Modifier genes of the intestinal and respiratory phenotype in Cystic Fibrosis pigs

von Melanie Folmer, geb. Janda

Inaugural-Dissertation zur Erlangung der Doktorwürde
der Tierärztlichen Fakultät der Ludwig-Maximilians-Universität München

Modifier genes of the intestinal and respiratory phenotype in Cystic Fibrosis pigs

von Melanie Folmer, geb. Janda

aus Fürth

München 2020

Aus dem Veterinärwissenschaftlichen Department der Tierärztlichen
Fakultät der Ludwig-Maximilians-Universität München

Lehrstuhl für Molekulare Tierzucht und Biotechnologie

Arbeit angefertigt unter der Leitung von: Univ.-Prof. Dr. Eckhard Wolf
Mitbetreuung durch: Prof. Dr. Nikolai Klymiuk und Dr. Andrea Bähr

Gedruckt mit Genehmigung der Tierärztlichen Fakultät
der Ludwig-Maximilians-Universität München

Dekan: Univ.-Prof. Dr. Reinhard K. Straubinger, Ph. D.

Berichterstatter: Univ.-Prof. Dr. Eckhard Wolf

Korreferent: Priv.-Doz. Dr. Bianka Schulz

Tag der Promotion: 25. Juli 2020

Meiner lieben Familie

TABLE OF CONTENTS

INDEX OF ABBREVIATIONS

aq. bidest	Bidistilled water
aq. dest.	Distilled water
ASL	Airway surface liquid
ATP	Adenosine triphosphate
BAC	Bacterial artificial chromosome
BW	Body weight
CACC	Calcium-activated chloride channel
cAMP	Cyclic adenosine monophosphate
CBAVD	Congenital bilateral absence of the vas deferens
cDNA	Complementary DNA
CF	Cystic Fibrosis
CFLD	Cystic Fibrosis-related liver disease
CFRD	Cystic Fibrosis-related diabetes mellitus
CFTR	Cystic fibrosis transmembrane conductance regulator
cLDLA	Combined linkage disequilibrium and linkage analysis
COPD	Chronic obstructive pulmonary disease
DIOS	Distal intestinal obstruction syndrome
DNA	Deoxyribonucleic acid
DNase	Deoxyribonuclease
dNTP	Deoxynucleoside triphosphate
DTT	Dithiothreitol
EDTA	Ethylenediaminetetraacetic acid
ENaC	Epithelial sodium channel
ET	Embryo transfer
EtOH	Ethanol
gDNA	Genomic DNA
GMS	Gene modifier study
GWAS	Genome-wide association study
h	Hour
HCl	Hydrochloric acid
i.c.	Intracardial
i.m.	Intramuscular

iFABP	Intestinal fatty acid-binding protein
IRT	Immunoreactive trypsinogen
IU	International unit
kb	Kilobase
KO	Knockout
L	Liter
LMU	Ludwig Maximilian University of Munich
M	Molar
mg	Milligramm
MI	Meconium ileus
min	Minute
mL	Milliliter
mM	Millimolar
mmol	Millimole
mRNA	Messenger RNA
NaCl	Sodium Chloride
NBD	nucleotide-binding domain
NBS	Newborn screening
NTC	Non-template control
PCR	Polymerase Chain Reaction
PFA	Paraformaldehyde
pH	Negative log of hydrogen ion concentration in water-based solution
qPCR	Quantitative PCR
rAAV	Recombinant adeno-associated virus
rcf	Relative centrifugal force
RNA	Ribonucleic acid
RNase	Ribonuclease
rpm	Revolutions per minute
s	Second
SCNT	Somatic cell nuclear transfer
SEM	Scanning electron microscopy
SNP	Single nucleotide polymorphism
TRIS	Tris (hydroxymethyl)-aminomethane
U	Unit
UNG	Uracil N-Glycosylase

UV	Ultraviolet
WT	Wild type
µL	Microliter

I. INTRODUCTION

Cystic Fibrosis (CF) is the most common life-threatening hereditary disorder among Caucasians and affects more than 100,000 people worldwide (reviewed in KLIMOVA et al., 2017). It is caused by mutations in the gene coding for the Cystic Fibrosis Transmembrane Conductance Regulator (CFTR) (WELSH & SMITH, 1993), leading to a defective anion transport on epithelial surfaces. CF constitutes a complex multi-organ disease affecting the airways, the gastrointestinal tract, including the pancreas and the hepatobiliary system, as well as the reproductive tract and the sweat glands, whereby clinical expression in individuals with CF shows a considerable variability (reviewed in AVERILL et al., 2017; HARUTYUNYAN et al., 2018; PARANJAPE & MOGAYZEL, 2018). While many organ systems can be affected, the major cause of morbidity and mortality is traced to pulmonary insufficiency (reviewed in CUTTING, 2015; PARKINS et al., 2018). Although CF remains incurable, the overall knowledge about the disease increased tremendously, so that not only life expectancy of up to 40 years, but also the quality of patients' life has significantly been improved over the last decades.

For a better understanding of pathophysiological mechanisms in CF and for developing novel therapeutic approaches, animal models turned out to be essential tools (reviewed in SEMANIAKOU et al., 2018). From the CF animal models developed so far in six species (mouse, rat, zebrafish, sheep, ferret and pig), the porcine CF model proves to be the model showing the closest similarity to hallmark features of human CF disease (reviewed in CUTTING, 2015). However, a lethal neonatal meconium ileus (MI) occurs in 100 % of all CF piglets (ROGERS et al., 2008b; KLYMIUK et al., 2012). If the intestinal obstruction is not corrected, CF piglets die within 48 hours after birth, considerably limiting the utility of pigs as animal models in CF research (KLYMIUK et al., 2012). Nonetheless, a previous thesis done at the Chair for Molecular Animal Breeding and Biotechnology, describes the occurrence of three CF piglets (#2850, #3137 and #4424) that showed a clear improved intestinal phenotype as meconium has passed autonomously; all other characteristic features of CF were still present (DMOCHEWITZ, 2016). Subsequent genome-wide analysis revealed the

hypothesis of two independent modifying loci on chromosome 10 (25.8–25.9 Mb) and on chromosome 16 (4.7–5.2 Mb) to rescue the severe intestinal phenotype. In my work, the hypothesis was tested and therefore the frequency of the desired genotype constellation on both candidate regions was enriched in the CF breeding herd in order to increase the probability of an improved intestinal manifestation in CF piglets. Eventually, an alternative evaluation of the genetic diversity was performed by genome-wide analysis on the basis of a larger population.

In addition, a variant respiratory phenotype was observed in some CF piglets during my thesis, independently from the CF gut-phenotype.

II. REVIEW OF THE LITERATURE

1. Cystic Fibrosis

Cystic Fibrosis (CF) is the most common, autosomal recessive monogenic disorder among Caucasians and indeed affects more than 100,000 people worldwide (reviewed in KLIMOVA et al., 2017). It is caused by mutations in the gene coding for the Cystic Fibrosis Transmembrane Conductance Regulator (CFTR), a controlled anion channel (WELSH & SMITH, 1993).
As early as in the Middle Ages, interesting notes told about children whose brows tasted salty and who died precociously (AGRONS et al., 1996), but only in 1938 Andersen firstly described clinical features of pancreatic fibrosis and pulmonary disease and finally introduced the term “cystic fibrosis” (ANDERSEN, 1938). Abnormal sweat gland electrolyte secretion was detected in 1953 (DI SANT'AGNESE et al., 1953), laying the foundation for the development of the “sweat test” in 1959 by Gibson and Cooke (GIBSON & COOKE, 1959) as a valuable diagnostic tool for CF, which is still in common use today. In 1983 the defective permeability of epithelium to chloride ions was recognized as the basic physiologic aberration in CF (QUINTON, 1983). With the identification of the disease causing *CFTR* gene (RIORDAN et al., 1989), a great breakthrough has been done and new diagnostic tests, prospects for novel therapeutic approaches and opportunities for further research came up.

The history of Cystic Fibrosis treatment can be considered a paradigm of the successful performance by collaborative international exertion in the basic and clinical research (reviewed in CASTELLANI & ASSAEL, 2017). Although CF remains incurable, the overall knowledge about the disease increased tremendously, so that not only life expectancy, but also the quality of patients’ life has significantly been improved over the last decades.

1.1. Genetics of Cystic Fibrosis

The identification of the *CFTR* gene in 1989 (RIORDAN et al., 1989) was a major breakthrough and paved the way for a more detailed diagnosis of CF, a better insight into the clinical features, and actually laid the foundation for new therapeutic agents (reviewed in DAVIS, 2006). The *CFTR* gene is located on the long arm of chromosome 7, consists of 27 exons, spanning over 250 kb and encodes the CFTR protein, which comprises 1,480 amino acids (MARINO et al., 1991; reviewed in DAVIS, 2006; reviewed in FANEN et al., 2014). CFTR is a membrane protein, expressed in many epithelial cells within the airways, pancreas, liver, intestine, sweat glands and vas deferens (reviewed in DAVIS, 2006) and functions as a cAMP-regulated channel, which transports anions, including chloride and bicarbonate. It belongs to the ABC-transporter family and is the only member of this family operating as an ion channel (reviewed in MENG et al., 2017; ROGERS et al., 2019).

CFTR structurally consists of five domains: two membrane-spanning domains (MSDs), taking part in the formation of the chloride channel pore, two nucleotide-binding domains (NBDs), interacting with cytosolic nucleotides, and one intracellular regulatory region (R) with multiple phosphorylation consensus sites. Coordinated interaction of NBDs and R domain systematically regulate channel activity (reviewed in WELSH & SMITH, 1993; MENG et al., 2017). Presently, there are more than 2,000 different mutations listed in the Cystic Fibrosis Mutation Database (CFTR1, 2015), of which at least 280 mutations are known to cause disease (IVANOV et al., 2018). The most common mutation worldwide, characterized by deletion of a single phenylalanine in position 508 (F508del), affects around 66 % of all CF patients (reviewed in RATJEN, 2009; CFTR1, 2015). Individuals homozygous for F508del represent the most common CFTR genotype, namely 50 % of all patients (CUTTING, 2010).

Based on their functional consequences on the CFTR protein, mutations are classified into six different groups (WELSH & SMITH, 1993; reviewed in ROGERS et al., 2019). Nonsense or splicing mutations lead to a complete absence of full-length, functional CFTR protein synthesis and are summarized in class I. Class II mutations, including the F508del mutation, stem from CFTR misfolding, resulting in a CFTR protein that fails to traffic through the endoplasmic reticulum to the cell surface. Mutant proteins that indeed reach the plasma membrane, but

due to mutations in the NBDs, do not respond to activation stimuli, such as phosphorylation, are cumulated in class III. As a result, these types of mutations lead to decreased chloride channel activity. A diminished chloride conductance defect is summed up in class IV mutations. Class V and VI mutations lead to normal CFTR protein, but there is either less amount of functional protein (class V) or less stability at the apical membrane combined with an increased turnover in the plasma membrane (class VI). Class I-III mutations are associated with the classical CF phenotype, whereas the other defects lead to milder phenotypes (reviewed in PROESMANS et al., 2008).

1.2. Pathophysiology of Cystic Fibrosis

Since the detection of the disease-causing *CFTR* gene, the knowledge of CF pathophysiology has increased significantly. Nevertheless, there are many aspects that still remain unclear and necessarily need to be clarified in order to conceivably escape the still unavoidable outcome of progressive lung dysfunction, the major cause of morbidity and mortality in CF-patients (reviewed in CUTTING, 2015).

In summary, an absent or malfunctioning CFTR protein leads to reduced chloride and bicarbonate conductance on the apical membrane of epithelial cells, resulting in dehydration and acidification of mucosal surfaces (reviewed in RATJEN, 2009; GENTZSCH & MALL, 2018). The so formed sticky and viscous mucus obstructs the luminal compartments of the affected organs, such as the lungs, the intestine and the pancreas.

It is of note, that, apart from being a chloride and bicarbonate channel, CFTR also acts as a regulator of other membrane channels. In this context, active CFTR inhibits the epithelial sodium channel ENaC, causing the absorption of sodium and water from the airway lumen (reviewed in CASTELLANI et al., 2018b), as well as chloride efflux via the outwardly rectifying chloride channel ORCC (reviewed in RATJEN, 2009).

From the beginning there were two different hypotheses, both of them trying to find a possible explanation for the development of CF lung disease, which reflects a failure of innate defense against bacterial infections (BOUCHER, 2007). The first hypothesis, the ‘high salt’ hypothesis, proposes an increased NaCl concentration in the airway surface liquid (ASL) as responsible for decreased activity of antimicrobial peptides, resulting in chronic airway infections. In contrast, the ‘low volume’ hypothesis focuses on the idea, that reduced chloride conductance leads to less water efflux, finally resulting in dehydrated airway surfaces. In turn, airway surface liquid depletion is recognized as the major cause of diminished mucus clearance due to ciliary collapse. Adherent mucus obstructs the airways and thus sets the stage for a vicious circle of chronic bacterial infection (GOLDMAN et al., 1997) and inflammation, in the end culminating in progressive lung dysfunction.

1.3. Phenotypical abnormalities in Cystic Fibrosis

Cystic Fibrosis is a complex multi-organ disease affecting the airways, the gastrointestinal tract, including the pancreas and the hepatobiliary system, as well as the reproductive tract and the sweat glands, whereby clinical expression in individuals with CF shows a comprehensive variability (reviewed in AVERILL et al., 2017; HARUTYUNYAN et al., 2018; PARANJAPE & MOGAYZEL, 2018).
While many organ systems can be affected, the major cause of morbidity and mortality is traced to pulmonary insufficiency (reviewed in CUTTING, 2015; PARKINS et al., 2018). At birth the lungs of CF patients appear normal, however from early age on individuals with common CF typically exhibit progressive respiratory manifestations. Impaired mucociliary clearance, resulting in mucus obstruction and chronic colonization of the airways by pathogenic bacteria, the latter clearly dominated by *Staphylococcus aureus* and *Pseudomonas aeruginosa* (reviewed in PROESMANS et al., 2008), remain the clinical hallmarks of classic CF. Frequent infections with repeated episodes of chronic and acute inflammatory and immune reaction lead to airway damage, manifesting as bronchiectasis, accompanied by fever, cough, dyspnea and weight loss. Finally, chronic cycles of infection and inflammation provoke respiratory failure with clinical end-stage lung disease. This is, why lung transplantation often remains the only therapeutic option at this stadium. It is of note, that the clinical appearance of CF lung disease shows wide variability (reviewed in CASTELLANI & ASSAEL, 2017).
Up to 90 % of individuals with classic CF suffer from gastrointestinal complications. Meconium ileus (MI), a life threatening obstruction of the distal small bowel by fetal feces, occurring in 15-20 % of all CF newborns (GUO et al., 2014), is often the first clinical indication of CF (AGRONS et al., 1996). Its occurrence is more frequently associated with more severe *CFTR* mutations and seems to be influenced by additional genetic factors (KNOWLES & DRUMM, 2012; DUPUIS et al., 2016). Two types of MI are admitted: the simple and the complicated form, both occurring with similar frequency (50-58 %). Simple MI typically appears in otherwise healthy infants within 48 hours after birth as an intestinal obstruction. The complicated form arises earlier and is characterized by more severe symptoms like volvulus or microcolon. Resolution of MI requires intensive treatment, including rectal infusion of Gastrografin or enema in the case of simple MI, as well as surgical intervention in about half of the cases (DUPUIS

et al., 2016). Thanks to great progress in the clinical management of MI, the survival of newborns with CF and MI increased significantly and is nowadays comparable to children with CF who do not suffer from MI.

Older patients may exhibit intestinal obstruction as well, leading to a sub occlusive or fully occlusive manifestation called distal intestinal obstructive syndrome (DIOS), that appears in up to 25 % of adult patients (reviewed in CASTELLANI & ASSAEL, 2017; SEMANIAKOU et al., 2018). Typically conservative measures like oral rehydration or osmotic laxatives are recommended (KELLY & BUXBAUM, 2015).

Another feature of classic CF, affecting 85-90 % of adults, is pancreatic exocrine insufficiency (reviewed in AVERILL et al., 2017; HARUTYUNYAN et al., 2018). Decreased levels of pancreatic enzymes lead to fat malabsorption, causing steatorrhea, malnutrition, deficiency of fat-soluble vitamins and characteristic fatty and foul-smelling stool. Similar to the occurrence of MI, pancreatic insufficiency is usually also associated with severe class I-III *CFTR* mutations (DURNO et al., 2002). As a result of progressive damage of pancreatic tissue, the pancreas can also lose its endocrine function, leading to Cystic Fibrosis-related diabetes mellitus (CFRD), which is a unique combination of type I and type II diabetes and can be handled with insulin.

Often hepatobiliary manifestation in CF is not clinically relevant. However, in some patients (3-5 %) Cystic Fibrosis-related liver disease (CFLD) is severe and counts as the third most common cause of mortality in CF individuals after respiratory failure and complications following transplantation. Usually, the onset of liver disease in the second decade of life or even later is characterized by fatty liver, fibrosis, biliary cirrhosis and portal hypertension. The so-called ‘micro-gallbladder’ is another reported abnormality in 10-30 % of all patients with CF (reviewed in LAVELLE et al., 2016). It is small or even absent and may be nonfunctioning.

Nearly all males with CF (over 95 %) are infertile due to congenital bilateral absence of the vas deferens (CBAVD) and obstructive azoospermia, whereas only a small percentage of women suffer from reduced fertility (reviewed in EDENBOROUGH, 2001; O'SULLIVAN & FREEDMAN, 2009).

1.4. Diagnosis of Cystic Fibrosis

In most cases, Cystic Fibrosis is diagnosed in the first year of life und normally diagnoses are unambiguous (reviewed in AVERILL et al., 2017).

At the moment there are three main tests to identify whether an individual suffers from CF: the newborn screening test, the confirmatory sweat-test and the diagnosis of specific mutations of the *CFTR* gene.

A diagnosis in the first days of life can be done by newborn screening (NBS), a technique established in 1979 (reviewed in COURSE & HANKS, 2019). In this test a blood sample is checked for higher than normal levels of pancreatic Immunoreactive Trypsinogen (IRT). Laboratories either perform two consecutive measurements or, if the first IRT level is increased, execute successive *CFTR* mutation testing (reviewed in PARANJAPE & MOGAYZEL, 2018). Proceeding that way, most children diagnosed with CF are nowadays detected when still in an asymptomatic stage (reviewed in COURSE & HANKS, 2019). Such an early diagnosis has been proven to bring substantial benefits in the following treatment and thus in the prognosis of patients with CF. When properly designed and managed, screening programs are cost effective and offer a high sensitivity and specificity (reviewed in CASTELLANI & ASSAEL, 2017). Over the past two decades, there has been a steady increase in national NBS programs. At present, in nearly all European countries, as well as in the United States, well-established nationwide protocols have been implemented (reviewed in COURSE & HANKS, 2019).

The gold-standard for diagnosing CF remains the pilocarpine iontophoresis sweat test (reviewed in COURSE & HANKS, 2019), developed by Gibson and Cooke in 1959, following the knowledge of increased chloride levels in the sweat as an unequivocal hallmark of CF (GIBSON & COOKE, 1959). A chloride concentration greater than 60 mmol/L is confirmatory of the CF diagnosis, while intermediate concentrations (40-60 mmol/L) are only indicative. In such cases, the identification of two CF-causing mutations on both alleles clearly verifies the before established suspicion (reviewed in KLIMOVA et al., 2017; CASTELLANI et al., 2018a). It has to be mentioned, that also in the case of a positive NBS test, a sweat test always has to confirm the diagnosis CF (CASTELLANI et al., 2009) .

Since mutation specific therapies are becoming increasingly available, the detection of *CFTR* mutations in an individual patient is now another important

tool (reviewed in DE BOECK et al., 2017). Most common disease-causing mutations in the examined population (covering 80-85 % of all mutations in the population) are identified with the help of a standard *CFTR* mutation panel. More complex analyses, conducted by certified laboratories, are realized, when two *CFTR* gene mutations could not be identified and the diagnosis of CF is nearly confident (diagnostic sweat chloride concentration above 60 mmol/L) or very likely due to typical clinical features as previously described. In the course of this, the entire *CFTR* gene is sequenced and after that, large deletions or insertions are being evaluated.

It is of note, that up to 7 % of CF cases are nowadays diagnosed in patients over the age of 16 years (reviewed in AVERILL et al., 2017), presenting with recurrent pancreatitis, chronic sinusitis or CBAVD. Often these patients exhibit one ‘mild’ *CFTR* mutation and retain a residual chloride channel activity. With only 10 % of the normal levels of *CFTR* mRNA remaining, individuals can show normal lung and pancreatic function, what is a formative difference from the before described classic CF phenotype diagnosed in childhood.

1.5. Treatment approaches for chronic aspects of Cystic Fibrosis

When first described in 1938, CF usually resulted in death during infancy (reviewed in CASTELLANI et al., 2018a; ROGERS et al., 2019). Early diagnosis, substantial progress in the management of especially pulmonary CF disease, important new therapy approaches and the establishment of multi-disciplinary treatment centers in the 1950s, altogether greatly improved the duration and particularly the quality of patients' life. Presently, 40-50 % of all CF patients are adults with a life expectancy of up to 40 years in countries with well-established CF programs (HODSON et al., 2008). For people born after the year 2000 it is even projected to be 50 years (HURLEY et al., 2014). CF cannot be cured, but with the help of careful monitoring and early aggressive pharmacological strategies, symptoms can be delayed.

Treatment approaches primarily focus on pulmonary manifestation of CF. In early stages of the disease, non-pharmacological treatment, mainly focusing on chest physical therapy, can help to loosen mucus (reviewed in KLIMOVA et al., 2017). The main challenge in CF remains the prevention and control of lung infections (reviewed in CASTELLANI & ASSAEL, 2017; KLIMOVA et al., 2017; RAFEEQ & MURAD, 2017). In this context, antibiotics in a high-dosage regime are prescribed, mainly consisting of inhaled forms of azithromycin, tobramycin, aztreonam and levofloxacin. Despite aggressive preventive measures, bacterial colonization of the lower airways, usually ending up in progressive lung damage, just like repeated episodes of inflammatory and immune action, remain major clinical difficulties. Anti-inflammatory therapy is able to slow down the progression of lung disease (reviewed in CHENG et al., 2013) and comprises the intake of ibuprofen (LANDS et al., 2007), as well as inhaled (beclomethasone, budesonide and fluticasone) or systemic (prednisone) corticosteroids. Another important aspect in dealing with CF pulmonary manifestation is the use of mucoactive substances, which help to remove thick, sticky mucus from the lungs and further dilate the airways. Mucolytics can be divided into non-specific, such as ambroxol, acetylcysteine and mesna, and in CF-specific like amiloride, NaCl and dornase α. In the worst cases, respiratory failure and end-stage lung disease make a lung transplantation, as the only remaining therapeutic option, necessary.

Pancreatic insufficiency is treated with well-established pancreatic enzyme replacement therapy rich in lipase, protease and amylase. Furthermore, a strict

high-energy and high-fat dietary nutrition and the supplementation of vitamins is mandatory (reviewed in KLIMOVA et al., 2017).

The therapy of CFLD focuses on improving biliary excretion and bile acid composting by oral supplementation of the bile salt ursodeoxycholic acid, which normalizes liver function. Only if hepatobiliary disease is complicated by portal hypertension, liver transplantation is considered (KELLY & BUXBAUM, 2015).

Even before the identification of the *CFTR* gene, genetic based therapy was suggested as possible treatment for CF (reviewed in GILL & HYDE, 2014). Gene therapy approaches mainly focus on gene complementation, where wild type (WT) *CFTR* cDNA is delivered to cells suffering from impaired CFTR function, a method feasible for all classes of mutations. A clinical study by British scientists, administering monthly treatments of a nebulized gene/liposome complex, run in clinical trial phase II and showed modest, but positive results in favor of improved lung function in 3.7 % of participating CF patients (reviewed in CASTELLANI & ASSAEL, 2017).

With the introduction of so-called CFTR modulators, treatment methods shifted from only symptomatic therapy towards personalized approaches, adjusted to the patients' underlying CFTR mutation (reviewed in SKOV et al., 2019). At the moment there are three different types of modulators available: potentiators, used in class III or IV mutations, raise the function of CFTR channels by increasing the channel open probability. Correctors, which augment the intracellular processing of class II mutations, allowing more protein to reach the plasma membrane. Moreover, read-through agents promote ribosomal read-through in class I *CFTR* mutations (reviewed in BRODLIE et al., 2015). The first available modulator was ivacaftor (Kalydeco), targeting class III mutations such as G551D, which is carried by 4 to 5 % of CF patients (ROWE et al., 2014). Ivacaftor was shown to significantly improve clinical parameters such as lung function and has actually been approved for treating patients with 38 different class III and IV mutations (reviewed in ROGERS et al., 2019). In 2015, the combination of ivacaftor together with the corrector lumacaftor (VX-809) was established in order to correct the most common class II mutation F508del (WAINWRIGHT et al., 2015). Unfortunately, compared to the previously described ivacaftor monotherapy, the effects of this combined method on lung function were relatively modest. Similar clinical effects, also tested in F508del mutations, have been observed with another potentiator/corrector combination ivacaftor/tezacaftor

(ROWE et al., 2017; TAYLOR-COUSAR et al., 2017). Ataluren (PTC124) is a read-through agent and has been trialed for use in class I mutations, affecting approximately 10 % of CF patients. It is now in phase III of clinical trials and so far, it showed moderate clinical improvement (KEREM et al., 2014). New and potentially more effective so-called next-generation modulators, aiming to be available for a much larger CF population, are presently tested in ongoing studies (reviewed in SKOV et al., 2019).

In summary it can be said, that, despite the positive outcomes of all the new agents, there are still limitations, including high costs for long-term treatment (reviewed in WHITING et al., 2014) and particularly the indispensable need to continue other symptomatic treatment (reviewed in RAFEEQ & MURAD, 2017). The development and improvement of novel treatment procedures for an even larger community of CF patients is a crucial need to enhance the patients' quality of live and will be a bold challenge in the near future.

2. Animal models for Cystic Fibrosis

Animal models are essential tools for better understanding pathophysiological mechanisms in Cystic Fibrosis and for developing new therapeutic approaches (reviewed in SEMANIAKOU et al., 2018). CFTR-deficient animal models offer several advantages for studying CF disease (reviewed in OLIVIER et al., 2015). They can be studied early in life, whereas studies in CF infants and children are limited due to ethical concerns. Moreover, animal models allow for controlled comparison of organ systems and even of the clinical spectrum between different species. Thus, they do not only give greater insights into CF pathogenesis, but also help to identify additional genetic modifiers possibly influencing the disease. Currently, CF model in six different species are available (mouse, rat, zebrafish, sheep, ferret and pig) and demonstrate the complexity of human CF manifestations, whereby various models present different specific advantages, but also major limitations (reviewed in SEMANIAKOU et al., 2018).

2.1. Animal models for Cystic Fibrosis (apart from the pig)

Shortly after the identification of the *CFTR* gene in 1989, the first CF mouse model was generated (SNOUWAERT et al., 1992). The most prominent hallmark in CF mice is the severe intestinal obstruction, including mucus accumulation, goblet cell hyperplasia and crypt dilatation, symptoms comparable with human intestinal manifestation (reviewed in GRUBB & BOUCHER, 1999). In contrast to CF patients in whom pancreatic insufficiency and liver disease are major features, CF mice develop only mild pancreatic disease (SNOUWAERT et al., 1992) and no obvious liver pathology (reviewed in ROSEN et al., 2018). Most of the male CF mice exhibit reduced fertility, but the complete bilateral absence of the vas deferens, typical for male humans, is missing (LEUNG et al., 1996; LAVELLE et al., 2016). The main problem of the CF mouse, limiting its usage as an animal model, is the lack of replicating CF-typical substantial und spontaneous bacterial infection and inflammation in the lungs (reviewed in GUILBAULT et al., 2007). A possible explanation for this divergent respiratory phenotype could be an adaptive dominance of the calcium-activated chloride channel (CACC), compensating the defective chloride transport (reviewed in MCCARRON et al.,

2018).

CF rat models are characterized by intestinal obstruction at weaning, complete bilateral absence of the vas deferens and missing signs of obvious hepatobiliary and pancreatic disease (TUGGLE et al., 2014). While CF rats do not spontaneously develop lung infection and inflammation, they still share respiratory abnormalities consistent with humans, such as congenital tracheal defects with reduced cartilage and gland area.

The CF zebrafish is a unique model of pancreatic disease progression in all developmental stages, demonstrating that pancreatic dysfunction starts early in life (NAVIS & BAGNAT, 2015).

FAN et al. (2018) generated the first CF sheep model, which is characterized by intestinal obstruction with 100 % incidence in CF KO lambs, pancreatic fibrosis, hepatobiliary abnormalities, including fibrosis and cirrhosis, as well as the absence of vas deferens in male individuals. However, lung pathology is not detectable.

Due to similarity in lung cell biology and anatomy to human CF patients, the ferret is a good animal model for CF research (reviewed in LAVELLE et al., 2016). Ferret CF models show a more severe intestinal phenotype compared to humans, as MI is present in approximately 75 % of CF ferret kits (SUN et al., 2010), resulting in death within 36 hours (reviewed in FISHER et al., 2011). Similar to human CF infants, CF KO kits are born with only mild pancreatic disease, but very early in life pancreatic inflammation is starting and within the first months the pancreas undergoes rapid tissue deterioration, finally resulting in pancreatic insufficiency in 85 % of adult CF ferrets and characteristics of CF-related diabetes mellitus (OLIVIER et al., 2012). While the hepatobiliary system appears normal at birth, increased liver enzymes indicate an early onset of liver disease and even gallbladder abnormalities are present in the majority of CF ferrets older than one month (SUN et al., 2014). An absent or degenerated vas deferens is another characteristic, typically found in CF ferrets. Most importantly, ferret models mirror the human respiratory phenotype, characterized by impaired mucociliary clearance, mucus-obstruction of the airways and submucosal glands, and particularly the development of spontaneous lung infections soon after birth (SUN et al., 2010; SUN et al., 2014).

2.2. The pig as an animal model for Cystic Fibrosis

From the CF animal models developed so far, the porcine CF model proves to be the model showing the closest similarity to typical CF phenotype in humans (reviewed in CUTTING, 2015). In view of pulmonary insufficiency, presenting the leading cause of mortality in CF patients, the pig as an animal model offers potential advantages, as its lung share many features with human lungs (ROGERS et al., 2008a; WELSH et al., 2009; AIGNER et al., 2010). In general, pigs and humans have a lot of similarities in terms of anatomy, physiology, histology, immunology, metabolism and even genomics. Moreover, the early sexual maturity, a short generation time and large litter sizes also recommend the pig as an ideal large animal model. The longevity of pigs enables for examining pathophysiological mechanisms in CF and long-term efficacy of pharmacological and other treatment approaches.

So far, three different porcine CF models, either carrying the complete disruption of both *CFTR* alleles (ROGERS et al., 2008b; KLYMIUK et al., 2012), or carrying the most common CF-associated mutation F508del (ROGERS et al., 2008a), have been generated. Rogers and colleagues used recombinant adeno-associated virus (rAAV) vectors targeting the porcine *CFTR* gene in fetal fibroblasts, followed by somatic cell nuclear transfer (SCNT) and embryo transfer (ET) to produce male heterozygous $CFTR^{+/-}$ offspring. At sexual maturity they were bred selectively over two generations by initially generating further male and also female heterozygotes in order to finally produce $CFTR^{-/-}$ piglets (ROGERS et al., 2008a). The first European pig model of CF was established by KLYMIUK et al. (2012) by using modified bacterial artificial chromosome (BAC) vectors for sequential targeting of the *CFTR* gene in porcine primary kidney cells.

Cystic Fibrosis pigs recapitulate many of the human phenotypical manifestations of CF. In newborn CF piglets, pancreatic insufficiency develops spontaneously, characterized by a variable severity of exocrine tissue destruction (ROGERS et al., 2008b; MEYERHOLZ et al., 2010b; KLYMIUK et al., 2012). Histologically, small and degenerative lobules with loose adipose tissue, mucus-dilated ducts, obstructed by eosinophilic material, and even signs of mild inflammation are generally detectable. Morphologically, pancreatic endocrine tissue appears intact (ROGERS et al., 2008b), however, glycemic abnormalities and even defects in insulin secretion are present findings in newborn CF pigs (UC et al., 2014).

Indeed, CF piglets demonstrate impaired glucose tolerance and an elevated glucose area, resulting in spontaneous hyperglycemia developing over time. Interestingly, obvious functional alterations in the pancreas of CF pigs are not associated with a decrease in islet cell mass, suggesting, that, independent of structural islet loss, functional deviations in pancreatic islets contribute to the early pathogenesis of CF-related diabetes mellitus (UC et al., 2014).

The liver of CF KO pigs infrequently exposes mild to moderate hepatic lesions, whereby signs of focal biliary cirrhosis, including increased cellular inflammation, bile ductal hyperplasia and mild fibrosis, are present. While all *CFTR*$^{-/-}$ piglets exhibit a micro-gallbladder, filled with mucin-containing material, in human CF patients this phenotypical abnormality occurs in only 10-30 % of all cases (reviewed in LAVELLE et al., 2016). It is of note, that the hepatic changes in CF pigs are irregular not only between different areas within the same tissue, but also between different individuals (KLYMIUK et al., 2012).

Moreover, male CF KO piglets reveal a degenerated or absent vas deferens, and in some cases also epididymis atresia, comparable with changes typically found in human CF patients (PIERUCCI-ALVES et al., 2011).

2.2.1. The respiratory phenotype in Cystic Fibrosis pigs

Due to anatomical, histological and physiological similarities between the human and porcine lung, the pig model presents an ideal model to examine pathophysiological mechanisms in CF lung disease (AIGNER et al., 2010). Interestingly, the porcine respiratory tract has already been used for a long time to study pulmonary abnormalities that are relevant to CF, such as infection and inflammation procedures (BRADLEY et al., 1976; PABST & BINNS, 1994).

In contrast to most of the CF animal models generated so far, the porcine CF model demonstrates several respiratory abnormalities. Common findings in all CF piglets are tracheal abnormalities, including a triangular to oval shaped trachea, in contrast to the circular shape in WT controls, reduced tracheal caliber extended through the mainstem bronchi, as well as thicker and more discontinuous cartilages (ROGERS et al., 2008b; KLYMIUK et al., 2012). Due to altered orientation of smooth muscle cell bundles, the caudal trachea and the large bronchi exhibit a variable thickening of the posterior wall. Moreover, submucosal

glands occur with similar frequency compared to control airways, but CF glands are small and hypoplastic (MEYERHOLZ et al., 2010a). In summary, the congenital tracheal defects are similar to changes found in CF infants (reviewed in MEYERHOLZ et al., 2010a; STOLTZ et al., 2015) and are furthermore awarded to contribute to CF disease development during postnatal life (WELSH et al., 2009; MEYERHOLZ et al., 2010a). Nevertheless, specific mechanisms for tracheal abnormalities and the question, how absent CFTR induces these effects during development, are still unknown (MEYERHOLZ et al., 2010a).

The lungs of newborn CF piglets morphologically appear normal at birth without evidence of pathological abnormalities (ROGERS et al., 2008b). Only within weeks to months after birth, they spontaneously develop characteristic features of CF lung disease, including infection, inflammation, mucus accumulation and remodeling procedures (STOLTZ et al., 2010). Interestingly, the manifestation of CF respiratory phenotype is, similar to humans, heterogeneous within and among pigs. Although newborn CF pigs morphologically do not show signs of inflammation, compared to non-CF littermates their lungs are less sterile. Harboring a huge amount of environmental bacteria led to the conclusion, that this is an equal opportunity host-defense defect (STOLTZ et al., 2015). Even after intrapulmonary bacterial challenge, CF piglets actually fail to eliminate bacteria, suggesting that airway infection precedes lung inflammation and not vice versa (STOLTZ et al., 2010). The reason for diminished degree of bacterial killing has been directly linked to reduced CFTR-dependent bicarbonate secretion, resulting in acidic airway surface liquid and decreased antibacterial activity (reviewed in STOLTZ et al., 2015). Suspecting that host-defense defects begin within hours of birth, preventive measures should be initiated immediately before secondary consequences, finally leading to respiratory failure, develop.

Moreover, pigs with CF demonstrate a defective mucociliary clearance, caused by the failure of mucus to detach from submucosal gland ducts. This defect is not imputable to insufficient periciliary liquid (BIRKET et al., 2014), but rather to basic loss of CFTR anion transport, indicating that this is a primary discrepancy and not dependent on processes like infection, inflammation or tissue remodeling (reviewed in STOLTZ et al., 2015).

Most significantly, studies on electrolyte transport in porcine CF airway tissue questioned the long-standing hypothesis, that sodium hyperabsorption via the epithelial sodium channel ENaC fundamentally contributes to CF pathogenesis.

CHEN et al. (2010), indeed demonstrated a lack of chloride conductance and impaired bicarbonate transport in airway epithelia in CF piglets, but also a clear absence of sodium hyperabsorption. This finding, together with lacking inflammation in the lungs of newborn CF pigs, contradicts the claim, that sodium hyperabsorption triggers respiratory failure (CHEN et al., 2010; STOLTZ et al., 2015). Instead, defects in chloride and bicarbonate transport are considered to initially initiate the pathogenesis of lung progression in CF patients.

2.2.2. The intestinal phenotype in Cystic Fibrosis pigs

Unfortunately, the development of CF lung disease in pig models is difficult to investigate, as an ever-present, severe intestinal phenotype with fatal meconium ileus (MI) represents the most prominent feature in pigs with Cystic Fibrosis. While only 15-20 % of all CF infants (GUO et al., 2014) suffer from the intestinal obstruction, in CF piglets MI actually occurs with a penetrance of 100 % (KLYMIUK et al., 2012). This dissimilarity in penetrance rate may potentially be explained by differences in anatomy and physiology combined with a restricted genetic background in pigs (ROGERS et al., 2008b). The pathogenesis of MI still remains unclear, but possible explanations are the lacking CFTR-mediated chloride and/or bicarbonate transport across epithelial membranes or perhaps pancreatic dysfunction (STOLTZ et al., 2013). Except from the frequency of occurrence, the general features of MI in pigs closely replicate those observed in humans. The site of obstruction ranges from the distal part of the jejunum to the proximal spiral colon (ROGERS et al., 2008b; MEYERHOLZ et al., 2010b). An atretic and stenotic microcolon with diminished diameter, distal to the site of obstruction, is a common finding in piglets with CF. The reason why the intestine distal to the site of obstruction fails to develop normally, is still uncertain. It is possible, that luminal content either prevents mechanical elongation, or because obstruction inhibits a distal transfer of the luminal content, assumed for adequate intestinal growth (AMODIO et al., 1986). A variably severe diverticulosis at the mesenterial side of the meconium-dilated jejunum is another intestinal lesion typically found in CF piglets (KLYMIUK et al., 2012). It appears as saccular bulges, histologically composing of lamina propria herniating through the lamina muscularis (MEYERHOLZ et al., 2010b). The proposed pathogenesis of such

diverticles is described as a combination of increased intraluminal pressure by sticky, adherent meconium and hypertrophic smooth muscles during fetal life. For some pig breeds a genetic predisposition toward diverticulosis has also been discussed (MEYERHOLZ et al., 2010b). The appearance of characteristic microcolon and diverticulosis in CF pigs is reported in human CF patients as well, however, with a lower incidence rate and a less severity. Further histological examinations of the porcine intestine demonstrate atrophic and degenerated villi, as well as mucus-obstructed Brunner's glands in the duodenum, lined by an atrophic epithelium (ROGERS et al., 2008b; KLYMIUK et al., 2012). Except as a secondary feature, initial signs of intestinal inflammation are not detectable (MEYERHOLZ et al., 2010b).

As clinical signs of an intestinal obstruction, the CF piglets stop eating, evolve abdominal distension, show bile-stained emesis and therefore continuously lose weight (ROGERS et al., 2008b). If MI is not corrected, CF piglets die within 48 hours after birth due to multifocal enteritis, peritonitis or even perforation, considerably limiting the usage of pigs as animal models in CF research (KLYMIUK et al., 2012). In CF infants, therapeutic strategies range from rectal infusion of Gastrografin or enema to complex surgical intervention, depending on the severity of MI (DUPUIS et al., 2016). However, nonsurgical approaches to rectify the intestinal obstruction fail in CF pigs (STOLTZ et al., 2013). Ensuring the survival of CF piglets, surgical ileostomy or cecostomy must be performed right after birth to bypass the obstruction (ROGERS et al., 2008b; STOLTZ et al., 2010). Although operative treatment may rescue the severe intestinal phenotype, the practicability in pigs is limited by intensive and time-consuming surgical-procedure as well as post-surgical care (KLYMIUK et al., 2012; GUILLON et al., 2015). Initially, in some CF pigs a surgical correction is basically not feasible in terms of complications associated with MI, such as intestinal atresia or perforation (STOLTZ et al., 2013). Even after surgical treatment, there is a high risk for postoperative complications, limiting the piglets' lifespan (KLYMIUK et al., 2012). These aspects, in addition to associated high costs, compromise surgical approaches as a regular technique to overcome the lethal intestinal phenotype in CF pigs (STOLTZ et al., 2013).

To circumvent these limitations, the prevention of MI rather than its treatment would obviously be an alternative method. Transgenic expression of *CFTR* under the control of gut-specific promoter results in an exclusive expression in the

intestine, while other organ systems stay unaffected (STOLTZ et al., 2013). As, in this way, the intestinal phenotype is able to be alleviated or even rescued, all other characteristic features of CF are still present. ZHOU et al. (1994) set the stage by using the rat intestinal fatty acid-binding protein (iFABP) promoter to express human *CFTR* in a murine model of CF, resulting in functional correction of cell hyperplasia and restored chloride secretion. STOLTZ et al. (2013) adopted that strategy to weaken the lethal intestinal phenotype, resulting in a "gut-corrected" porcine model of Cystic Fibrosis. They used the rat iFABP promoter to express WT porcine CFTR protein (pCFTR) in CF KO pigs (STOLTZ et al., 2013). In this study, piglets from 3 out of 5 transgenic lines had an improved intestinal phenotype, while still exhibiting pancreatic destruction, liver disorder and lung disease. An expression rate of approximately 20 % of WT *CFTR* seems to be adequate to largely prevent MI. It has to be mentioned, that a supportive treatment with Gastrografin enemas is still necessary to assure the piglets' survival. Interestingly, BALLARD et al. (2016) evaluated the "gut-corrected" approach in CF pigs and unexpectedly found other complications among the piglets, including a high neonatal mortality, severe systematic edema and cardiovascular abnormalities.

3. Modifier genes in Cystic Fibrosis

In general terms, Cystic Fibrosis is a monogenic recessive Mendelian disorder with complex, heterogeneous phenotypic expression (reviewed in WEILER & DRUMM, 2013; O'NEAL & KNOWLES, 2018). Apart from the causative *CFTR* defect itself, there are multiple sources that contribute to the striking phenotypic diversity, including the specific *CFTR* mutation, environmental factors, as well as additional non-*CFTR* genetic influences, so called 'modifier genes'. Each of the affected organ systems in CF demonstrates a specific phenotypic variability and uniquely responds to *CFTR* mutations and modifier effects. The correlation between *CFTR* genotype and clinical manifestation of the disease is well-known (KEREM et al., 1990). However, even among patients carrying the same *CFTR* mutation, there is a wide range of clinical manifestation, most notably lung disease diversity. As early as 1990, the potential role of genetic modifiers in determining the complexity of CF, has been proposed (SANTIS et al., 1990). Twin and sibling studies, determining the relative contribution of genetic and environmental factors, demonstrated high degrees of heritability for several traits, such as the severity of lung disease (MEKUS et al., 2000; VANSCOY et al., 2007), the risk for developing CFRD (BLACKMAN et al., 2009), early exocrine pancreatic insufficiency (SONTAG et al., 2006) and also the occurrence of intestinal obstruction at birth (BLACKMAN et al., 2006). In sum, those studies generally pointed to significant role of genetic modifiers in disease presentation, but the specific impact on the severity in CF still remains unclear (reviewed in SHANTHIKUMAR et al., 2019).

It is clear, that identifying and comprehensively understanding the effect of non-*CFTR* genetic influences in the context of CF pathogenesis and clinical variability, help to figure out novel therapeutic targets, hopefully resulting in new effective treatment strategies. In this context, observing a patient's particular genetic profile, disease-modifying genes actually open the door to personalized medicine (reviewed in WEILER & DRUMM, 2013).

Initial studies on modifier genes contributing to disease variability, evaluated candidate genes or regions implied in pathways that are already known to be relevant in CF (reviewed in WEILER & DRUMM, 2013; SHANTHIKUMAR et al., 2019). In view of still limited understanding of disease pathophysiology,

genetic locations beyond those are not detected. Further challenges of early candidate gene approaches are the limitation of statistical power due to relatively small cohort sizes and lots of conflicting results (reviewed in BÜSCHER & GRASEMANN, 2006). Larger, unbiased studies using a genome-wide approach examine either the overall exome, the coding region of the gene, via whole-exome sequencing, or all single nucleotide polymorphisms (SNPs), common genetic variations in an individual's DNA sequence (DAVIES et al., 2005), via genome-wide association study (GWAS). Thus, novel chromosomal regions and genes, previously not considered, can be identified. So far, a variety of individual genetic modifiers for multiple CF phenotypes has been detected, though there is no single definitive contributor that universally predicts disease severity or secondary complications (reviewed in DORFMAN, 2012). Rather combinations of genetic variants seem to contribute to overall disease manifestation. Due to this complex constellations, current study approaches are limited by disparate findings, confined replication and a relative lack of clinical influence. Future work has to overcome these limitations and finally assess, whether validated modifiers can actually be used in clinical management of CF patients.

3.1. Gene modifiers for the respiratory phenotype in Cystic Fibrosis

Considering the great relevance of pulmonary insufficiency in the progression of CF, the main focus of gene modifier approaches is the identification of additional non-*CFTR* genetic influences for lung disease progression (reviewed in O'NEAL & KNOWLES, 2018). The complex, heterogeneous phenotypic expression in CF appears, as previously mentioned, even among CF patients with the same *CFTR* mutation. While some patients exhibit relatively mild lung disease until adolescence and adulthood, others show a faster decline in lung function and suffer from poor respiratory condition even at very young age (KEREM et al., 1990). Also, in various CF animal models, the manifestation of pulmonary disease severely differs, as ferrets and pigs spontaneously develop lung infection and inflammation, whereas mice, rats and sheep lack this CF-typical abnormality. It was determined, that genetic modifiers could account for 50-80 % of lung disease variability in CF patients carrying an equal *CFTR* genotype (VANSCOY et al., 2007).

For the divergent pulmonary phenotype, a huge amount of modifier genes has been described, with *TGFB1* and *MBL* being the first ones that have been identified (reviewed in SHANTHIKUMAR et al., 2019). Transforming growth factor beta 1 (TGFB1), a major fibrogenic cytokine (GRAINGER et al., 1999), is one of the most widely examined potential gene modifiers in CF lung disease, as it plays a key role in the regulation of inflammation and tissue remodeling (AKHURST, 2004). Its impact on other lung disorders, such as asthma and chronic obstructive pulmonary disease (COPD), has already been described (PULLEYN et al., 2001; WU et al., 2004). Moreover, there is also evidence that interaction between *TGFB1* genotype and tobacco smoke exposure additionally influences CF lung disease severity (COLLACO et al., 2008). Several studies on *TGFB1* as a modifier of CF, including the large Gene Modifier Study (GMS), revealed, that a codon 10 CC genotype has been associated with enhanced expression of *TGFB1*, leading to increased inflammation and fibrosis, in turn resulting in more severe respiratory manifestation (DRUMM et al., 2005).

The lack of mannose-binding lectin (MBL), a serum protein participating in innate immune response, is related to increased susceptibility to infections. (reviewed in TURNER, 2003). Consequently, as actually proved in a number of candidate modifier studies, a *MBL*-deficient genotype is suggested to be connected with worse clinical manifestation, characterized by higher infection rate and reduced lung function (reviewed in SHANTHIKUMAR et al., 2019). However, since the findings of numerous studies are in part contradictory, and the most robust study actually could not find any effect of *MBL* on lung disease diversity (DRUMM et al., 2005), the role of *MBL* as a modifier gene of CF still remains a matter of debate.

Apart from *TGFB1* and *MBL*, many other genes have been suggested as modifiers contributing to the diverse pulmonary phenotype in CF patients, such as homeostatic iron regulator (*HFE*) (REID et al., 2004; PRATAP et al., 2010; SMITH et al., 2019), endothelin receptor type A (*EDNRA*) (DARRAH et al., 2010) and carcinoembryonic antigen-related cell adhesion molecules (*CEACAM*) (STANKE et al., 2010).

Moreover, current systematic GWAS identified five more regions that are correlated to lung disease severity (reviewed in O'NEAL & KNOWLES, 2018; SHANTHIKUMAR et al., 2019). On chromosome 3 mucin 4 (*MUC4*) and mucin 20 (*MUC20*) have been detected, however, neither the region, nor the genes have

been identified in subsequent studies. In contrast, solute carrier family 9 member A3 (*SLC9A3*) on chromosome 5, as well as major histocompatibility complex (*HLA*) class II on chromosome 6 could both be detected as possible gene modifiers in additional investigations. The X chromosome revealed solute carrier family 6 member A14 (*SLC6A14*) to be associated with lung function and the risk of *Pseudomonas aeruginosa* infection. Further research detected ETS homologous factor (*EHF*) and APAF1 interacting protein (*APIP*) on chromosome 11 as potential gene modifiers. All hypothesized genes are of biological interest with high mechanistic probability (reviewed in O'NEAL & KNOWLES, 2018). However, it has to be mentioned that the loci of highest correlation are intergenic and hence very likely of regulatory function. Understanding the mechanistic effect of the suspected genes and expanding the present findings to even larger investigations will be an important challenge in future CF gene modifier research.

3.2. Gene modifiers for the intestinal phenotype in Cystic Fibrosis

Although the presentation of neonatal intestinal obstruction with meconium ileus (MI) is pathognomonic for Cystic Fibrosis (AGRONS et al., 1996), only 15-20 % of all CF infants are born with this characteristic trait. On the contrary, animal models for CF remarkably exhibit a more severe, but among each other, a still variable intestinal phenotype. In CF rats an intestinal obstruction at weaning is actually the most prominent feature (TUGGLE et al., 2014), whereas in CF mice the development of this trait usually depends on their genetic background (reviewed in FIOROTTO et al., 2019). CF ferrets are characterized by severe MI, appearing in approximately 75 % of all ferret kits (SUN et al., 2010). As a major drawback of the promising CF pig model, fatal MI even occurs with a penetrance of 100 % (KLYMIUK et al., 2012). While the respiratory phenotype is highly penetrant in CF patients, regardless of mutation class (DORFMAN et al., 2008), the occurrence of neonatal MI is usually associated with severe class I-III *CFTR* mutations in both alleles (KNOWLES & DRUMM, 2012; DUPUIS et al., 2016). Beyond that, studies in CF twins and siblings undoubtedly indicate a predominant impact of additional non-*CFTR* genetic modifiers on both, the contribution to and the protection against the occurrence of MI (BLACKMAN et al., 2006). In striking contrast to MI, the development of distal intestinal obstruction syndrome

(DIOS), a trait with clinical and pathologic similarities to MI in older CF patients, is not significantly influenced by modifier genes.

The study of ROZMAHEL et al. (1996) initially described the role of further genetic factors on the intestinal disease in a murine model of CF, revealing a region on chromosome 7 to apparently influence intestinal obstruction. Examining the corresponding region of the human genome, located on chromosome 19, indeed indicated an association between variants in this region and the risk for MI (ZIELENSKI et al., 1999), but a causative gene has never been identified and also in later work this finding was not confirmed. (BLACKMAN et al., 2006).

Genome-wide analyses revealed a few potential candidate loci, including polymorphisms in the genes coding for several members of the solute carrier family, either promoting (*SLC6A14* on chromosome X, *SLC9A3* on chromosome 13, *SLC26A9* on chromosome 1) or preventing the development of MI (*SLC4A4* on chromosome 4) (DORFMAN et al., 2009; SUN et al., 2012). Studies on murine models of CF clearly confirmed the protective effect of *SLC4A4* variants against obstruction (GAWENIS et al., 2007). HENDERSON et al. (2012) confirmed an association between *MSRA* on chromosome 8, encoding for methionine sulfoxide reductase A, as CF mice lacking functional *MSRA* exhibit decreased incidence of intestinal obstruction in comparison to CF mice with functional *MSRA*. Another examination provided evidence for MI-promoting locus on chromosome 12 and suggested the involvement of the gene adiponectin receptor 2 (*ADIPOR2*) (DORFMAN et al., 2009). Just recently, two new potential modifier genes of MI have been identified, namely ATPase H^+/K^+ transporting non-gastric alpha2 subunit (*ATP12A*) on chromosome 13, and a suggestive locus on chromosome 7 near serine protease 1 (*PRSS1*) (GONG et al., 2019).

For the porcine genome there are none potential modifiers that have been described so far, but the major contribution of additional non-*CFTR* genetic factors to neonatal intestinal obstruction in humans, as well as in murine models of CF, permits the assumption that also in CF pigs the severity of the intestinal disease might be modified.

Aims of my thesis

KLYMIUK et al. (2012) generated the first European CF pig model at the Chair for Molecular Animal Breeding and Biotechnology, LMU Munich, Germany. As the CF pig exhibit hallmark features of human CF disease, it turned out to be an indispensable model for different cooperation partners working on CF research. In order to regularly provide porcine tissue material to different partners, a *CFTR* breeding herd with heterozygous female and male $CFTR^{+/-}$ pigs has been established. Since an ever-present, severe intestinal phenotype with fatal MI constitutes the most prominent trait in CF piglets, the use of the pig as an animal model for CF is strongly limited. However, a previous thesis done at the Chair for Molecular Animal Breeding and Biotechnology describes the occurrence of three CF KO piglets (#2850, #3137 and #4424) that showed a clear improved intestinal phenotype (DMOCHEWITZ, 2016). In those piglets, the meconium has passed through the cecum and was stuck in middle to distal parts of the colon. Moreover, the CF-typical microcolon was not detectable, but the size and diameter of the colon was similar to a WT one. To clarify the relevance of the genetic background for this naturally occurring improvement, a genome-wide analysis has been performed. This SNP typing revealed, that there are two potential modifier loci on chromosome 10 (25.8–25.9 Mb) and on chromosome 16 (4.7–5.2 Mb), whereby the three rectified piglets were homozygous for a specific haplotype at both loci. It was therefore hypothesized that the severity of the intestinal phenotype might be improved in those CF piglets that show homozygosity for specific haplotypes on both chromosomes. Based on these findings, the aim of my thesis was to test the hypothesis of two independent loci on chromosomes 10 and 16 to protect CF piglets from MI. In the case the hypothesis was verified, the probability of an improved manifestation in CF piglets should be increased by enriching the frequency of the desired genotype on chromosomes 10 and 16 in the CF pig breeding herd. Eventually, an alternative evaluation of the genetic diversity was performed by genome-wide analysis on the basis of a larger population. Independently from the CF gut-phenotype, a variant respiratory phenotype was observed in some CF piglets during my thesis.

III. ANIMALS, MATERIALS AND METHODS

1. Animals

The animals included in this work were wild type (WT), heterozygous *CFTR*$^{+/-}$ and homozygous *CFTR*$^{-/-}$ (*CFTR* KO) piglets generated by selected breeding of heterozygous female and male *CFTR*$^{+/-}$. All animal experiments were approved by the responsible animal welfare authority (Regierung von Oberbayern, AZ 55.2-1-54-2532-70-12).

2. Materials

2.1. Chemicals

Acetic Acid (glacial)	Carl Roth, Karlsruhe, Germany
Bromophenolblue	Carl Roth
Chloroform (Trichloromethane)	Sigma-Aldrich, St. Louis, USA
EDTA (Ethylenediaminetetraacetic acid)	Carl Roth
Ethanol	Carl Roth
GelRed® Nucleic Acid Gel Stain	Biotium, Fremont, USA
Glutardialdehyde solution 25 %	Merck, Darmstadt, Germany
Glycerin (Glycerol)	Carl Roth and Sigma-Aldrich
HCl (Hydrochloric acid) 1 mol/L	Bernd Kraft GmbH, Duisburg, Germany
Methanol	Carl Roth
$MgCl_2$ (Magnesium chloride)	Thermo Fisher Scientific, Waltham, USA
NaOH (Sodium hydroxide 2N)	Carl Roth
Paraformaldehyde	Sigma-Aldrich
Perfadex®	XVIVO Perfusion, Gothenburg, Sweden
Sodium cacodylate trihydrate	Sigma-Aldrich
Tris (Tris-(hydroxymethyl)-aminomethane)	Carl Roth

TRIzol® Reagent	Thermo Fisher Scientific
Universal Agarose	Bio&SELL, Nuremberg, Germany

2.2. Devices

Chyo Petit Balance MK-2000B	YMC CO, Kyoto, Japan
Eppendorf Centrifuge 5417 R	Eppendorf, Hamburg, Germany
Eppendorf Centrifuge 5424	Eppendorf
Eppendorf Centrifuge 5910 R	Eppendorf
Gel documentation system	Bio-Rad Laboratories, Hercules USA
Grant JB Nova 5 water bath	Grant Instruments Ltd, Royston, UK
Hettich Rotina 380 R	Andreas Hettich GmbH & Co. KG, Tuttlingen, Germany
Incubator	Memmert GmbH & Co. KG, Schwabach, Germany
inoLab® pH meter 7110	WTW, Weilheim in Oberbayern, Germany
Labcycler	SensoQuest GmbH, Göttingen, Germany
LightCycler® 96	Roche Diagnostics, Basel, Switzerland
Mastercycler® gradient	Eppendorf
Microwave	DAEWOO, Gangnam, South Korea
Owl™ EasyCast™ B1A and B2 Mini gel electrophoresis systems	Thermo Fisher Scientific
Pipettes (1000 µL, 200 µL, 20 µL, 10 µL, 2 µL)	Gilson Inc, Middleton, USA
Polytron homogenizer PT 2500 E	Kinematica, Luzern, Switzerland
Power Pac 300 gel electrophoresis unit	Bio-Rad Laboratories
Power Station 300 gel electrophoresis unit	Labnet International, Edison,

	USA
RH Basic heating plate with magnetic stirrer	IKA, Staufen im Breisgau, Germany
Select vortexer	Select BioProducts, Edison, USA
SimpliNano™ spectrophotometer	Biochrom GmbH, Berlin; Germany
Spectrafuge 24D Microcentrifuge	Labnet International
Thermo-Shaker TS-100	bioSan, Riga, Latvia
Varioklav 400 autoclave	H+P Labortechnik GmbH, Oberschleißheim, Germany

2.3. Drugs, enzymes and oligonucleotides

Drugs

Altrenogest (Regumate®)	MSD Animal Health, Unterschleißheim, Germany
Azaperon (Stresnil®)	Elanco Animal Health, Bad Homburg, Germany
Choriongonadotropine (hCG) (Ovogest®)	MSD Animal Health
Cloprostenol (Estrumate®)	MSD Animal Health
Embutramid, Mebezonium, Tetracain (T61®)	MSD Animal Health
Ketamine hydrochloride (Ursotamin®)	Serumwerk Bernburg AG, Bernburg, Germany
Peforelin (Maprelin®)	Veyx-Pharma GmbH, Schwarzenborn, Germany

Enzymes

BigDye® Terminator v3.1	Applied Biosystems, Foster City, USA
DNase I, RNase-free (1 U/µL)	Thermo Fisher Scientific
FastStart Essential DNA Green Master	Roche Diagnostics

Herculase II Fusion DNA Polymerase	Agilent Technologies, Santa Clara, USA
HotStarTaq Plus DNA Polymerase (5 U/µL)	Qiagen, Hilden, Germany
Proteinase K, ready to use	Agilent Technologies
SuperScript™ III Reverse Transcriptase (200 U/µL)	Thermo Fisher Scientific
Qiagen® LongRange PCR Enzyme Mix (5 U/µL)	Qiagen
Uracil N-Glycosylase (UNG) (1 U/µL)	Thermo Fisher Scientific

Oligonucleotides

All oligonucleotides were designed with the PrimerQuest Tool by IDT and were purchased from Thermo Fisher Scientific.

Cg2f	**5′** AGA AGA GTA GGG CCT TTG GCA T **3′**
Cg1r	**5′** TGG CTG AAC TGA GCG AAC AAG T **3′**
Cg5r	**5′** AGC ACA TGT GGG TCT TAG AGT ACG **3′**
c105b1	**5′** TGG AGC CTC AGG CTG AAA GCA **3′**
c105g1	**5′** CCT TGA AGA AGC TCT GCA ATA C **3′**
c105g2	**5′** CCT TGA AGA AGC TCT GCA AAA C **3′**
c105g3	**5′** CCT TGA AGA AGC TCT GCA AAT C **3′**
c105g4	**5′** CCT TGA AGA AGC TCT GCT ATA C **3′**
c105g5	**5′** CCT TGA AGA AGC TCT GCA ATT C **3′**
c105g6	**5′** CCT TGA AGA AGC TCT GCA TTA C **3′**
c105g7	**5′** TGG AGC CTC AGG CTG AAA GCG **3′**
c105g8	**5′** TGG AGC CTC AGG CTG AAA CAG **3′**
c167b1	**5′** CAA GTT TAT GGT TCA GAG AAC CA **3′**
c167g1	**5′** CTT TAG AGT TAT AGA AGC TCA GC **3′**
c167b2	**5′** CAA GTT TAT GGT TCA GAG AAG CA **3**
c167b3	**5′** CAA GTT TAT GGT TCA GAG ATG CA **3′**
c169b1	**5′** TCT ACT CTC AGG AAT GAG ATA CG **3′**
c169g1	**5′** TTG GGT CTC ATT CAT AAG GGG AT **3′**

c104f1	**5′** GGG AGG AGG AGC CCT CAT AA **3′**
c104r1	**5′** GTG ATT GGT GCC TTG ACT GC **3′**
c104f2	**5′** CTG TGG CCC TGT CCC TTA TG **3′**
c104r2	**5′** TTG GTG CCT TGA CTG CCT AC **3′**
c105f1	**5′** AGT GCT AGG CAG CAA TGT GT **3′**
c105r1	**5′** GGC ATC AGA TGT CCA AGG CT **3′**
c105f2	**5′** CTA GCT CCC ATC CAC ACT GC **3′**
c105r2	**5′** AGC TTA GGG AGC CCA TGA GA **3′**
c105f3	**5′** TGT GAG GAC ATA TCC TCC **3′**
c105r3	**5′** CAT TGC CAT GGT GAG CAG C **3′**
c167f1	**5′** GGT AGC AGC TTC CCT GAT TT **3′**
c167r1	**5′** CTC TTG GTG TGG ATG CTA TCT T **3′**
c167f2	**5′** GTG GTT TCT TGG TGA GCT CTT A **3′**
c167r2	**5′** CCA TAA AGG GAG GCT TAG TGA TG **3′**
c169f1	**5′** CTA TCC CTG CCC TTG CTC AG **3′**
c169r1	**5′** CAA CCC CTA GTG TGG GAA CC **3′**
c169f2	**5′** CCC ATC ATG GCA CAG TAG TT **3′**
c169r2	**5′** CTT CCC ATT TCT TTG GGT ACT TTC **3′**
c169f3	**5′** TCA CAA ATT AGC ACA GTA CC **3′**
c169r3	**5′** TGT CTT AGT GAG TTC AGG C **3′**
ch10f1	**5′** GCC CTG CAT GAA TGA ATG ACC **3′**
ch10r1	**5′** TCT CGG AGT TCC CAC CAT GT **3′**
ch10f2	**5′** CTT TGC TGA CAG GGA CAC TCA **3′**
ch10r2	**5′** TGG AGG CAC GGG TTC AAT C **3′**
ch10f3	**5′** GAA TGA CCC AGA GAT GGA GAA G **3′**
ch10r3	**5′** AGA TGT GTG ATG GCA GGT AAA **3′**
ch10f4	**5′** ACA GCA ACA CCA GAT CCG AG **3′**
ch10r4	**5′** TGT GTG ATT GGG TCT TCG GG **3′**
ch10f5	**5′** TTA TGG GTG CAG AGC AGT GG **3′**
ch10r5	**5′** AGT CAG GCT CGT CCT GAG TA **3′**
ch10f6	**5′** ACA CCA GTG CCC AAA TAG AG **3′**
ch10r6	**5′** GAG AGA TGA CCC AAG CCA AAT A **3′**
ch10s11	**5′** CAC ACC CTA TTC CAC TAA G **3′**
ch10s12	**5′** GGA AAG AAT ATT GAG AAG TGC **3′**
ch10s13	**5′** TCT CTC TGT GAC TGA GAC AGC **3′**

ch10s14	**5′** CTT GCA CAG AAC ACA GAG G **3′**
ch10s21	**5′** TGA CTT CAA GCT GTG TGA CC **3′**
ch10s22	**5′** AGC TGA TAA TAG TCT CTC C **3′**
ch10s23	**5′** GAT TTA CCA AGC TAG TGG AC **3′**
ch10s24	**5′** CGT CTT CCA ATA GAT TCC GC **3′**
ch10s25	**5′** TAC ACT AAT AAT GCC AGG **3′**
ch10s61	**5′** AAG ATA GCG TTT CTA GCA G **3′**
ch10s62	**5′** ATA AGC AGT TAA CCA TTG C **3′**
ch10s63	**5′** AGA TCA CCT GCT GCC CTG AG **3′**
ch10s64	**5′** CTC ACA GGC TGT TGT TCA G **3′**
ch10s71	**5′** AGC TGC CTT ATC AAG CTC TG **3′**
ch10s72	**5′** ATG CTG TTG TCG CAT GCC **3′**
ch10s73	**5′** TGG AGA GTC CTG TAA AGT GC **3′**
ch10s74	**5′** GAT CCT GCA TTC CTG TGA GC **3′**
nek1f	**5′** CTC TCA GTG CTA CAC AGG ATT T **3′**
nek1r	**5′** GCA ACC TCA TGG TTC CTA GTT **3′**
nek2f	**5′** CCA ACC GAA TCC AAC AAC ATA TC **3′**
nek2r	**5′** CTG TCA GAC CTC CAT TAT CAC C **3′**
nek3f	**5′** TGA GTC TAT CGC CCT CCC AA **3′**
nek3r	**5′** GGA ACA GAG GCA GTC TCC AC **3′**
nek4f	**5′** CTG GTG CGG TGT AAG GAA GT **3′**
nek4r	**5′** CTG TCG TGT CTC GCT GAA CT **3′**
nek5f	**5′** GGT CTT AGC ATT GCA GCT TTC **3′**
nek5r	**5′** ATA CGG GCT AAA GGT AGG TTT C **3′**
nek6f	**5′** GCA CAC ATT ACC CAA GGC **3′**
nek6r	**5′** GTA CAA TCA TGA GTA GAG C **3′**
nek7f	**5′** TGA ATT GAT ATG AGA AGC AG **3′**
GAPqf1	**5′** CAG AAC ATC ATC CCT GCT TC **3′**
GAPqr1	**5′** GCT TCA CCA CCT TCT TGA TG **3′**
gapdhF1	**5′** CAG CAA TGC CTC CTG TAC CA **3′**
gapdhR1	**5′** GAT GCC GAA GTT GTC ATG GA **3′**
tbpF	**5′** GAT GGA CGT TCG GTT TAG G **3′**
tbpR	**5′** AGC AGC ACA GTA CGA GCA A **3′**
ywhazF	**5′** ATG CAA CCA ACA CAT CCT ATC **3′**
ywhazR	**5′** GCA TTA TTA GCG TGC TGT CTT **3′**

Lars2f **5′** AAC CTG AAC AAG TTT GAT GAA G **3′**
Lars2ra **5′** AAG GCA AGT CCA CAG AAG GC **3′**

2.4. Buffers and solutions

Water deionized in a Millipore device (Barnstead™ EASYpure™ II, Wilhelm Werner GmbH, Leverkusen, Germany) and termed as aq. bidest. was used as solvent. All buffers and other solutions were stored at room temperature if not indicated otherwise

Buffers and solutions for PCR and agarose gels

DNA loading buffer (10×)
10 % glycerol in aq. bidest.
1 spatula tip of Bromophenol Blue
Add 0.5 M NaOH until color turns blue
Stored aliquoted at 4 °C.

dNTP-mix
2 mM dATP, dCTP, dGTP, dTTP
Mixed in aq. bidest.
Stored aliquoted at -20 °C.

TAE buffer (50×)
242 g 2 M Tris
100 mL 0.5 M EDTA (pH 8.0)
57 mL acetic acid (glacial)
Ad 1000 mL aq. bidest.
Buffer solution was filtrated and autoclaved for storage.
Before usage the buffer solution was diluted to single concentration.

Gene Ruler™ 1 kb DNA
100 µL Gene Ruler™ 1 kb DNA
100 µL 6x loading dye

400 µL aq. bidest.
Stored aliquoted at -20 °C.

Sequencing buffer (5×)
17.5 mL 1 M Tris/HCl (pH 9.0)
125 µL 1 M $MgCl_2$
Ad 50 mL aq. bidest.
Stored aliquoted at -20 °C.

Buffers and solutions for RNA isolation and cDNA synthesis

10 mM Tris/HCl, pH 8.0
10 mM Tris
Adjust pH to 8.0 with HCl

10 mM dNTPs
10 mM dATP, dCTP, dGTP, dTTP
Mixed in aq. bidest.
Stored aliquoted at -20 °C.

Buffers and solutions for fixation

Methacarn
60 % methanol
30 % chloroform
10 % acetic acid (glacial)
Prepared freshly, stored in the dark.

4 % PFA solution
4 % PFA
1× PBS buffer
Solution was heated to 50 °C in a water bath and was vigorously shaken several times. For complete dissolution of PFA, 200 µL of 5 M NaOH were added to raise the pH. After cooling down to room temperature, the

solution was adjusted to pH 7.4 with HCl, filtered and stored at 4 °C.

Modified Karnovsky fixative

2 % PFA

2.5 % of glutardialdehyde solution 25 %

Mixed in 0.05 M sodium cacodylate buffer, pH 7.2

Stored aliquoted at -20 °C.

0.05 M sodium cacodylate buffer, pH 7.2

Sodium cacodylate trihydrate

Dissvoled in aq. bidest

Adjust pH to 7.2 with HCl

Stored aliquoted at -20 °C.

2.5. Kits

Double Pure Kombi Kit	Bio&SELL
Easy-DNA™ Kit	Invitrogen, Carlsbad, USA
Nexttec™ Genomic DNA Isolation Kit From Tissue and Cells	Nexttec Biotechnologie GmbH, Leverkusen, Germany

2.6. Other reagents

0.1 M DTT	Thermo Fisher Scientific
10× CoralLoad PCR buffer	Qiagen
10× DNase reaction buffer with $MgCl_2$	Thermo Fisher Scientific
10× LongRange PCR Buffer	Qiagen
5× Herculase II Reaction Buffer	Agilent Technologies
5× Reaction Buffer for RT	Thermo Fisher Scientific
6× DNA loading dye	Thermo Fisher Scientific
dNTPs (dATP, dCTP, dGTP, dTTP)	Thermo Fisher Scientific
Gene Ruler™ (1 kb DNA ladder)	Thermo Fisher Scientific
Oligo$(dT)_{18}$ primer (0.5 µg/µL)	Thermo Fisher Scientific

2.7. Software

BioEdit Sequence Alignment Editor

FinchTV Version 1.3.1, Geospiza Inc.

LightCycler® 96 Application Software 1.1.0.1320

3. Methods

3.1. Sampling of piglets

Autopsy of piglets

For molecular analyses and for experiments performed by cooperation partners, samples were taken from WT and *CFTR*$^{-/-}$ piglets. For this purpose, the piglets were anaesthetized i.m. with ketamine hydrochloride (2 mL/10 kg BW) and azaperone (0.5 mL/kg BW), followed by euthanasia via i.c. injection of Embutramid, Mebezonium, Tetracain (1 mL/10 kg BW).

Preparation of the airways

After euthanasia, the thorax was opened and, starting from the larynx, the connected trachea, the lungs and the heart were explanted. Then the heart, the esophagus, attached nerves and big blood vessels were removed. In pulmonary tissue the pH was measured for experiments on alternative airway chloride channels, performed by Karl Kunzelmann and Roberta Benedetto from the Institute for Physiology at the University of Regensburg. For experiments on mucociliary transport, performed by Anna Ermund from the Mucin Biology Group at the University of Gothenburg, Sweden, all pulmonary tissue was carefully pulled away with anatomical forceps until only the trachea and the bronchial tree were left. Meanwhile, the airways were repeatedly bathed in Perfadex® transport solution, which has been adjusted to pH 7.4 with 1 M Tris solution. For histopathological exploration, tracheal and bronchial tissue were put in 4 % PFA and immediately sent to Lars Mundhenk from the Institute of Animal Pathology at the Free University of Berlin, Germany. For scanning electron microscopy (SEM), the airways were fixed in modified Karnovsky fixative for 24 hours. After transferring the samples to 0.05 M sodium cacodylate buffer, pH 7.2, they were sent to the Mucin Biology group in Gothenburg for further investigation. For RNA isolation purposes, tissue samples were cut into small pieces and quick-frozen on dry ice as fast as possible to prevent degradation. Samples were transferred to 1.5 mL Eppendorf tubes and stored at -80 °C until further examination. After the sampling of each tissue, the surgical instruments

were disinfected with 70 % ethanol to prevent contamination. The airways were photographed to document the phenotypical manifestation.

Preparation of the intestine

To document the severity of the intestinal phenotype, pictures were taken of the opened abdomen, the intestinal convolute in whole and the intestine laid out in full length. For histopathological examination tissue samples were collected from the pancreas, liver, gall bladder, different parts of the intestine (duodenum, jejunum, ileum, caecum, colon ascendens divided into gyri centripetales and gyri centrifugales, colon descendens and rectum), and in the case of male piglets also the testicles. For fixation, the tissue samples were put in either 4 % PFA or methacarn solution. Samples in methacarn fixative were stored in fridge, protected from light exposure, and transferred to 100 % methanol after approximately 48 hours. For histological investigation PFA- and methacarn-fixed samples were sent to Lars Mundhenk from the Institute of Animal Pathology at the Free University of Berlin, Germany.

3.2. Analysis at molecular level

3.2.1. Genotyping of pigs

Due to the fatal MI, health status of newborn *CFTR*$^{-/-}$ piglets deteriorates shortly after birth. Therefore, it was necessary to select relevant animals by fast genotyping, including fast isolation of DNA and time-saving genotyping Polymerase Chain Reaction (PCR). This was done for the *CFTR* genotype, as well as for the candidate regions on chromosomes 10 and 16 that presumably improve the intestinal phenotype.

Isolation of genomic DNA

From freshly cut tails of newborn piglets, genomic DNA was isolated using the nexttec™ Genomic DNA Isolation Kit from Tissue and Cells according to the manufacturer's instructions. A small amount of tissue (5-30 mg) was transferred

to a 1,5 mL Eppendorf tube containing a lysis buffer, which is composed of three included components, and then incubated in a thermomixer with 1200 rpm at 60 °C for at least 30 min. To ensure proper lysis of the tissue 3 µL DTT were added and the sample was vortexed vigorously several times during incubation time. The lysate was then transferred to an equilibrated cleaning column and centrifuged for 1 min at 700 rcf. The occurred eluate containing the purified DNA was immediately used for subsequent PCR.

For genome-wide analysis, genomic DNA was isolated according to the manufacturer's instructions described in "protocol #8 - isolation of DNA from mouse tails" from the Easy-DNA^{TM} Kit. The obtained DNA pellet was air dried for 6 minutes to remove residual ethanol and resuspended in 100 µL of 10 mM Tris/HCl, pH 8.0. The DNA concentration was finally diluted to 70 ng/µL.

PCR

A robust PCR for *CFTR* genotyping has been established in previous work (doctoral thesis of Michaela Désirée Dmochewitz, done at the Chair for Molecular Animal Breeding and Biotechnology, LMU Munich, Germany) and was used for genotyping each litter. Table 1 and Table 2 show the master mix composition and the cycler protocol. To rapidly identify the desired constellation at the candidate regions on chromosomes 10 and 16, PCRs for specific markers in the modifier loci were established and optimized. First, the proposed markers were confirmed by sequencing of amplified PCR products using primers indicated in Table 3. The applied master mix composition and the running conditions are shown in Table 4 and Table 5. Then, marker-specific PCRs were developed for chosen sites, using one primer specifically binding to one of the marker variants and one unspecific primer (see Table 6). For each of the chosen sites, one PCR was established for each of the marker variants. PCRs were either conducted with the HotStarTaq Plus DNA Polymerase kit or with the Herculase II Fusion DNA Polymerase kit. The PCR components were mixed on ice to a final volume of 20 µL (HotStarTaq) or 25 µL (Herculase) in 0.2 mL reaction tubes.

Table 1: Master mix composition for *CFTR*-genotyping PCRs.

10× CoralLoad PCR buffer	2.0 µL
dNTPs (2 mM)	2.0 µL
Primer f (10 µM)	0.4 µL
Primer r (10 µM)	0.4 µL
HotStarTaq (5 U/µL)	0.2 µL
aq. dest.	13 µL
DNA template	2 µL

Table 2: Cycler protocol for *CFTR*-genotyping PCRs.

Denaturation	95 °C	5 min	
Denaturation	95 °C	20 s	35×
Annealing	56 °C	20 s	
Elongation	72 °C	30 s	
Final elongation	72 °C	5 min	
Termination	4 °C	5 min	

Table 3: Primers tested for amplification and sequencing of marker regions.

c104f1	**5′** GGG AGG AGG AGC CCT CAT AA **3′**
c104r1	**5′** GTG ATT GGT GCC TTG ACT GC **3′**
c104f2	**5′** CTG TGG CCC TGT CCC TTA TG **3′**
c104r2	**5′** TTG GTG CCT TGA CTG CCT AC **3′**
c105f1	**5′** AGT GCT AGG CAG CAA TGT GT **3′**
c105r1	**5′** GGC ATC AGA TGT CCA AGG CT **3′**
c105f2	**5′** CTA GCT CCC ATC CAC ACT GC **3′**
c105r2	**5′** AGC TTA GGG AGC CCA TGA GA **3′**
c105f3	**5′** TGT GAG GAC ATA TCC TCC **3′**
c105r3	**5′** CAT TGC CAT GGT GAG CAG C **3′**
c167f1	**5′** GGT AGC AGC TTC CCT GAT TT **3′**
c167r1	**5′** CTC TTG GTG TGG ATG CTA TCT T **3′**
c167f2	**5′** GTG GTT TCT TGG TGA GCT CTT A **3′**
c167r2	**5′** CCA TAA AGG GAG GCT TAG TGA TG **3′**
c169f1	**5′** CTA TCC CTG CCC TTG CTC AG **3′**
c169r1	**5′** CAA CCC CTA GTG TGG GAA CC **3′**
c169f2	**5′** CCC ATC ATG GCA CAG TAG TT **3′**
c169r2	**5′** CTT CCC ATT TCT TTG GGT ACT TTC **3′**
c169f3	**5′** TCA CAA ATT AGC ACA GTA CC **3′**

Table 4: Master mix composition for marker PCRs.

5× Herculase II Reaction Buffer	5.0 µL
dNTPs (2 mM)	2.5 µL
Primer f (10 mM)	0.4 µL
Primer r (10 mM)	0.4 µL
Herculase II	0.2 µL
aq. dest.	15.5 µL
DNA template	1 µL

Table 5: Cycler protocol for marker PCRs.

Denaturation	95 °C	5 min	
Denaturation	94 °C	20 s	35×
Annealing	58 °C	20 s	
Elongation	72 °C	1 min	
Final elongation	72 °C	10 min	
Termination	4 °C	5 min	

Table 6: Primers tested for marker-specific genotyping PCRs.

c105b1	**5′** TGG AGC CTC AGG CTG AAA GCA **3′**
c105g1	**5′** CCT TGA AGA AGC TCT GCA ATA C **3′**
c105g2	**5′** CCT TGA AGA AGC TCT GCA AAA C **3′**
c105g3	**5′** CCT TGA AGA AGC TCT GCA AAT C **3′**
c105g4	**5′** CCT TGA AGA AGC TCT GCT ATA C **3′**
c105g5	**5′** CCT TGA AGA AGC TCT GCA ATT C **3′**
c105g6	**5′** CCT TGA AGA AGC TCT GCA TTA C **3′**
c105g7	**5′** TGG AGC CTC AGG CTG AAA GCG **3′**
c105g8	**5′** TGG AGC CTC AGG CTG AAA CAG **3′**
c105f1	**5′** AGT GCT AGG CAG CAA TGT GT **3′**
c105r1	**5′** GGC ATC AGA TGT CCA AGG CT **3′**
c105f2	**5′** CTA GCT CCC ATC CAC ACT GC **3′**
c105r2	**5′** AGC TTA GGG AGC CCA TGA GA **3′**
c105f3	**5′** TGT GAG GAC ATA TCC TCC **3′**
c105r3	**5′** CAT TGC CAT GGT GAG CAG C **3′**
c167b1	**5′** CAA GTT TAT GGT TCA GAG AAC CA **3′**
c167g1	**5′** CTT TAG AGT TAT AGA AGC TCA GC **3′**
c167b2	**5′** CAA GTT TAT GGT TCA GAG AAG CA **3′**
c167b3	**5′** CAA GTT TAT GGT TCA GAG ATG CA **3′**
c167f1	**5′** GGT AGC AGC TTC CCT GAT TT **3′**

c167r1	**5′** CTC TTG GTG TGG ATG CTA TCT T **3′**
c167f2	**5′** GTG GTT TCT TGG TGA GCT CTT A **3′**
c167r2	**5′** CCA TAA AGG GAG GCT TAG TGA TG **3′**
c169b1	**5′** TCT ACT CTC AGG AAT GAG ATA CG **3′**
c169g1	**5′** TTG GGT CTC ATT CAT AAG GGG AT **3′**
c169f1	**5′** CTA TCC CTG CCC TTG CTC AG **3′**
c169r1	**5′** CAA CCC CTA GTG TGG GAA CC **3′**
c169f2	**5′** CCC ATC ATG GCA CAG TAG TT **3′**
c169r2	**5′** CTT CCC ATT TCT TTG GGT ACT TTC **3′**
c169f3	**5′** TCA CAA ATT AGC ACA GTA CC **3′**
c169r3	**5′** TGT CTT AGT GAG TTC AGG C **3′**

Agarose gel electrophoresis

For agarose gel electrophoresis, a 1 % agarose gel was produced by heating 1× TAE buffer with 1 g/100 mL Universal Agarose in a microwave till agarose completely dispersed. After cooling down to about 60 °C, GelRed® was added in a concentration of 5.0 µL/100 mL agarose gel and then the mixture was poured into an electrophoresis chamber. After solidifying, the chamber was filled with 1× TAE buffer as running buffer. PCR samples and 4.5 µL of Gene Ruler™ 1 kb DNA were pipetted into individual gel slots. After separating in the electric field, DNA fragments were visualized under UV light. In order to verify a correct amplification of the PCR product, bands of the correct size were excised from the agarose gel, followed by elution and sequencing of the DNA.

DNA-elution

DNA was eluted according to the manufacturer's instructions described in "protocol 1: isolation of DNA from agarose gels" from the Bio&Sell Double Pure Kombi Kit. To increase the final DNA yield, 30 µL of elution buffer, preheated to 50 °C, were used. The successful extraction of the DNA was confirmed by mixing

5 µL eluted DNA
2.5 µL 10× DNA loading buffer
10 µL aq. bidest.

and loading this compound as well as 4.5 µL Gene Ruler™ 1 kb DNA on prepared 1 % agarose gel. The eluted DNA was stored at -20 °C or immediately

used for following sequencing PCR.

Sequencing PCR

Sanger sequencing was performed with the BigDye® Terminator v3.1 Cycle Sequencing Kit. The master mix components (see Table 7) were mixed on ice to a final volume of 10 µL in 0.2 mL reaction tubes. Each DNA amplicon was sequenced either with the amplification and/or with internal sequencing primers. Table 8 indicates the running conditions for sequencing PCRs.

Table 7: Master mix composition for sequencing PCRs.

5× Sequencing buffer	4 µL
BigDye®	1 µL
Primer (10 µM)	1 µL
DNA template	4 µL

Table 8: Cycler protocol for sequencing PCRs.

Denaturation	95 °C	1 min	
Denaturation	95 °C	5 s	40×
Annealing	54 °C	10 s	
Elongation	60 °C	4 min	
Termination	4 °C	15 min	

Purification of sequencing reactions

Sequencing products were purified by ethanol precipitation. For this purpose, 2.5 µL of 125 mM EDTA and 30 µL of 100 % EtOH were added to the amplified PCR. This mixture was then transferred to a fresh 1.5 mL Eppendorf tube and incubated on ice for 15 min. The samples were centrifuged at 13,000 rpm for 30 min at 4 °C and the supernatant was carefully removed with a pipette. The pellet was washed in 150 µL of 70 % EtOH. After centrifugation at 13,000 rpm for 2.5 min, the supernatant was removed again. The pellet was air-dried for 6 min, resuspended in 30 µL aq. dest. and finally transferred to a 96-well plate for capillary electrophoresis. The latter was performed at the Genome Analysis

Center, Helmholtz Zentrum Munich, Germany. Electropherograms were compared and evaluated with FinchTV Version 1.3.1 and the BioEdit Sequence Alignment Editor.

3.2.2. Examination of candidate regions

Within the candidate region on chromosome 10, three different genetic elements were investigated in more detail by sequencing of amplified PCR products. Table 9 lists all primers that were tested for the amplification and sequencing of all three elements. PCRs were either conducted with the Herculase II Fusion DNA Polymerase kit or with the Qiagen® LongRange PCR kit. The optimal conditions for each PCR are presented in the results section. Amplified PCR products were sequenced via the Sanger approach following the same protocol as described under 3.2.1. "Genotyping of pigs" above.

Table 9: Primers tested for amplification and sequencing of candidate region on chromosome 10.

ch10f1	**5′** GCC CTG CAT GAA TGA ATG ACC **3′**
ch10r1	**5′** TCT CGG AGT TCC CAC CAT GT **3′**
ch10f2	**5′** CTT TGC TGA CAG GGA CAC TCA **3′**
ch10r2	**5′** TGG AGG CAC GGG TTC AAT C **3′**
ch10f3	**5′** GAA TGA CCC AGA GAT GGA GAA G **3′**
ch10r3	**5′** AGA TGT GTG ATG GCA GGT AAA **3′**
ch10f4	**5′** ACA GCA ACA CCA GAT CCG AG **3′**
ch10r4	**5′** TGT GTG ATT GGG TCT TCG GG **3′**
ch10f5	**5′** TTA TGG GTG CAG AGC AGT GG **3′**
ch10r5	**5′** AGT CAG GCT CGT CCT GAG TA **3′**
ch10f6	**5′** ACA CCA GTG CCC AAA TAG AG **3′**
ch10r6	**5′** GAG AGA TGA CCC AAG CCA AAT A **3′**
ch10s11	**5′** CAC ACC CTA TTC CAC TAA G **3′**
ch10s12	**5′** GGA AAG AAT ATT GAG AAG TGC **3′**
ch10s13	**5′** TCT CTC TGT GAC TGA GAC AGC **3′**
ch10s14	**5′** CTT GCA CAG AAC ACA GAG G **3′**
ch10s21	**5′** TGA CTT CAA GCT GTG TGA CC **3′**
ch10s22	**5′** AGC TGA TAA TAG TCT CTC C **3′**
ch10s23	**5′** GAT TTA CCA AGC TAG TGG AC **3′**

ch10s24	**5′** CGT CTT CCA ATA GAT TCC GC **3′**
ch10s25	**5′** TAC ACT AAT AAT GCC AGG **3′**
ch10s61	**5′** AAG ATA GCG TTT CTA GCA G **3′**
ch10s62	**5′** ATA AGC AGT TAA CCA TTG C **3′**
ch10s63	**5′** AGA TCA CCT GCT GCC CTG AG **3′**
ch10s64	**5′** CTC ACA GGC TGT TGT TCA G **3′**
ch10s71	**5′** AGC TGC CTT ATC AAG CTC TG **3′**
ch10s72	**5′** ATG CTG TTG TCG CAT GCC **3′**
ch10s73	**5′** TGG AGA GTC CTG TAA AGT GC **3′**
ch10s74	**5′** GAT CCT GCA TTC CTG TGA GC **3′**
nek1f	**5′** CTC TCA GTG CTA CAC AGG ATT T **3′**
nek1r	**5′** GCA ACC TCA TGG TTC CTA GTT **3′**
nek2f	**5′** CCA ACC GAA TCC AAC AAC ATA TC **3′**
nek2r	**5′** CTG TCA GAC CTC CAT TAT CAC C **3′**
nek3f	**5′** TGA GTC TAT CGC CCT CCC AA **3′**
nek3r	**5′** GGA ACA GAG GCA GTC TCC AC **3′**
nek4f	**5′** CTG GTG CGG TGT AAG GAA GT **3′**
nek4r	**5′** CTG TCG TGT CTC GCT GAA CT **3′**
nek5f	**5′** GGT CTT AGC ATT GCA GCT TTC **3′**
nek5r	**5′** ATA CGG GCT AAA GGT AGG TTT C **3′**
nek6f	**5′** GCA CAC ATT ACC CAA GGC **3′**
nek6r	**5′** GTA CAA TCA TGA GTA GAG C **3′**
nek7f	**5′** TGA ATT GAT ATG AGA AGC AG **3′**

3.2.3. RT-PCR

For expression analysis, RNA was isolated from porcine tissue samples and subsequently reversely transcribed into cDNA. *CFTR* expression was compared to the housekeeping genes *GAPDH*, *TBP* and *YWHAZ*.

RNA isolation

For isolation of tRNA from tissue samples stored at -80 °C, the acid guanidinium thiocyanate-phenol-chloroform extraction with TRIzol® was performed. To avoid possible RNase contamination all working steps were done under a separate hood. At first tissue was powdered in liquid nitrogen by using a hammer and mortar. 50-100 mg of tissue powder was then transferred to a 2 mL Eppendorf tube filled

with 1 mL TRIzol® and immediately homogenized for 10 s at 30,000 rpm with the Polytron homogenizer PT 2500 E. After each sample, the grinder was cleaned carefully with aq. dest. for several times to avoid carry-over of contaminating material. After centrifugation at 12,000 rcf for 10 min at 4 °C, the clear supernatant was transferred to a new 1.5 mL Eppendorf tube and RNA was isolated according to the manufacturer's protocol. RNA concentration was determined with a spectrophotometer by measuring the absorbance at a wavelength of 260 nm and 280 nm. Prepared and measured RNA samples were stored at -80 °C.

DNase digestion

In order to eliminate a possible contamination with genomic DNA (gDNA), RNA samples were treated with DNase I, RNase-free, an endonuclease that digests single- and double-stranded DNA.

2 µL	10× reaction buffer with $MgCl_2$
1 µL	DNase I, RNase-free
16 µL	aq. dest.
1 µL	RNA (500 ng/µL)

were mixed together and incubated for 30 min at room temperature. Afterwards 1 µL of 25 mM EDTA was added to each sample and incubated at 65 °C for 10 min to inactivate DNase. From each sample 10 µL were used for confirmation of complete DNA digestion.

cDNA synthesis

The residual 10 µL of the DNase digest were applied for first-strand cDNA synthesis, performed with SuperScript™ III Reverse Transcriptase. cDNA synthesis was implemented according to the manufacturer's instructions, whereby $Oligo(dT)_{18}$ was used as primer. The obtained cDNA was stored at -20 °C until further processing. The integrity of the obtained cDNA was verified by amplification of the housekeeping gene *GAPDH*. The master mix composition as well as the running conditions for this PCR are shown in Table 10 and Table 11.

Table 10: Master mix composition for cDNA-verification PCRs.

10× CoralLoad PCR buffer	2.0 µL
dNTPs (2 mM)	2.0 µL
Primer f (10 µM)	0.4 µL
Primer r (10 µM)	0.4 µL
HotStarTaq (5 U/µL)	0.1 µL
aq. dest.	14.1 µL
DNA template	1 µL

Table 11: Cycler protocol for cDNA-verification PCRs.

Denaturation	95 °C	5 min	
Denaturation	95 °C	20 s	35×
Annealing	58 °C	20 s	
Elongation	72 °C	45 s	
Final elongation	72 °C	5 min	
Termination	4 °C	5 min	

qPCR

The *CFTR* expression in tissue samples of WT, *CFTR*$^{-/-}$ and respiratory improved *CFTR*$^{-/-}$ piglets was determined by comparing to housekeeping genes *GAPDH*, *TBP* and *YWHAZ*. Primers for different sets of qPCR have been tested in endpoint PCR in previous work (doctoral thesis of Michaela Désirée Dmochewitz, done at the Chair for Molecular Animal Breeding and Biotechnology, LMU Munich, Germany). My work was based on these conditions, but running conditions were optimized, whereby the optimal conditions are presented in the results section. The quality of each cDNA sample was tested by determining the amplification efficacy in a serial dilution with primers for *GAPDH*. For this purpose, five serial 1:8 dilutions were prepared:

1:8	10 µL cDNA	+	70 µL of 10 mM Tris/HCl, pH 8.0
1:16	40 µL of 1:8 dilution	+	40 µL of 10 mM Tris/HCl, pH 8.0
1:32	20 µL of 1:8 dilution	+	60 µL of 10 mM Tris/HCl, pH 8.0
1:64	10 µL of 1:8 dilution	+	70 µL of 10 mM Tris/HCl, pH 8.0
1:128	5 µL of 1:8 dilution	+	75 µL of 10 mM Tris/HCl, pH 8.0

Each dilution was run in duplicates and a non-template control (NTC) served as a negative control. The qPCR master mix (see Table 12) was mixed on ice and 10

µL were used for each well in a LightCycler® 480 Multiwell Plate 96. Table 13 indicates the running conditions for qPCR. The PCR efficacy was calculated by the LightCycler® 96 Application Software and cDNA showing improper amplification was excluded from further analysis and newly synthesized from DNase-digested RNA. Appropriate cDNA was used at the 1:16 dilutions and C_t-values (threshold cycle) for *CFTR*, *GAPDH*, *TBP* and *YWHAZ* were determined in duplicates. Relative *CFTR* expression was calculated as ΔC_t-levels.

Table 12: Master mix composition for qPCRs.

FastStart Essential DNA Green Master	6.25 µL
UNG	0.075 µL
Primer f (10 µM)	xx µL
Primer r (10 µM)	xx µL
aq. bidest.	ad 10 µL
Template (cDNA)	2.5 µL

Table 13: Cycler protocol for qPCRs.

UNG activation	50 °C	2 min	
Denaturation	95 °C	10 min	
Denaturation	95 °C	10 s	45×
Annealing	xx °C	90 s	
Melting	95 °C	10 s	
	65 °C	1 min	
	97 °C	1 s	
Cooling	37 °C	30 s	

IV. RESULTS

1. The improved intestinal phenotype in *CFTR*$^{-/-}$ piglets

The relevance of the genetic background for an improved intestinal phenotype was initially evaluated by a genome-wide survey of single nucleotide polymorphism (SNP) variations using the PorcineSNP60 DNA Analysis Kit v2 (Illumina, San Diego, USA). SNP typing was implemented by Doris Seichter, Tierzuchtforschung e.V. München (TZF Grub, Germany) and data were analyzed by Sophie Rothammer and Ivica Medugorac, Population Genomics Group, Department of Veterinary Sciences, LMU Munich, Germany. This SNP typing revealed that there are two potential modifier loci on chromosome 10 (25.8–25.9 Mb) and on chromosome 16 (4.7–5.2 Mb), whereby the three rectified piglets (#2850, #3137 and #4424) were homozygous for a specific haplotype at both loci. The findings are described in more detail in the doctoral thesis of Michaela Désirée Dmochewitz, done at the Chair for Molecular Animal Breeding and Biotechnology, LMU Munich, Germany. First goal of my thesis was to check the hypothesis of two modifying loci on chromosomes 10 and 16. For this, it was necessary to increase the frequency of the desired genotype constellation in the breeding herd and then to produce the CF piglets with this constellation at larger scale. All available pigs of the breeding herd were screened for the potential modifier loci on chromosome 10 and on chromosome 16. Marker-specific genotyping-PCRs were established to rapidly identify the desired genotype constellation.

1.1. Evaluation of candidate regions on chromosomes 10 and 16

1.1.1. Marker-based selection of breeding animals

The desired haplotype constellation on chromosome 10 was covered by 6 marker positions and on chromosome 16 by 10 marker positions. To avoid costly and time-consuming SNP-typing for each breeding animal and each CF piglet, I aimed at establishing marker-specific PCRs that discriminate the desired haplotype “g/g”

from any of the non-desired constellations. Via genome-wide association study (GWAS) the three CF KO piglets with the improved intestinal phenotype were compared to all CF KO littermates as well as with any parents and grandparents for which samples were available. For the two candidate loci on chromosome 10 and on chromosome 16 all haplotype patterns were compared (see Figure 1). In both cases only one specific haplotype (haplotype 1) is postulated to be beneficial for the manifestation of an improved intestinal phenotype in *CFTR*$^{-/-}$ piglets, all other haplotypes are presumably unfavorable. To distinguish the desired haplotype from unwanted ones with a minimal effort, markers on positions 1, 4, 5 or 6 for chromosome 10 and markers on positions 7 and 9 for chromosome 16 must be applied. All potential markers were examined in the context of the porcine reference genome; marker 4 on chromosome 10 turned out to be an artefact, whereas the other positions were identified in the reference genome. We decided to use marker 5 as indicative for chromosome 10 and a combination of markers 7 and 9 as indicative for chromosome 16. Each of these indicative markers is evaluated for both allele variants. If both alleles on the marker position correspond to the desired variant, the haplotype is “g/g” (g = good), whereas the haplotype is “g/b” (b = bad) or “b/b”, if one or none allele is congruent.

At first the markers were confirmed by sequencing of amplified PCR products. For this purpose, two different primer pairs were tested for amplification of each marker sequence under standard conditions (see Table 4 and Table 5 in III., 3.2.1.). For each marker we chose the better of the two primer pairs, excised the band from the gel and verified the nucleotide sequence (see Figure 2). Each sample was sequenced independently with a forward and/or a reverse primer. On the basis of the verified marker positions, SNP-specific primer pairs were designed. To increase the probability of the desired haplotype constellation in CF piglets, all animals of the existing breeding herd were screened for the candidate regions on chromosome 10 and on chromosome 16 (see Figure 3) and selected for breeding according to their haplotype.

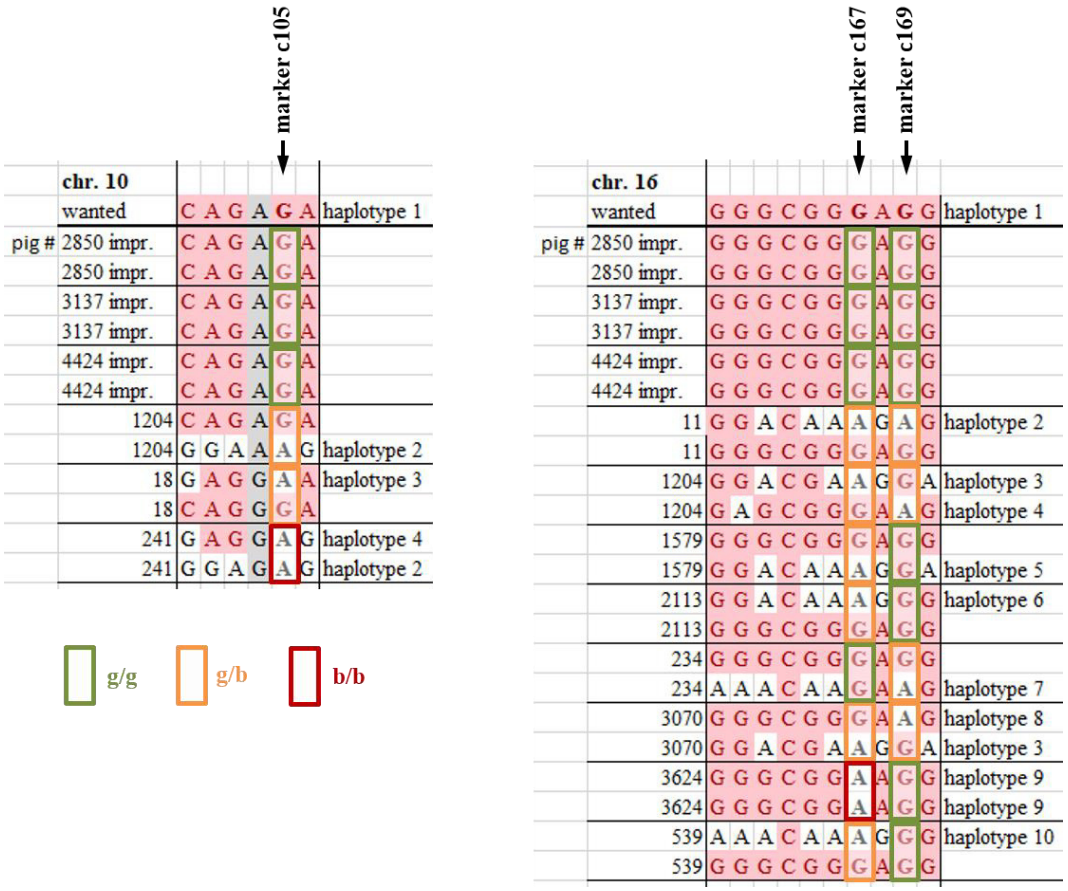

Figure 1: Distinguishing the desired haplotype from unwanted ones by detecting informative markers. Marker 5 on chromosome 10 and markers 7 and 9 on chromosome 16 are suitable SNPs to differentiate the desired haplotype (haplotype 1) from all others. As marker 4 (marked gray) on chromosome 10 turned out to be an artefact, it was not taken into further consideration. The haplotypes are described as “g/g”, “g/b” or “b/b” depending on whether both, only one or none of the two alleles comply with the wanted haplotype. The three intestinal improved piglets (#2850, #3137 and #4424) show homozygosity for the desired haplotype at both candidate loci.

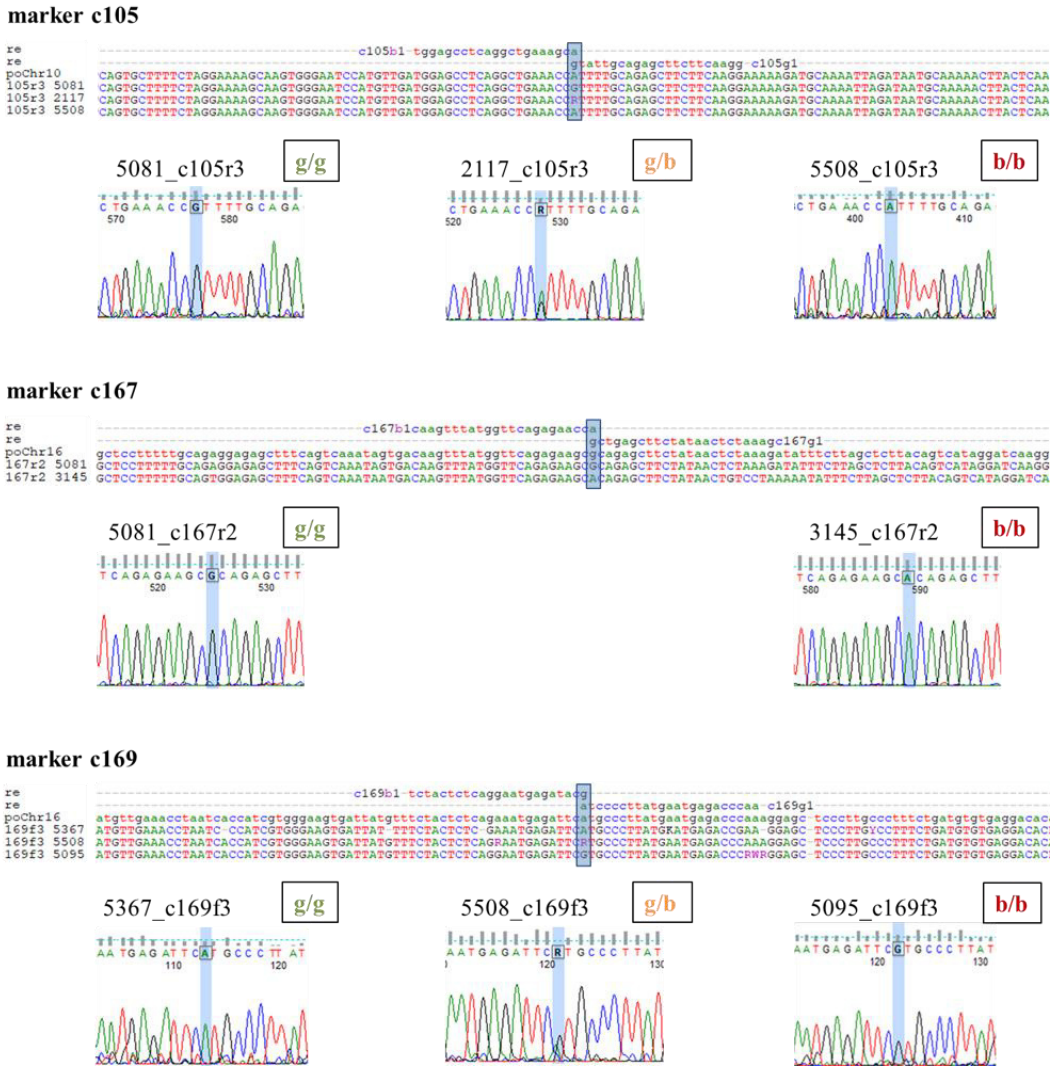

Figure 2: Exemplary electropherograms of the marker regions. An animal's haplotype is discriminated by SNPs (marked blue) with the help of marker-specific primer pairs, whereby the sequence of the primer pairs is indicated in the upper lines (see chapter IV.1.1.2.). It should be noted that no single individual showed a "g/b" constellation on marker c167, wherefore no electropherogram for the heterozygous constellation is shown.

♂	chr. 10	chr. 16	
	c105	c167	c169
pig #5081	g/g	g/g	b/b
5367	g/g	g/b	g/g
5368	g/g	g/b	g/g

♀	chr. 10	chr. 16	
	c105	c167	c169
pig #2116	g/g	g/b	b/b
2117	g/b	g/b	b/b
5078	g/g	g/g	b/b
5095	g/g	g/g	b/b
5372	g/g	g/g	g/b
5373	g/g	g/g	b/b
5375	g/g	g/g	b/b

Figure 3: Haplotypes of the initial breeding herd. Marker c105 was indicative for the desired candidate region alone, while for chromosome 16 the "g" constellation only on both, the c167 and the c169 marker, suggested the desired haplotype.

1.1.2. Establishment of marker-specific genotyping PCRs

Since sequencing of marker regions is very time-consuming, marker-specific genotyping-PCRs were established to rapidly identify the desired genetic constellation at both candidate regions. For each marker on chromosome 16, marker 7 and marker 9, two individual PCRs were designed. One PCR identifies the desired ("g") haplotype, the second one detects the undesired ("b") constellation. For marker 5 on chromosome 10 only one PCR was established that ruled out any unwanted haplotype. To establish robust PCRs, various sets of SNP-specific primer pairs as well as different master mix compositions were tested. Table 14 and Table 15 demonstrate the final conditions for each discrimination PCR. Genotyping by marker-specific PCRs and Sanger sequencing gave consistent results (see Figure 4).

While on chromosome 10 the desired haplotype "g/g" was abundant at high frequency, the desired haplotype on chromosome 16 was low and almost extinct in female animals (see Figure 3 above). However, in a parallel attempt on reducing inbreeding by mating with unrelated WT animals, a higher frequency of the desired haplotype was achieved (see Figure 5 and Figure 6).

Table 14: Final master mix compositions for discrimination PCRs.

Marker	Primer pair *	$MgCl_2$	HotStarTaq	DNA template
c105-b	c105b1/c105r3	0.0 µL	0.1 µL	1 µL
c167-b	c167b3/c167r2	0.0 µL	0.1 µL	2 µL
c167-g	c167f1/c167g1	2.0 µL	0.2 µL	1 µL
c169-b	c169b1/c169r3	0.0 µL	0.2 µL	1 µL
c169-g	c169f2/c169g1	0.0 µL	0.1 µL	1 µL

* 0.4 µL of 10 µM stock solution was applied for each primer.

Table 15: Cycler protocol for discrimination PCRs.

Denaturation	95 °C	5 min	
Denaturation	94 °C	20 s	35×
Annealing	58 °C	20 s	
Elongation	72 °C	1 min	
Final elongation	72 °C	10 min	
Termination	4 °C	5 min	

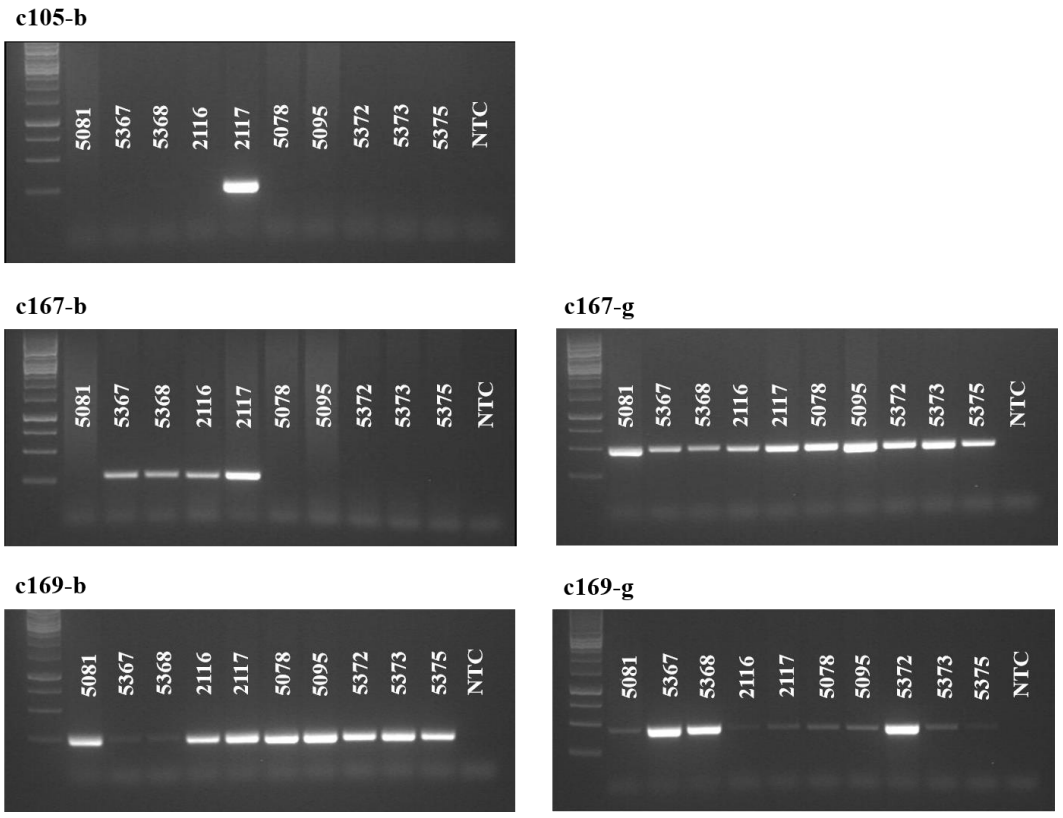

Figure 4: Confirming the sequenced haplotypes of the initial breeding herd by marker-specific discrimination PCRs. To identify the haplotype of each marker, the separate PCRs are considered in combination. The detection of a single band in

the “b”- or “g”-PCR only, defines the “g/g” or the “b/b” constellation. If there are bands in both PCRs detectable, the “g/b” haplotype exists.

♂	chr. 10	chr. 16	
	c105	c167	c169
pig #5554	g/g	g/b	g/g
5655	g/g	g/g	g/b
5656	g/g	g/g	g/b

♀	chr. 10	chr. 16	
	c105	c167	c169
pig #5509	g/g	g/g	g/b
5562	g/g	g/g	g/b
5666	g/g	g/g	g/b
5780	g/g	g/g	g/b

Figure 5: Haplotypes of the additional breeding animals. Heterozygous *CFTR*$^{+/-}$ sows of the initial breeding herd were inseminated with sperm of WT boars to generate further *CFTR*$^{+/-}$ pigs as potential new breeding animals.

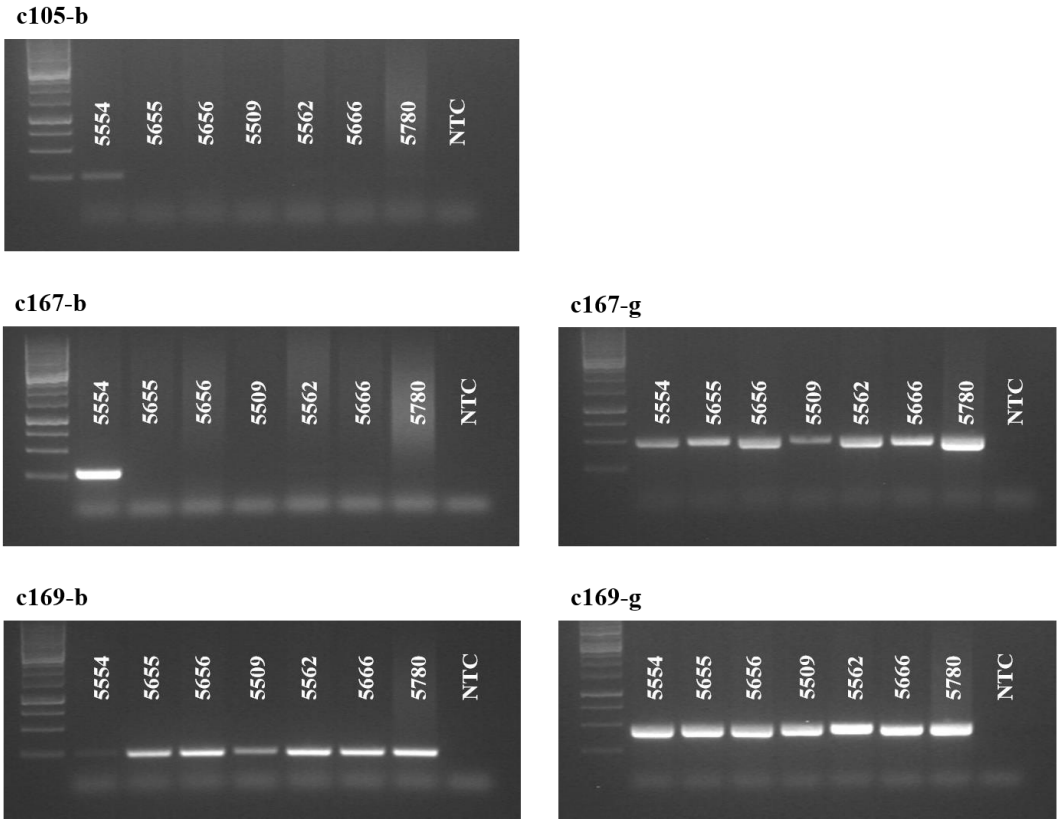

Figure 6: Discrimination of the additional breeding animals by marker-specific discrimination PCRs.

1.1.3. *CFTR*$^{-/-}$ piglets with the desired genotype constellation

Outbreeding delivered new heterozygous *CFTR*$^{+/-}$ pigs with an increased frequency of the desired haplotypes. Animals with homozygous “g/g” on chromosome 10 and heterozygous “g/b” on chromosome 16 were raised and mated to have a higher probability of the desired haplotype combination in the CF offspring.

Immediately after birth, all piglets were evaluated by genotyping PCRs for *CFTR* as well as for the markers c105, c167 and c169. CF KO piglets were euthanized and examined for their intestinal phenotype. During a period from February to December 2018, marker-specific genotyping PCRs revealed 10 out of 55 *CFTR*$^{-/-}$ piglets in 19 litters that showed homozygosity for the desired haplotype at both candidate regions. Genotyping and pedigree of an exemplary *CFTR* litter is shown in Figure 7 and Figure 8. None of the *CFTR*$^{-/-}$ animals showed autonomous release of meconium. This is confirmed by the macroscopic and histological examination of the CF piglet #6491 which exhibited the desired genotype constellation on chromosome 10 and on chromosome 16 in comparison to the CF piglet #6345 which lacked the desired genotype constellation (see Figure 9 to Figure 11). Obviously, there was no phenotypic difference between the animals. The distinct localization of the intestinal obstruction reflected the typical variation seen in CF piglets. In sum, all CF KO piglets with the desired genotype on chromosome 10 and on chromosome 16, showed an MI similar to normal CF KO piglets. The naturally occurring improvement of the intestinal phenotype found in the previously described animals (#2850, #3137 and #4424), could not be replicated by selected breeding for the proposed modifier loci. The hypothesis of the beneficial influence of these loci was therefore clearly rejected.

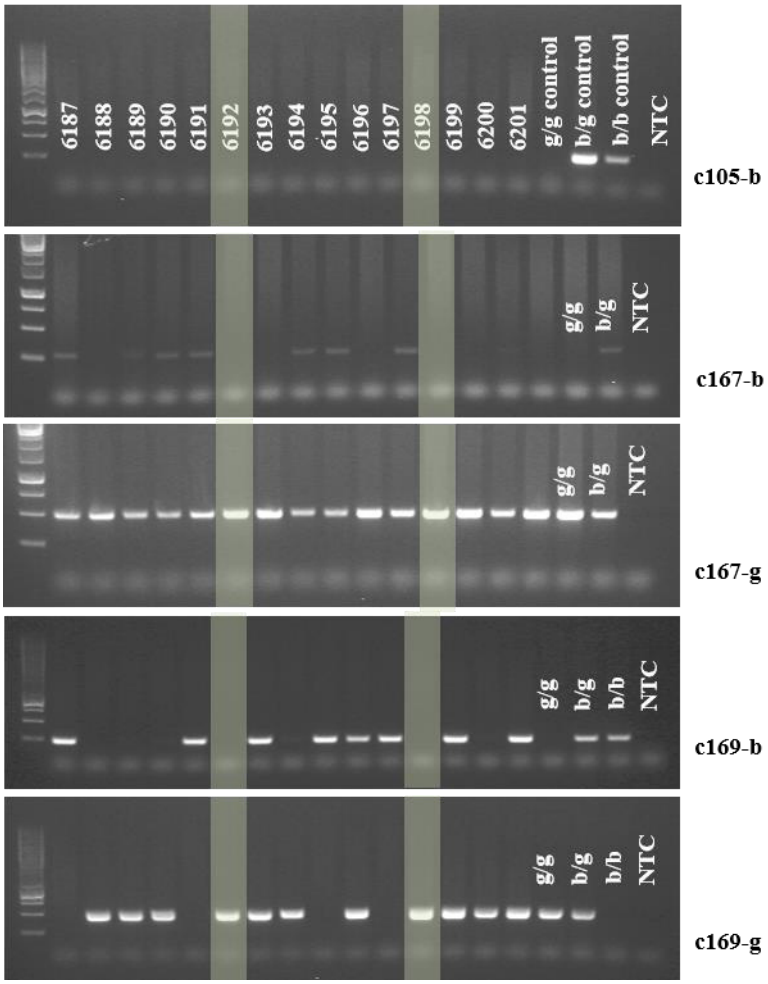

Figure 7: Marker-specific discrimination PCRs performed in an exemplary *CFTR* litter. The *CFTR*$^{-/-}$ piglets #6192 and #6198 (marked green) are homozygous for the desired haplotype at all markers. Previously discriminated animals served as controls.

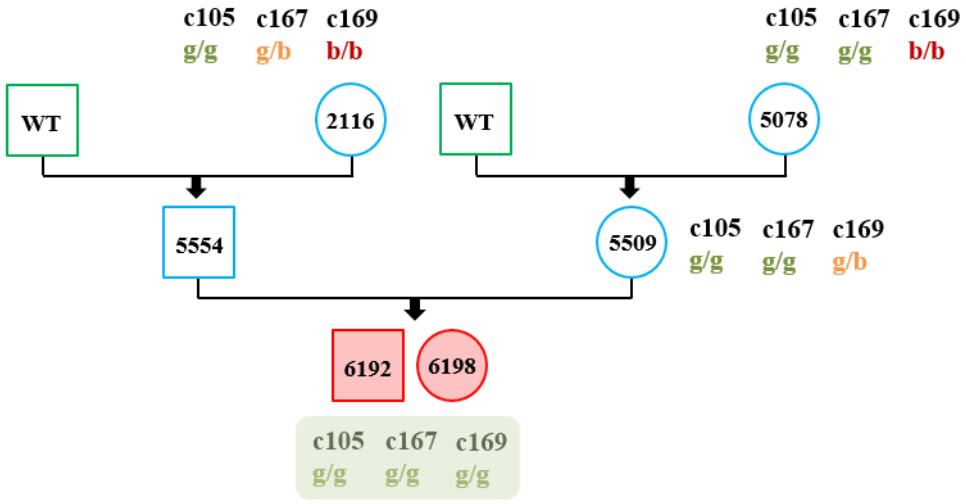

Figure 8: Pedigree of promising *CFTR*$^{-/-}$ piglets from an exemplary *CFTR* litter. Green constitutes WT pigs, heterozygous *CFTR*$^{+/-}$ breeding animals are represented in blue and red remarks *CFTR*$^{-/-}$ piglets. Boxes stand for male pigs; females are indicated by circles. The promising genetic structure found in the CF KO piglets #6192 and #6198 was attained over two generations by outbreeding and particular mating of heterozygous *CFTR*$^{+/-}$ animals.

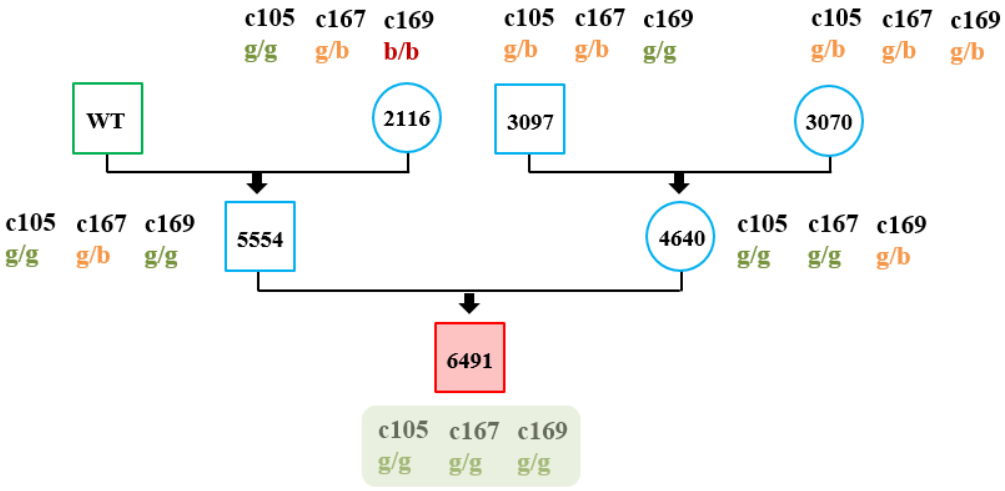

Figure 9: Pedigree of *CFTR*$^{-/-}$ piglet #6491 with the desired genotype. Based on the promising CF piglet #6491, the expression of the intestinal phenotype was exemplary investigated by comparing with a normal CF KO piglet that did not demonstrate the desired genetic constellation in previously implemented discrimination PCRs.

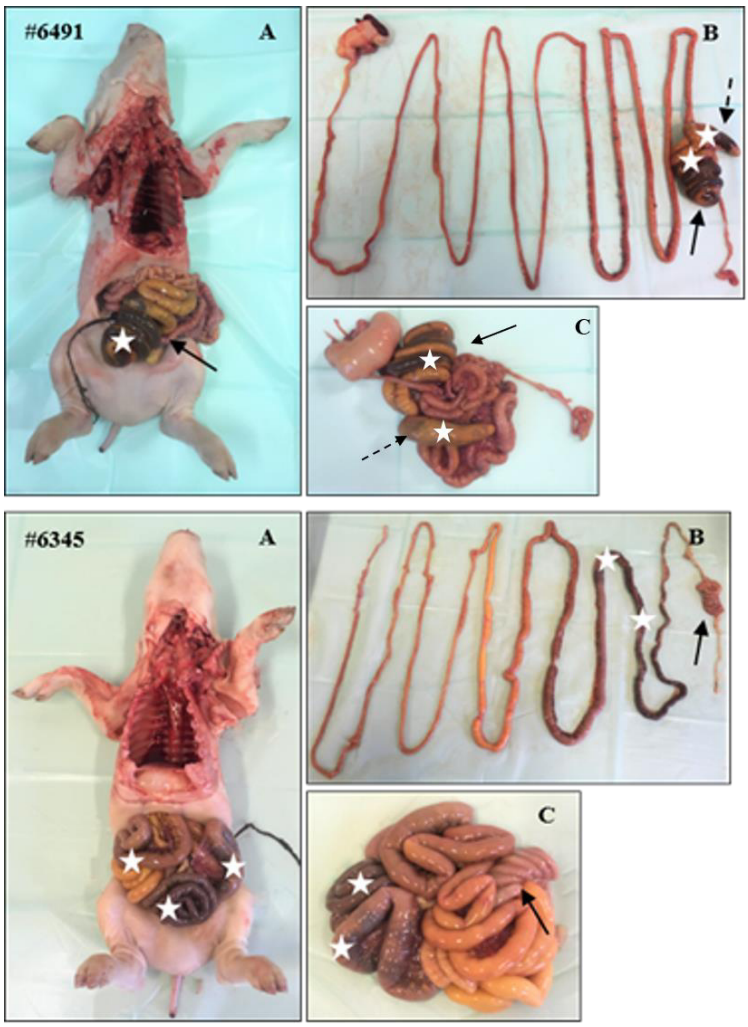

Figure 10: Intestinal phenotype of the promising *CFTR*$^{-/-}$ piglet #6491 compared with a normal *CFTR*$^{-/-}$ piglet #6345. (A) View of the intestinal convolute after opening the abdomen. (B) and (C) The intestinal convolute after resection. White asterisks mark the presence of meconium. Black arrows point to the colon, the cecum is marked by discontinuous black arrows. A severe MI is present in both animals. In piglet #6491 the cecum and the colon ascendens are severely enlarged by stuck meconium. The reduced diameter of the following colon descendens is similar to the CF-typical microcolon apparent in piglet #6345. The severity of the intestinal phenotype is comparable in both the CF KO piglet exhibiting the desired genotype and the CF piglet without the special constellation.

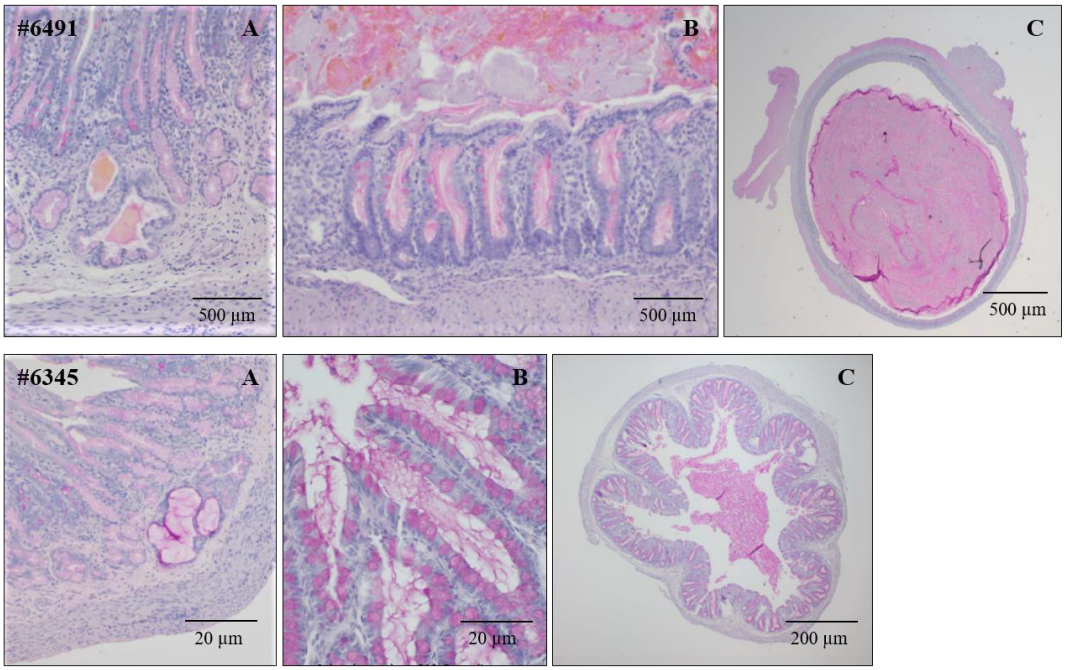

Figure 11: Histopathological examination of intestinal tissue in the promising *CFTR*$^{-/-}$ piglet #6491 compared with a normal *CFTR*$^{-/-}$ piglet #6345. (A) PAS-staining of 4 % PFA- (#6491) and methacarn-fixed (#6345) duodenal tissue. (B) PAS-staining of 4 % PFA-fixed colon ascendens (#6491) and colon descendens (#6345). (C) PAS-staining of methacarn-fixed colon ascendens (#6491) and 4 % PFA-fixed colon descendens (#6345). In both animals, duodenal Brunner's glands (A), as well as crypts in the colon (B) are severely dilated and filled with mucus. The colon itself (C) is stuffed with large amounts of mucous material, whereby in piglet #6345 the additional CF-typical microcolon with reduced diameter is apparent (data kindly provided by Lars Mundhenk from the Institute of Animal Pathology at the Free University of Berlin, Germany).

1.1.4. Detailed examination of the candidate region on chromosome 10

The postulated candidate region on chromosome 10 (25.8–25.9 Mb) was defined by a specific pattern of 6 marker positions. Within this region, there was no annotated genetic element in the Sscrofa 10.2 reference genome. A multi-species alignment of chromosome 10 however revealed two loci within the candidate region that are characterized by high homology among different species, are

covered by bioinformatically predicted genetic elements and are consistent with potential regulatory function by the PreMod algorithm (Figure 12). Further, the last exon of NIMA related kinase 7 (NEK7) was located outside the region covered by the markers, but situated inside the nearest up-stream marker. Therefore, all three loci were investigated in more detail for a potential causative mutation.

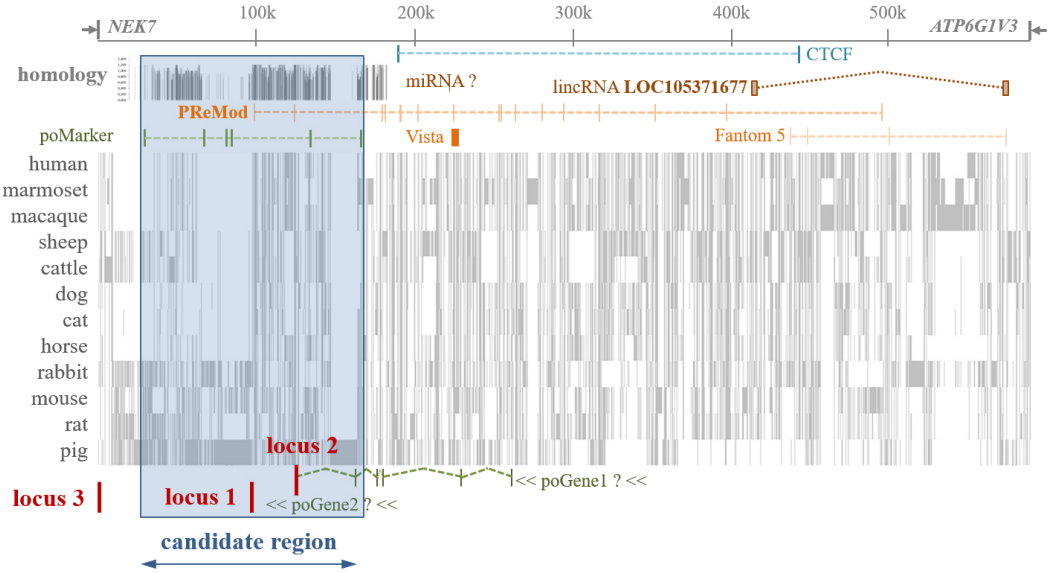

Figure 12: Multi-species alignment of chromosome 10. In a multi-species alignment, the similarity among genomic sequences of different species is studied. Shared patterns with possible regulatory or functional relevance can thus be identified. The performed alignment detected two loci that are highly homologous among the species. The PreMod database suggested a potential regulatory function of this loci and the GeneScan tool predicted them to be part of not clearly specified genetic elements.

All three regions were investigated by sequencing of PCR products amplified from CF pigs with a g/g, g/b or b/b haplotype, as determined by Sanger sequencing of the marker site c105 (see chapter IV.1.1.1.). Standard conditions, according to Table 12 and Table 13, proved sufficient for PCR amplification of locus 1 and locus 2 (see Figure 13). For amplifying locus 3, several primer pairs were tested (see Figure 14). Finally, the primers nek3f and nek2r used in an optimized master mix composition and cycler protocol, resulted in efficient amplification (Table 16 and Table 17). Overall six animals with different c105

haplotypes were explored: two animals exhibiting the g/g constellation, three animals with the g/b haplotype and one b/b individual. Sequencing of PCR products was performed with amplification and internal sequencing primers. By comparing the PCR amplicons, SNPs were found in locus 1 and locus 2. Locus 1 revealed six SNPs and in locus 2 seven SNPs were identified. Examination of locus 3 did not reveal any polymorphisms between the different c105 haplotypes (see Figure 15 A). As the patterns of SNPs in locus 1 and locus 2 were not consistent with the marker-defined haplotypes, none of the identified polymorphisms could present a causative mutation that supports the initial hypothesis of a modifier region on chromosome 10 (see Figure 15 B, Figure 16 and Figure 17). This finding correlated to the rejection of the hypothesis by selected breeding (see chapter IV.1.1.3.). A further examination of the second postulated candidate region on chromosome 16 (4.7-5.2 Mb) was therefore not performed.

	Primer pair		
	Primer f	**Primer r**	**length**
1	ch10f1	ch10r1	2251 bp
2	ch10f6	ch10r6	2387 bp

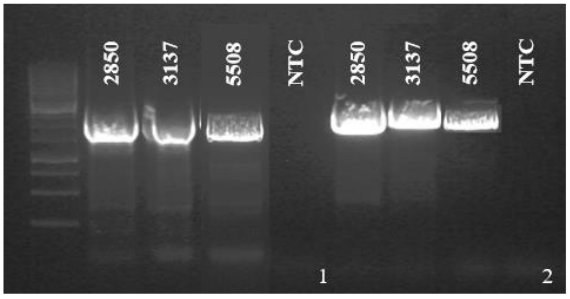

Figure 13: Amplification of locus 1 and locus 2 in exemplary *CFTR* animals. After testing different primer pairs, the most promising ones (primer pair 1 for locus 1 and primer pair 2 for locus 2) were optimized. Under UV-light, amplified PCR products of the correct size were cut out of the agarose gel, DNA was eluted and subsequently used for sequencing reaction.

	Primer pair		
	Primer f	**Primer r**	**length**
1	nek1f	nek1r	5359 bp
2	nek2f	nek2r	5115 bp
3	nek3f	nek3r	3661 bp
4	nek3f	nek2r	3166 bp

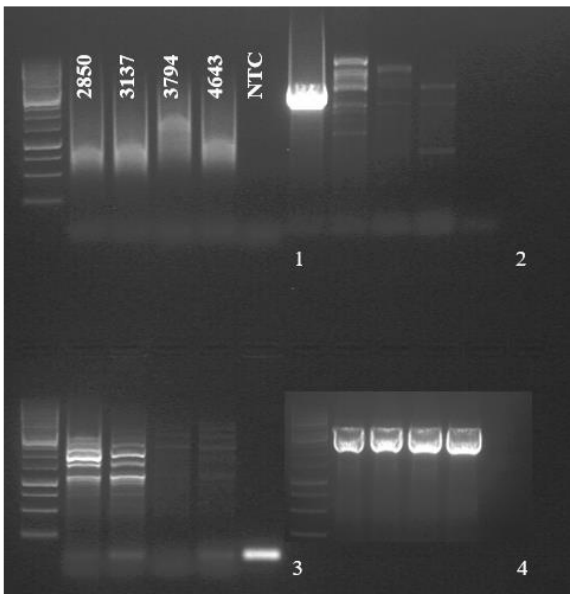

Figure 14: Amplification of locus 3 in exemplary *CFTR* animals. (1-3) Testing of primer pairs for amplification of locus 3. Primer pairs were tested with the Herculase II Fusion DNA Polymerase kit with a volume of 0.4 µL each. Primer pairs 2 and 3 were selected for further optimization by different combination of the primers. (4) Final amplification of locus 3 with the primer pair nek3f / nek2r by using the Qiagen® LongRange PCR kit. Bands of the correct bp size were cut out of the gel and eluted DNA was applied in following sequencing reaction.

Table 16: Master mix composition for locus 3-PCR.

10× LongRange PCR Buffer	2.5 µL
dNTPs (10 mM)	1.25 µL
Primer f (10 µM)	0.5 µL
Primer r (10 µM)	0.5 µL
LongRange (5 U/µL)	0.2 µL
aq. dest.	18.05 µL
DNA template	2 µL

Table 17: Cycler protocol for locus 3-PCR.

Denaturation	93 °C	3 min	
Denaturation	93 °C	15 s	35×
Annealing	62 °C	30 s	
Elongation	68 °C	3.5 min	
Termination	4 °C	15 min	

A

	SNPs	
	Locus 1	**Locus 2**
1	nt 560	nt 881
2	nt 767	nt 1166
3	nt 1641	nt 1307
4	nt 1957	nt 1483
5	nt 1967	nt 1637
6	nt 1996	nt 1744
7		nt 1906

B

		c105	Locus 1						Locus 2						
pig#	**GWAS**	**seq**	**1**	**2**	**3**	**4**	**5**	**6**	**1**	**2**	**3**	**4**	**5**	**6**	**7**
2850	g/g	g/g	G	G	R	A	C	C	A	C	T	A	A	T	G
3137	g/g	g/g	G	G	G	A	C	C	A	C	T	A	A	T	G
2117	b/g	g/b	R	R	G	R	Y	Y	C	A	C	T	T	C	A
3097	b/g	g/b	R	R	G	R	Y	Y	C	A	C	T	T	C	A
3132	b/g	g/b	R	R	R	R	Y	Y	C	A	C	T	T	C	R
5508	b/b	b/b	R	R	G	R	C	Y	M	M	Y	T	W	Y	R

Figure 15: Evaluation of SNPs in the candidate region of chromosome 10. (A) Identified SNPs in the three specified loci. SNPs were found in locus 1 and locus 2, with their position relative to the 5′-end of the forward primer indicated. In locus 1 six SNPs were identified and locus 2 revealed seven possible SNPs. Investigating locus 3 did not detect any polymorphisms between the examined animals. (B) Overview of all examined SNPs in two individuals with the g/g constellation, three animals with the g/b haplotype and one individual exhibiting the b/b constellation. Regarding the latter, we identified only one single animal in our herd with the specific genotype. As the identified SNPs in locus 1 and locus 2 were not consistent with the marker-defined haplotypes, none of these polymorphisms could present a causative mutation according to the initial hypothesis of a modifier region on chromosome 10.

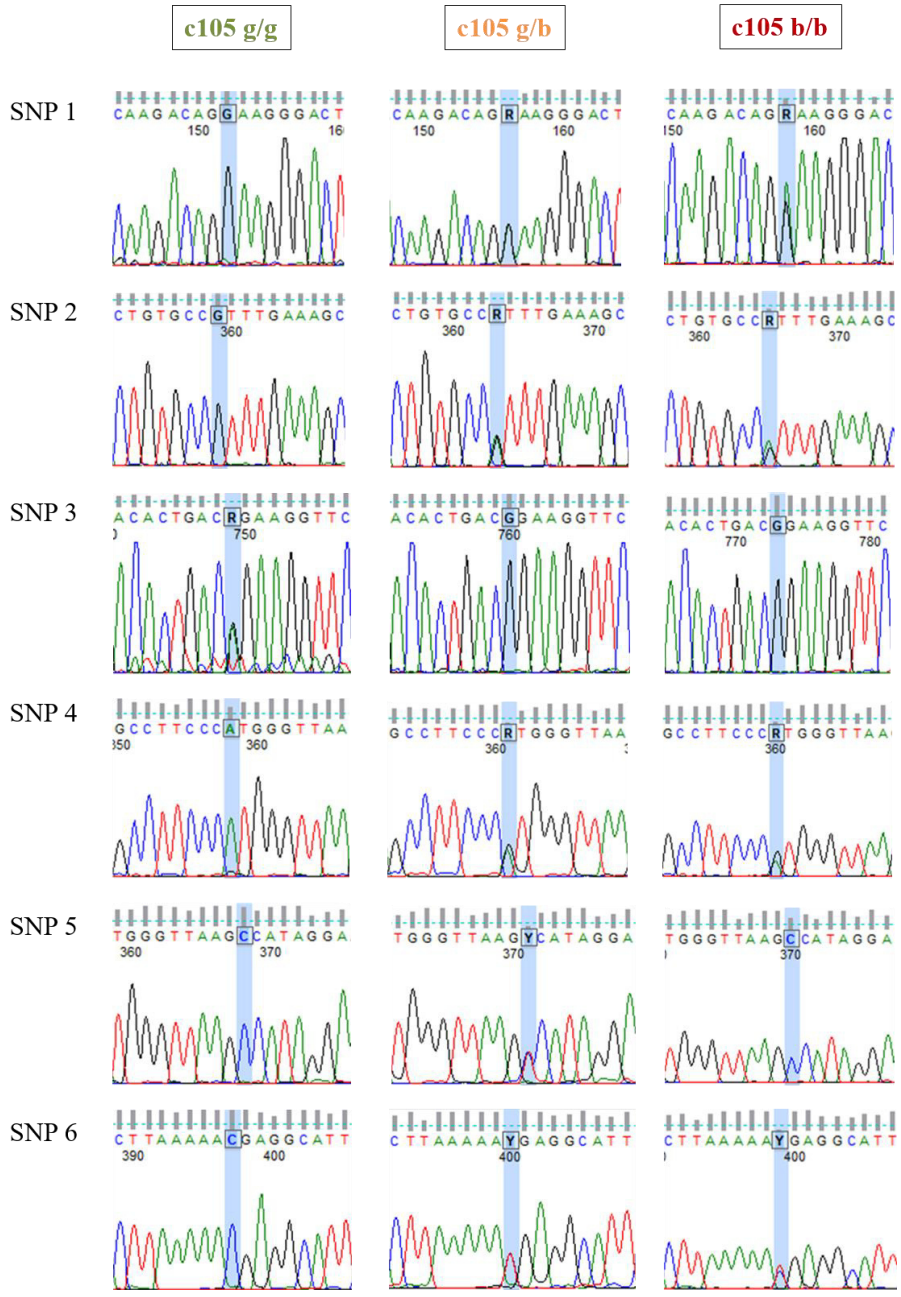

Figure 16: SNP patterns in locus 1. For each SNP, representative electropherograms from pigs with marker constellations g/g, g/b or b/b are shown. The SNP-position is highlighted by a blue box.

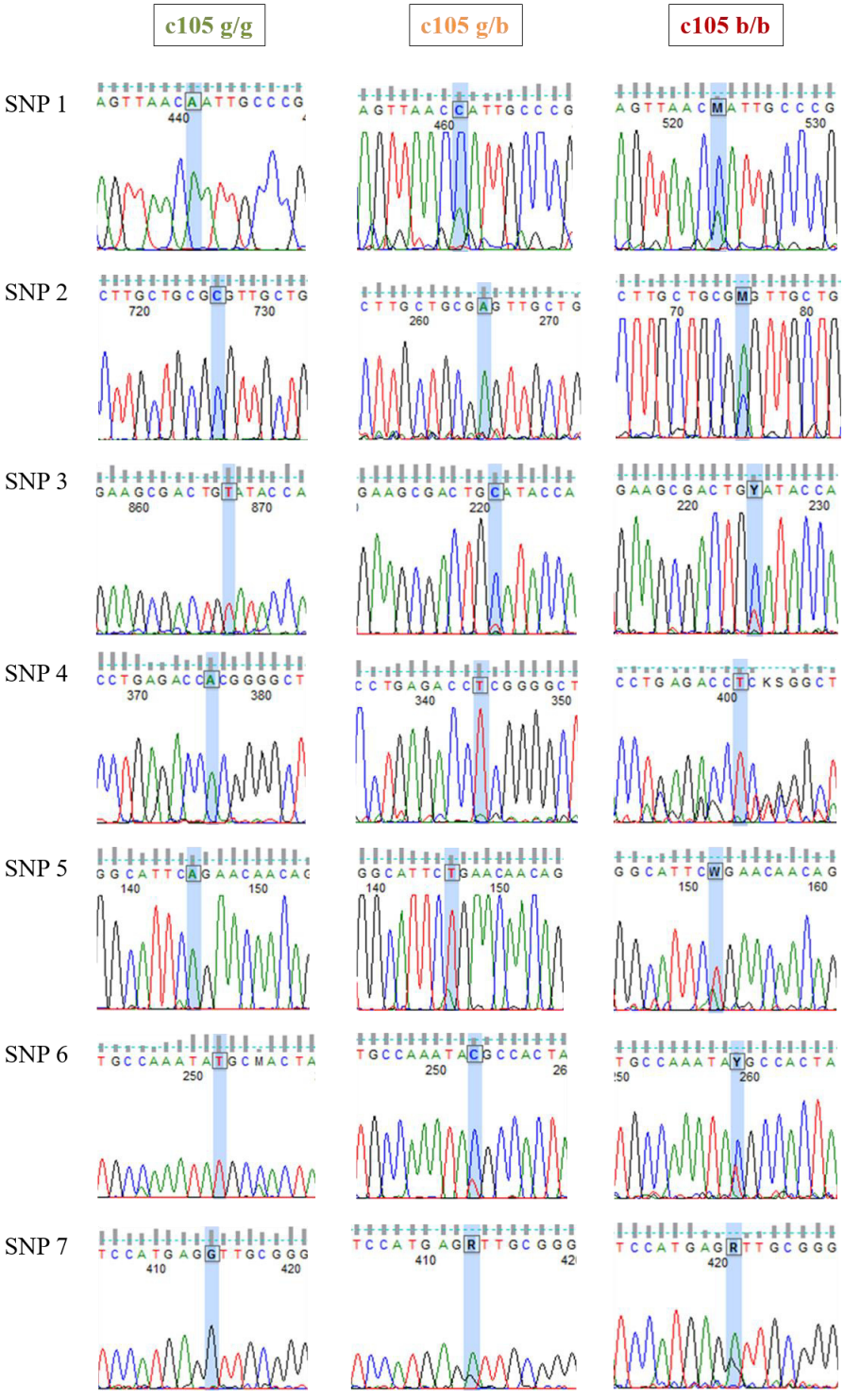

Figure 17: SNP patterns in locus 2. For each SNP, representative electropherograms from pigs with marker constellations g/g, g/b or b/b are shown. The position of the SNP is highlighted by a blue box.

1.2. Novel genome-wide analysis

Although the initial hypothesis of two modifying loci on chromosome 10 and on chromosome 16 was fully rejected and no additional piglet with an improved gut-phenotype was born, the close familial relation of these animals suggested an influencing effect by the genetic background. Therefore, we performed an alternative analysis based on a combined linkage disequilibrium and linkage analysis (cLDLA) (MÜLLER et al., 2017) on the basis of a more extended population of animals. This included all initial 146 *CFTR*$^{-/-}$ piglets, three of them with the gut improved phenotype, and 50 heterozygous *CFTR*$^{+/-}$ breeding animals as well as 55 additional *CFTR*$^{-/-}$ animals that were born between February and December 2018 as well as 14 new breeding animals that were involved in the extended pedigree. The animals were investigated using the PorcineSNP60 DNA Analysis Kit v2 (Illumina, San Diego, USA). SNP typing was performed by Doris Seichter, Tierzuchtforschung e.V. München (TZF Grub, Germany) and data were analyzed by Ivica Medugorac, Population Genomics Group, Department of Veterinary Sciences, LMU Munich, Germany. The newly obtained data were combined with the data set from the previous analysis.

As in human CF patients the variability of the intestinal phenotype is proven to be dependent on modifying loci, the regions covering the proposed modifier genes *SLC6A1* (AHMADI et al., 2018), *SLC26A9* (LIU et al., 2015), *SLC9A3* (LI et al., 2014), *ZG16* (BERGSTROM et al., 2016), *CLCA1* (VAN DER DOEF et al., 2010), *MSRA* (HENDERSON et al., 2012), *ADIPOR2* (DORFMAN et al., 2009) and *GUCY2C* (ARORA et al., 2017) have been investigated regarding their relevance in porcine CF. A detailed examination indicated that none of these human modifiers were involved in similarly modulating CF in pigs (see Figure 18). Instead, cLDLA revealed two significant peaks on chromosome 5 and on chromosome 13 that have been studied in more detail (see Figure 19).

The candidate region on chromosome 5 is spanning over a segment of 1.5 Mb according to the Sscrofa 10.2 reference genome and corresponding to the regions chr12p13.33 and chr2q11.21 in the human genome. The locus is indicated by two sharp, closely adjacent peaks and contains 12 genes (see Figure 19 A). Haplotype analysis suggested a heterozygous influence of three haplotypes, narrowing the candidate region down to a size of 1.13 Mb covered by five markers. This genomic sequence covers a number of genes in all examined animals, including

ATP6V1E1 located within the center of the candidate region. The encoded protein of this gene is a component of the multi-unit vacuolar ATPase, a proton pump acting on the acidification of intracellular organelles and extracellular compartments (MCGUIRE et al., 2017). The abundance of other genes or genetic elements in the gut was low or almost absent (NCBI) or the submitted function described in the literature or the OMIM database give only little hint for an involvement in compensating lacking *CFTR*.

Examination of the candidate region on chromosome 13 revealed a segment of 0.41 Mb. This region corresponds to the human chr3p24.1, is indicated by a broad single peak and comprises only four genes (see Figure 19 B). Haplotype analysis presumes the involvement of a small region covered by only three markers, narrowing the candidate region down to 180 kb. The suggested region resembles the upstream region of *TGFBR2*, a gene that is expressed in almost any tissue (NCBI). Its protein is well known for its diverse roles in cell proliferation, including the continuous turnover of epithelial cells in the gut (FLENTJAR et al., 2007; ZHANG et al., 2016).

Is has to be mentioned that cLDLA analysis revealed further peaks apart from the investigated candidate regions, but none of them reached a peak level of similar height as the suggested modifying loci on chromosomes 5 and 13. Nonetheless, the new hypothesis has to be verified in future studies, whereby a more detailed characterization of the submitted modifier genes *ATP6V1E1* and *TGFBR2* is indispensable. The described data are part of a manuscript in preparation.

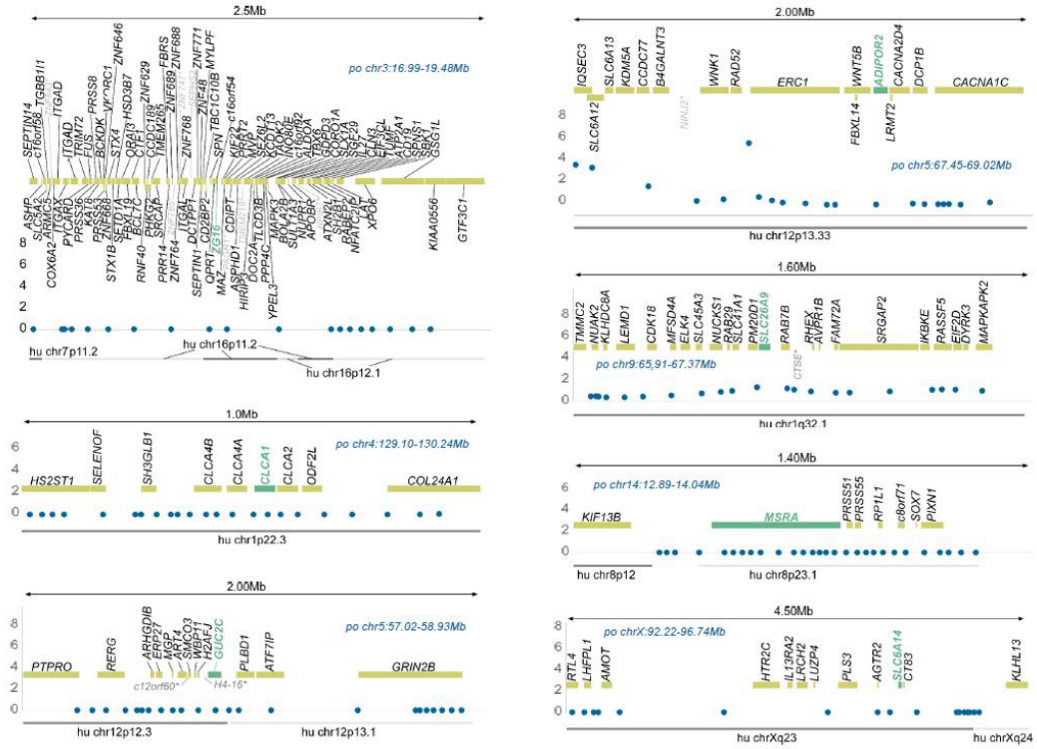

Figure 18: Combined linkage disequilibrium and linkage analysis (cLDLA) of intestinal improved *CFTR*$^{-/-}$ piglets compared with normal *CFTR*$^{-/-}$ piglets. Detailed examination of the proposed modifier genes of the gut-phenotype in human CF patients indicated that none of the candidate loci *ZG16*, *CLCA1*, *GUCY2C*, *ADIPOR2*, *SLC26A9*, *MSRA* or *SLC6A14* is relevant in porcine CF. For each locus, the likelihood-ratio test (LRT) values, illustrated by blue dots, are indicated for the respective gene, presented in green, plus 10 LRT sites up- and downstream. The position of genes in the respective loci were taken from the Sscrofa 10.2 reference genome, after correlating to the corresponding genomic regions in the human reference genome. The corresponding genomic locations in the human genome are indicated for each locus. The y-axis (LRT value) is at the same scale for each locus.

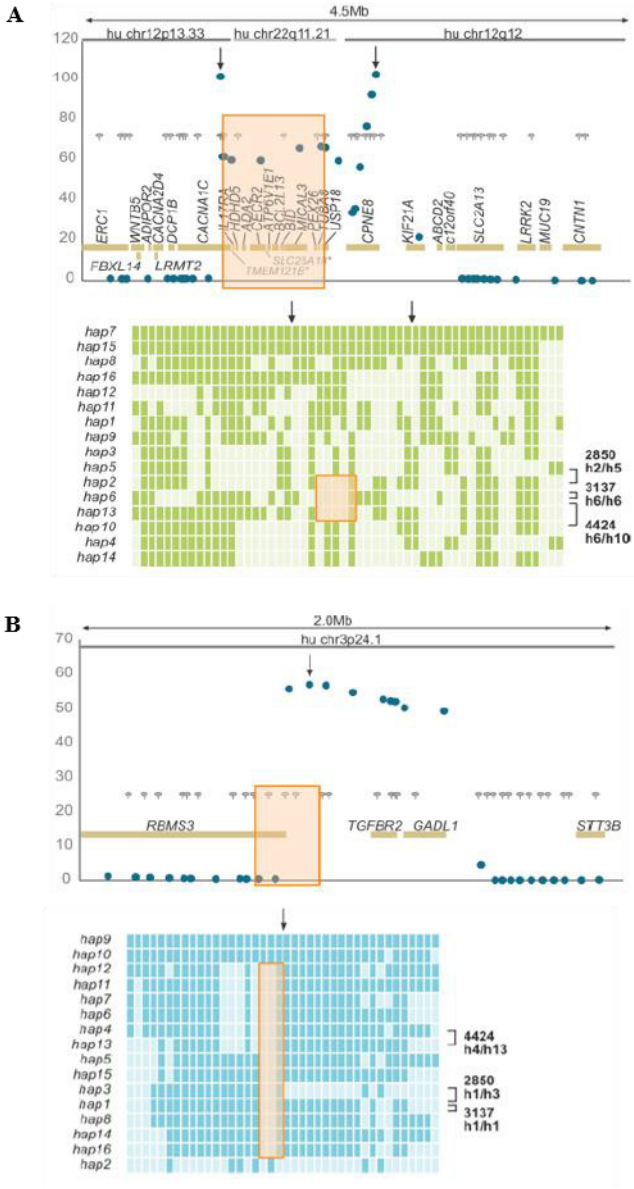

Figure 19: Further examination of new candidate regions on chromosomes 5 and 13. (A) Analysis of candidate region on chromosome 5. The locus on chromosome 5 is indicated by two sharp, closely adjacent peaks and is packed by genes (upper illustration). Haplotype analysis suggests a heterozygous constellation of a region covered by five markers (marked orange). This genomic segment covers a number of genes in all examined animals, including *ATP6V1E1*. (B) Examination of candidate region on chromosome 13. The locus on chromosome 13 is indicated by a broad single peak and covers only few genes. Haplotype analysis suggests the involvement of a small region covered by only three markers (marked orange) which resembles the upstream region of *TGFBR2*.

2. The improved respiratory phenotype in *CFTR*$^{-/-}$ piglets

During my thesis, the routine breeding program continued and overall, a number of 119 CF piglets has been produced. While we did not observe any further piglets with a modified phenotype of the gut, we found in total five CF piglets (#5703, #5704, #5786, #6046, #6704) that showed morphological changes in the airways at the time of examination. Those piglets exhibited a WT-like round trachea with a greater diameter in comparison to a typically triangular-shaped trachea with reduced diameter in all other *CFTR*$^{-/-}$ piglets.

2.1. Finding genetic causes for the improved respiratory phenotype

During routine section it became obvious that initially three animals (#5703, #5704, #5786) differed from normal CF piglets in their trachea by presenting a WT-like round caliber with greater diameter, while their genotype and also a significant MI clearly indicated common signs of CF. Experiments on mucociliary clearance, done by Anna Ermund from the Mucin Biology Group at the University of Gothenburg, Sweden, demonstrated a mucus bundle velocity which is at least as fast as in a WT trachea. To clarify a potential involvement of the genetic background in the naturally occurred modification of the CF airways, the parental animals of improved piglets (boar #5081, sow #5373) have been mated systematically (see Table 18). In this manner, we succeed in reproducing the modified phenotype in two more piglets (#6046, #6704). For a precise description of the origin of the respiratory improved piglets and their parents in the context of the entire *CFTR* breeding herd, a pedigree containing all the ancestors and littermates was created (see Figure 20). The close familial relation of all airway-improved animals and the reproduction of the phenotype by selected breeding, suggested an influence of modifier genes.

Table 18: Overview of all respiratory improved *CFTR*$^{-/-}$ piglets.

Boar #	Sow #	CF KOs #	Phenotype
5081	3506	5703	respiratory improved
		5704	respiratory improved
5081	5373	5786	respiratory improved
		5788	normal CF KO
		5790	normal CF KO
5081	5373	6046	respiratory improved
		6051	normal CF KO
		6056	normal CF KO
5081	5373	6438	normal CF KO
5081	5373	6702	normal CF KO
		6704	respiratory improved

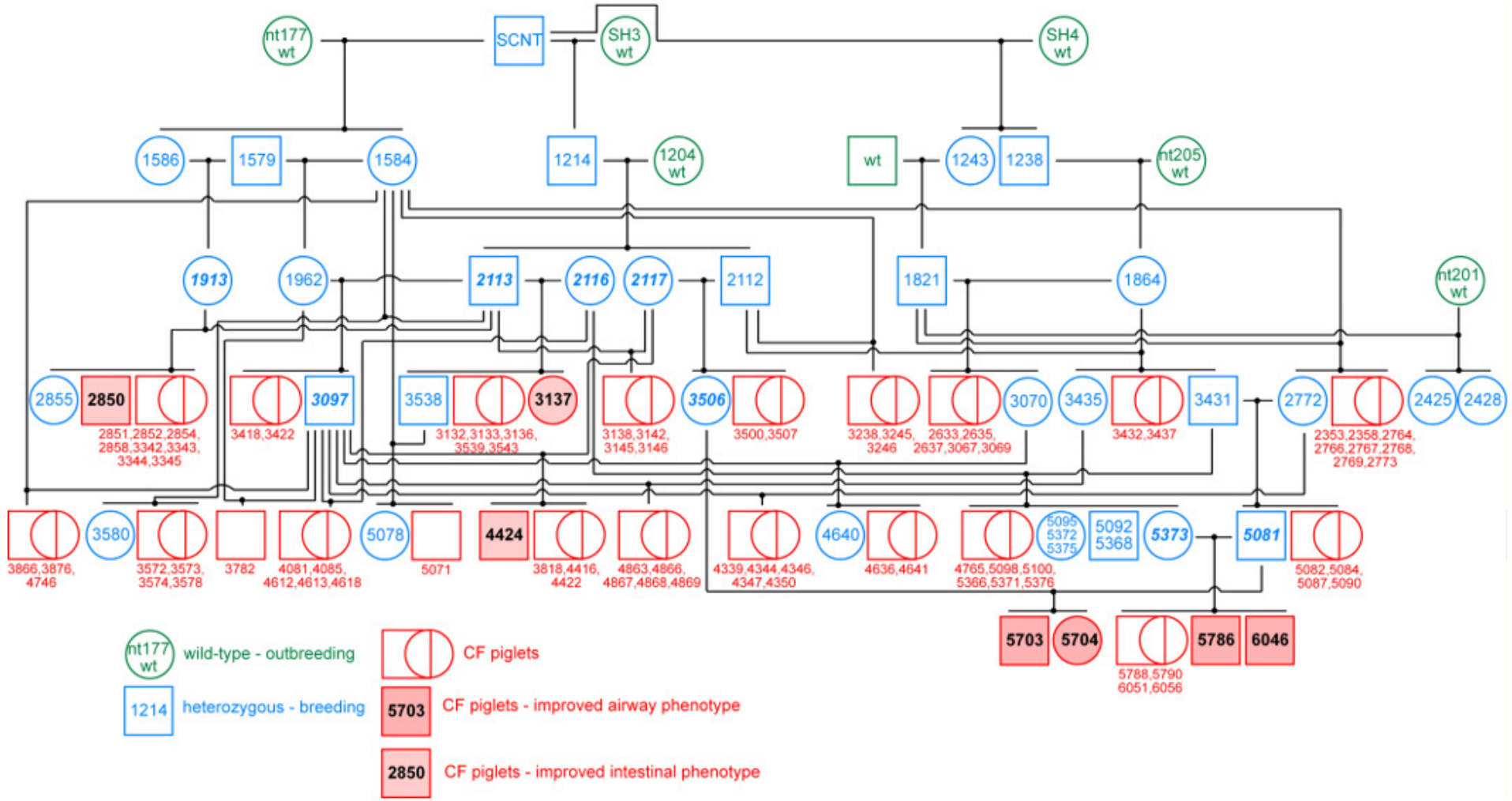
nt177 wt
SCNT
SH3 wt
SH4 wt
1586
1579
1584
1214
1204 wt
wt
1243
1238
nt205 wt
1913
1962
2113
2116
2117
2112
1821
1864
nt201 wt
2855
2850
2851,2852,2854, 2858,3342,3343, 3344,3345
3418,3422
3097
3538
3137
3132,3133,3136, 3539,3543
3138,3142, 3145,3146
3506
3500,3507
3238,3245, 3246
2633,2635, 2637,3067,3069
3070
3435
3432,3437
3431
2772
2353,2358,2764, 2766,2767,2768, 2769,2773
2425
2428
3580
3866,3876, 4746
3572,3573, 3574,3578
3782
4081,4085, 4612,4613,4618
5078
5071
4424
3818,4416, 4422
4863,4866, 4867,4868,4869
4339,4344,4346, 4347,4350
4640
4636,4641
4765,5098,5100, 5366,5371,5376
5095 5372 5375
5092 5368
5373
5081
5082,5084, 5087,5090
5703
5704
5788,5790 6051,6056
5786
6046
nt177 wt
wild-type - outbreeding
1214
heterozygous - breeding
CF piglets
5703
CF piglets - improved airway phenotype
2850
CF piglets - improved intestinal phenotype

Figure 20: Pedigree of the *CFTR* breeding herd. WT pigs are represented in green, blue constitutes heterozygous *CFTR*$^{+/-}$ breeding animals and red remarks *CFTR*$^{-/-}$ piglets. Males are indicated by boxes; circles stand for female pigs. CF piglets of both sexes are symbolized by combined boxes and circles. All respiratory improved piglets #5703, 5704, 5786 and 6046, highlighted in dark red, descends from one single boar #5081 and two different sows, #3506 and #5373.

2.2. Macroscopic examination of the improved respiratory phenotype

Macroscopically, the airway-modified phenotype is characterized by a WT-like trachea with an almost round caliber and a greater diameter in comparison to the CF-typical triangular trachea with clearly reduced diameter (see Figure 21). Is has to be mentioned that in some cases the modification did not extend regularly over the total length of the trachea, but only partially in the middle part, whereas the sections close to the larynx and the main bronchi branching off the trachea, showed CF-typical features. Nevertheless, in all cases of modification, the overall trachea appeared to be less fragile than the tender structure of a CF-trachea, whereby a WT-trachea is even more robust. Apart from the improved respiratory phenotype, all other characteristic features of CF, including a severe intestinal obstruction by MI as well as a micro-gallbladder, were still present.

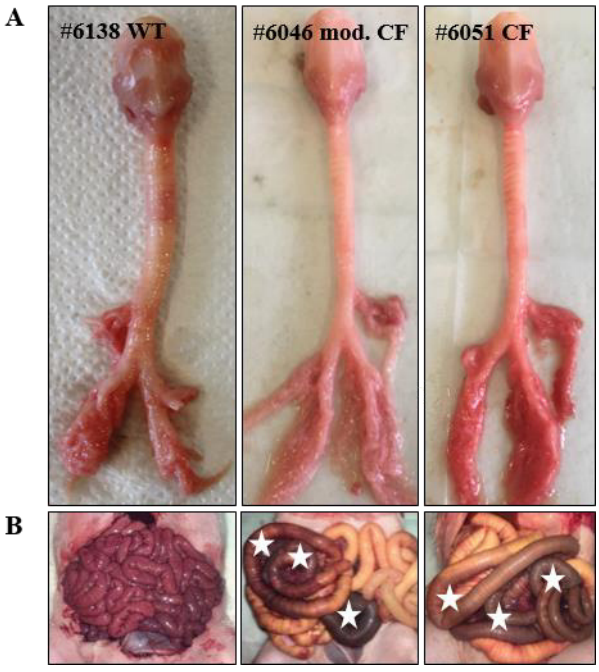

Figure 21: The improved respiratory phenotype (#6046) compared with a normal *CFTR*$^{-/-}$ piglet (#6051) and a WT piglet (#6138). (A) The airways after resection. In comparison to the triangular shaped trachea with clearly reduced diameter in a normal CF pig, the trachea of the respiratory improved CF piglet showed a WT-like round caliber with greater diameter. (B) The intestinal convolute after opening the abdomen. White asterisks mark the presence of meconium. In contrast to the changes in the respiratory tract, the intestinal phenotype of piglet #6046 was typical for CF.

2.3. Detailed examination of the improved respiratory phenotype

To initially verify a lack of *CFTR* expression in respiratory modified *CFTR*$^{-/-}$ piglets, a quantitative PCR (qPCR) was performed. By comparing to housekeeping genes, the relative quantification of *CFTR* expression in pulmonary tissue of two respiratory improved CF piglets (#5786, #6046), two normal CF pigs (#5788, #6051) and one WT piglet (#6138) was determined (see Figure 22). The optimal conditions for the established qPCRs are presented in Table 19. Since the expression of housekeeping genes varies also within the same tissue material, we chose three different genes, *GAPDH*, *TBP* and *YWHAZ,* in order to exclude artifacts. qPCR revealed that, although there is a certain variance, the housekeeping genes are generally expressed in all examined animals. However, an expression of *CFTR* was only detectable in the WT control. Normal CF piglets as well as the airway-improved piglets lacked expression of *CFTR*.

A histopathological exploration was performed by Lars Mundhenk from the Institute of Animal Pathology at the Free University of Berlin, Germany. By comparing the bronchus trachealis of a modified piglet with a normal CF piglet, the greater diameter in the case of the improved animal was clearly apparent (see Figure 23). For a further examination of the improved respiratory phenotype, tracheal tissue was analyzed by Anna Ermund from the Mucin Biology Group at the University of Gothenburg, Sweden. For experiments on mucociliary transport, three airway-improved CF piglets, seven normal CF pigs and overall 14 WT animals have been analyzed. The studies revealed a mucus bundle velocity along the tracheal tissue of the improved animals which is at least as fast as in WT ones (see Figure 24 A). Typically, the examined normal CF piglets did not show any

movement of the mucus due to ciliary collapse. An additional scanning electron microscopic (SEM) analysis, visualized the more expanded mucus in the airways of an improved CF piglet, whereas in a normal CF pig, the mucus network seemed to be more compressed (see Figure 24 C). The appearance of the airway mucus network in an examined WT animal was comparable to the improved animal. Moreover, a measurement of the surface pH in tracheal tissue was performed in four modified piglets, 18 normal CFs and 20 WT piglets, resulting in a similar starting pH value of nearly 6.8 in the improved piglets and the WT controls (see Figure 24 B). Normal CF piglets exhibited a lower pH value of approximately 6.5. For a more detailed examination, the potential role of other modifier elements, in this case responsible for the variant respiratory phenotype, has to be investigated by future genome-wide mapping.

Table 19: Final conditions for respiratory improved qPCRs.

Gene	Primer pair	Concen.	Annealing
CFTR	Lars2f/Lars2ra	0.5 µL	60 °C
GAPDH	GAPqf1/GAPqr1	0.5 µL	60 °C
TBP	tbpF/tbpR	0.7 µL	63 °C
YWHAZ	ywhazF/ywhazR	0.3 µL	63 °C

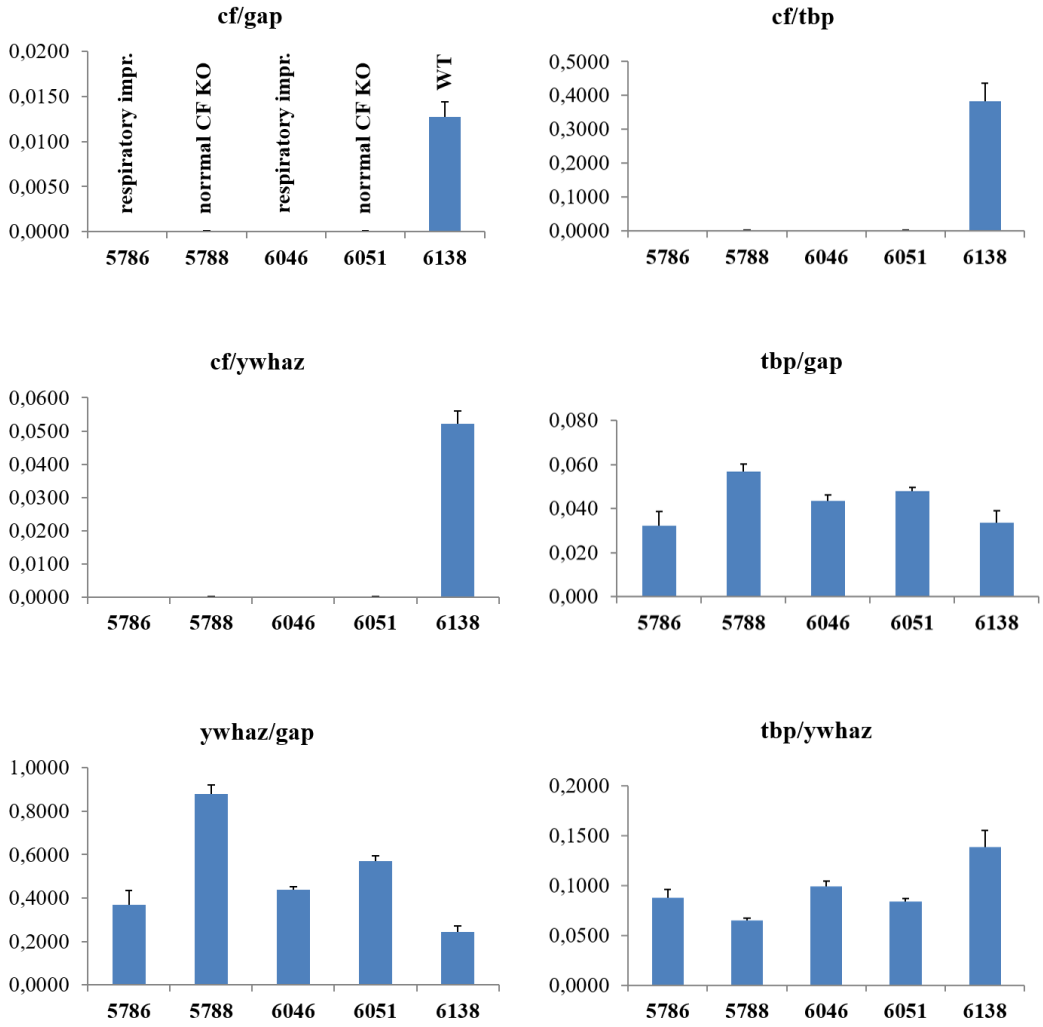

Figure 22: Relative quantification of *CFTR* expression in pulmonary tissue of respiratory improved *CFTR*$^{-/-}$ piglets (#5786, #6046) compared with normal *CFTR*$^{-/-}$ piglets (#5788, #6051) and a WT piglet (#6138). In contrast to the housekeeping genes *GAPDH*, *TBP* and *YWHAZ* that are generally expressed in all examined animals, a *CFTR* expression is only detectable in the WT control. Normal CF KO piglets as well as the airway-improved CF piglets typically lack an expression of *CFTR*.

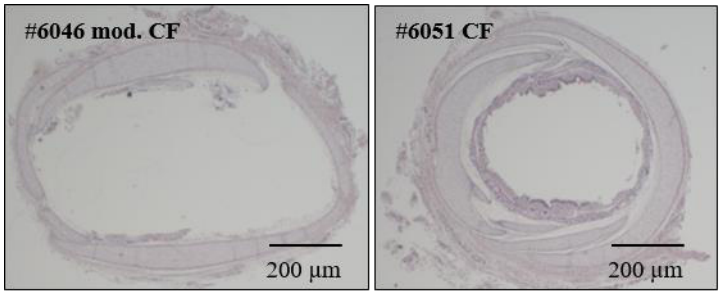

Figure 23: Histopathological examination of bronchial tissue of a respiratory improved *CFTR*$^{-/-}$ piglet (#6046) compared with a normal *CFTR*$^{-/-}$ piglet (#6051). HE-staining of 4 % PFA-fixed tissue of the bronchus trachealis. In comparison to the normal CF piglet that exhibits a clearly reduced diameter, the diameter of the improved animal appears to be significantly enlarged. In both cases, the epithelium is lost due to tissue preparation (data kindly provided by Lars Mundhenk from the Institute of Animal Pathology at the Free University of Berlin, Germany).

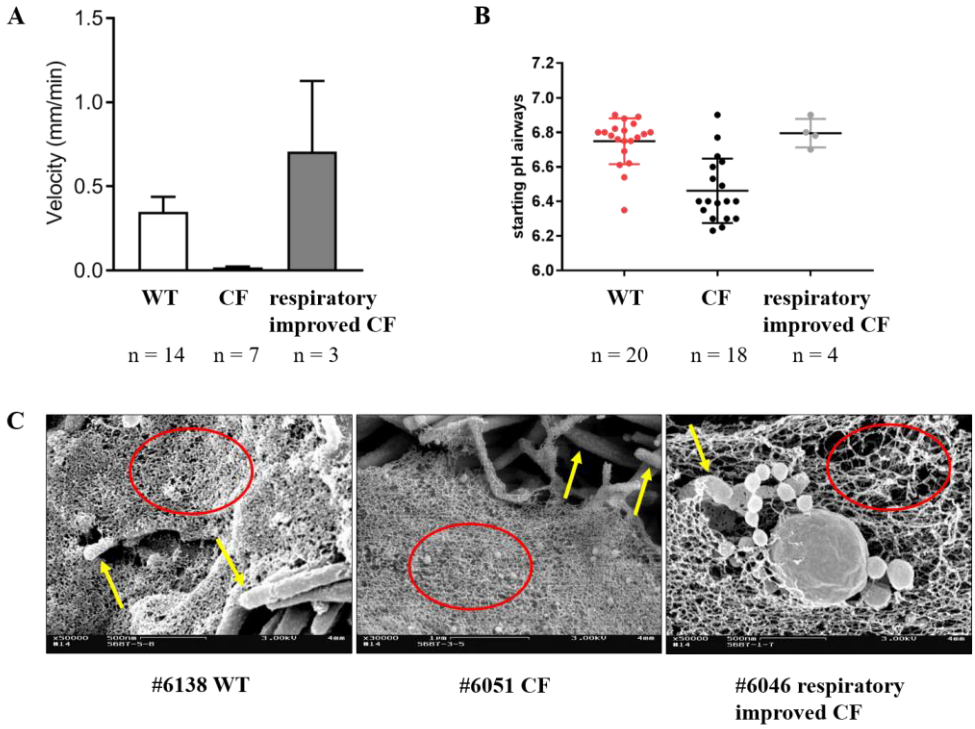

Figure 24: Further examination of tracheal tissue of respiratory improved *CFTR*$^{-/-}$ piglets compared with normal *CFTR*$^{-/-}$ piglets and WT piglets. (A) Analysis of the mucus bundle velocity. For visualizing, the mucus was stained with Alcian blue. The mean of five measurement points per time-lapse revealed that mucus transport in modified piglets is at least as fast as in WT ones, whereas

normal CFs did not show any mucus movement. (B) Surface pH measurement. Improved CF piglets and WT ones show a similar starting pH value of nearly 6.8, whereas normal CF animals exhibit a lower pH value of approximately 6.5. (C) Scanning electron microscopic (SEM) analysis. Red circles indicate the airway mucus network. Cilia are represented by yellow arrows. In the exemplary improved piglet, the mucus network seems to be more expanded than in the normal CF piglet that shows a more compressed network. The appearance of the airway mucus in the examined WT animal, is comparable to the modified pig (data kindly provided by Anna Ermund from the Mucin Biology Group at the University of Gothenburg, Sweden).

V. DISCUSSION

Although Cystic Fibrosis remains incurable, the overall knowledge about this monogenic disease appearing with striking phenotypic diversity, increased tremendously (reviewed in WEILER & DRUMM, 2013; O'NEAL & KNOWLES, 2018). Not only life expectancy, but also the quality of patients' life has significantly been improved over the last decades. The development of first animal models for CF just shortly after the identification of the disease-causing *CFTR* gene in 1989 (RIORDAN et al., 1989; SNOUWAERT et al., 1992), significantly contributed to this successful progression. Animal models turned out to be essential tools for a better understanding of pathophysiological mechanisms in CF and for developing new therapeutic approaches (reviewed in SEMANIAKOU et al., 2018). From the CF animal models developed so far in six species, the porcine CF model proves to be the model showing the closest similarity to hallmark features of human CF disease (reviewed in CUTTING, 2015) and it is therefore not surprising that CF pigs became an important model in CF research. However, a lethal neonatal intestinal obstruction by meconium represents a significant limitation in CF piglets. If MI is not corrected, CF piglets die within 48 hours after birth, considerably limiting the usage of pigs as animal models in CF research (KLYMIUK et al., 2012). While only 15-20 % of all CF infants (GUO et al., 2014) suffer from the intestinal obstruction, in CF piglets MI actually occurs with a penetrance of 100 % in both available CF pig models, in the United States as well as in Europe (ROGERS et al., 2008b; KLYMIUK et al., 2012). Nonetheless, a previous thesis done at the Chair for Molecular Animal Breeding and Biotechnology, describes the occurrence of three CF piglets (#2850, #3137 and #4424) that showed a clear improved intestinal phenotype as meconium has passed autonomously; all other characteristic features of CF, such as mucus sticking in the airways, a triangular trachea, hypoplastic exocrine pancreas and a micro-gallbladder, were still present (DMOCHEWITZ, 2016). Genome-wide analysis suggested two independent modifying loci on chromosome 10 (25.8–25.9 Mb) and on chromosome 16 (4.7–5.2 Mb) to rescue the severe intestinal phenotype. In my work, this hypothesis was tested. Therefore, the frequency of the promising genotype constellation on both candidate regions was

enriched in the CF breeding herd by selective breeding in order to increase the probability of the desired genotype constellation and the consequent expectation of additional CF piglets with an improved intestinal manifestation.

The relevance of the genetic background for an improved intestinal phenotype was evaluated by a genome-wide survey of single nucleotide polymorphism (SNP) variations using the PorcineSNP60 DNA Analysis Kit v2 (Illumina, San Diego, USA). The PorcineSNP60 v2 BeadChip is the most comprehensive genome-wide genotyping array for the porcine genome (RAMOS et al., 2009; ILLUMINA, 2020). It has been validated in seven economically important pig breeds, including Duroc, Landrace, Pietrain, Large White as well as in wild boar as the ancestor of all modern pig breeds. The chip features more than 64,232 SNPs that uniformly span the porcine genome with an average spacing of 43.4 kb, and thus enables a broad range of applications such as genome-wide selection, linkage disequilibrium studies, identification of quantitative trait loci, evaluation of genetic merit, cross-breed mapping, comparative genetic studies, and breed characterization for determining biodiversity. High call rates and accurate genotype calls ensuring the highest accuracy and reliability for successful whole-genome association studies. Overall, validation of the PorcineSNP60 v2 BeadChip proved it to be a valuable tool for most types of pig genetic studies (RAMOS et al., 2009).

The Axiom™ Porcine Genotyping Array even includes 658,692 SNPs, validated in a diverse set of commercial and non-commercial pig breeds (THERMOFISHER). An accordance with 56,000 SNPs of the PorcineSNP60 v2 BeadChip allows well compatibility with previous studies. A key benefit of this high-density array is the ability to genotype samples without experiencing marker dropout or missing data, which might occur with other porcine genotyping products. Compared with the PorcineSNP60 v2 BeadChip, the Axiom™ Porcine Genotyping Array offers the power for a more detailed fine mapping of the porcine genome. Nonetheless, considering the specification of the proposed haplotype constellation on chromosome 10 by six markers and on chromosome 16 by ten markers, it is questionable whether a denser coverage of the proposed modifying loci would be favorable. These concerns appear even more true if the costs (approximately tenfold) are considered. The very same is true also for whole-genome surveys; although they would allow the most comprehensive

evaluation of a genome (in case of the nucleotide resolution). Further, analysis can only be performed in specialized laboratories and the evaluation requires specific bioinformatic equipment and expertise. Finally, at this point in time, whole-genome approaches in the pig are limited by the low number of reference genome and would therefore require the sequencing of numerous control animals. For these reasons, we decided to do SNP typing with the PorcineSNP60 v2 BeadChip only.

Although the marker-based haplotyping of animals is an effective and relatively cheap option for identifying candidate regions, its application in daily routine is difficult. This is not only due to the requirement of high-quality DNA, the scale of 96 samples per run and the necessary access to specialized equipment, but also because genotyping of CF piglets needs to be carried out within the first hours after birth. To achieve this in a preferably simple, cheap and time-saving way, I established marker-specific genotyping PCRs. The discrimination PCRs distinguish the desired haplotypes at the modifier regions on chromosomes 10 and 16 from unwanted ones. In total, every single piglet of a litter was characterized by performing seven PCRs. PCR for *CFTR* genotyping comprises two PCRs amplifying the WT and the mutated *CFTR* sequence. Five additional PCRs discriminate genetic constellations at the candidate regions on chromosomes 10 and 16 (see chapter IV.1.1.2.). For marker 7 and marker 9 on chromosome 16, in each case, two individual PCRs were designed. One PCR determines the desired (“g”) haplotype, the second one detects the undesired (“b”) constellation. For marker 5 on chromosome 10 only one PCR was established that ruled out any unwanted haplotype.

The marker-based genotyping was first used to enrich the desired haplotypes in the breeding herd. After screening all available pigs of the breeding herd for the potential modifier loci on chromosomes 10 and 16, the pigs have been mated selectively according to their haplotype constellations. By mating with unrelated WT animals, the frequency of the desired genotype constellation in the breeding animals has been increased. By selective breeding, I obtained the desired haplotypes on chromosome 10 and on chromosome 16 in 10 out of 55 *CFTR*$^{-/-}$ piglets (see chapter IV.1.1.3.). However, none of these animals showed the previously described autonomous release of meconium. Even a macroscopic and histological examination of the exemplary CF piglet #6491 with the desired

genetic constellation, did not reveal any indicative improvement of the intestinal phenotype compared to the CF piglet #6345 which lacked the wanted genotype. The initial hypothesis of two independent loci on chromosome 10 and on chromosome 16 to protect *CFTR*$^{-/-}$ piglets from MI was therefore clearly rejected. The influence of the genetic background on the intestinal phenotype in the CF pig, based on the report on three closely related CF piglets that had passed meconium autonomously, is still likely. However, the small number of affected CF piglets (three out of 23 CF piglets that showed the initial gut-improved phenotype) suggests a low frequency of a protective genetic constellation in the original breeding herd. Furthermore, I propose that by following a wrong initial hypothesis, the rare beneficial genotype constellation was finally sorted out. It is likely that both, the marker-based selection of breeding animals as well as the outbreeding with unrelated WT animals contributed to this elimination.

Independently from the intestinal phenotype in CF pigs, a variant respiratory phenotype was observed in some CF piglets. During routine section it became obvious that three animals (#5703, #5704, #5786) differed from normal CF piglets by showing a WT-like round trachea with greater diameter, while their genotype and a significant MI clearly indicated common signs of CF (see chapter IV.2.2.). By systematically mating the parents of improved piglets (boar #5081, sow #5373), the randomly occurred improvement of the respiratory phenotype has been reproduced in two more *CFTR*$^{-/-}$ piglets (#6046, #6704). It is thus consequent to suppose that both, the intestinal as well as the respiratory phenotype in the CF pig are independently modified by variants of genetic background elements. A contribution of distinct genetic elements to the manifestation of the gut- and the lung-phenotype is very likely at the basis of the GWAS studies and reflects the situation in patients, where the phenotypical manifestation of CF in different organ systems uniquely responds to *CFTR* mutations and modifier effects (reviewed in WEILER & DRUMM, 2013; O'NEAL & KNOWLES, 2018). As early as 1990, the potential role of genetic modifiers in determining the complexity of CF, has been proposed (SANTIS et al., 1990). So far in human patients with CF, a variety of individual genetic modifiers for multiple CF phenotypes has been detected, though there is no single definitive contributor that universally predicts the disease severity or secondary complications (reviewed in DORFMAN, 2012). Rather combinations of several genetic variants seem to

contribute to overall disease manifestation.

Regarding the intestinal phenotype, studies in CF twins and siblings undoubtedly indicate a predominant impact of additional non-*CFTR* genetic modifiers on both, the contribution to and the protection from MI (BLACKMAN et al., 2006). Subsequent genome-wide analyses on human CF patients revealed a few potential candidate loci, including polymorphisms in the genes coding for several members of the solute carrier family, either promoting (*SLC6A14* on chromosome X, *SLC9A3* on chromosome 13, *SLC26A9* on chromosome 1) or preventing the development of MI (*SLC4A4* on chromosome 4) (DORFMAN et al., 2009; SUN et al., 2012). Just recently, two new potential modifier genes of MI have been identified, namely ATPase H^+/K^+ transporting non-gastric alpha2 subunit (*ATP12A*) on chromosome 13, and a suggestive locus on chromosome 7 near serine protease 1 (*PRSS1*) (GONG et al., 2019).

In CF patients carrying an identical *CFTR* genotype it was determined that genetic modifiers could account for 50-80 % of lung disease variability (VANSCOY et al., 2007). For the divergent pulmonary phenotype in humans, numerous modifier genes have been described, with transforming growth factor beta 1 (*TGFB1*) and mannose-binding lectin (*MBL*) being the first ones that have been identified (reviewed in SHANTHIKUMAR et al., 2019). Apart from *TGFB1* and *MBL*, there are other genes that have been suggested as potential modifiers, such as homeostatic iron regulator (*HFE*) (REID et al., 2004; PRATAP et al., 2010; SMITH et al., 2019), endothelin receptor type A (*EDNRA*) (DARRAH et al., 2010) and carcinoembryonic antigen-related cell adhesion molecules (*CEACAM*) (STANKE et al., 2010).

In contrast to the significant evidence of modifier genes for human CF disease, none such elements have been described in the pig so far. The most striking explanation for this finding is the limited number of CF piglets that have been produced. Even if the number of such animals in the US and European breeding herds reaches a several hundreds, the obviously limited genetic diversity in the breeding herds descending from a handful of individuals and their systematic breeding for less than ten generations, would prevent a constellation similar to humans where founder individuals have distributed their mutations among huge populations for centuries. Therefore, the appearance of unusual phenotypes in closely related $CFTR^{-/-}$ piglets showing either autonomous remove of meconium or a WT-like anatomy of the trachea, must be seen as strong evidences that also in

CF pigs modifier genes might play a crucial role in altering disease severity.

In parallel to testing the hypothesis of modifier loci on chromosome 10 and on chromosome 16 by marker-assisted breeding, a detailed analysis of the candidate region on chromosome 10 has been conducted. Based on the assumption that a potential causative mutation would preferentially be located in a region with a specific function and that such functional region would often be conserved between species, we performed a multi-species alignment of the candidate region on chromosome 10 and identified genetic elements proposed by different prediction tools. This procedure suggested three regions of several kb size which were therefore examined by Sanger sequencing in animals of the different marker-defined haplotypes “g/g”, “g/b” and “b/b”. The identified SNPs in locus 1 and locus 2 did not reveal a pattern according to the marker-based analysis, and locus 3 did not reveal any polymorphisms between the different c105 haplotypes. As this finding correlated to the results from the selected breeding procedure, the initial hypothesis of modifier regions on chromosome 10 and on chromosome 16 was finally rejected. For reasons of completeness, however, one could question, if not a region outside the three examined loci contained a genetic variant responsible for the differences in the intestinal phenotype. Although this cannot be excluded, I think the assumption of functional properties in conserved and/or annotated genetic elements is a valuable and efficient strategy. Notably, not only the GeneScan tool predicted locus 1 and locus 2 as significant genetic elements, but both loci are also characterized by high homology among different species. Assuming the maintenance of genetic elements during the evolution only in the case of a beneficial function, this finding implies a potential regulatory function of locus 1 and locus 2. The finding of a potential regulatory capacity of two loci by the PreMod database, supports this consideration. No other region within the candidate region on chromosome 10, except the terminal exon of NEK7 (locus 3) showed similar evidence for a potential regulatory function. On the other hand, there is also evidence that such biased assumptions do not always correctly identify all regulatory elements. This is particularly true if such elements are species-specific. Two such examples have previously been published in the cattle: The first one was the responsibility of genetic duplications, located in a large intergenic region, for genetically induced lack of horn (MEDUGORAC et al., 2012). Although the mechanism of how these mutations prevent the growing of

horn is not completely understood (reviewed in ALDERSEY et al., 2020), the introgression of such a modification by gene editing proved transformation of a horned cattle genome into a polled version (TAN et al., 2013). The second one was the identification of a common, dominant genetic variant that causes a white belt around the body of otherwise colored cattle (AWASTHI MISHRA et al., 2017; ROTHAMMER et al., 2018). Again, the causative mutation is fairly distant to its closest annotated genetic element, TWIST2. Importantly, however, both phenotypic characteristics, the formation of horned appendices at the skull bones and the coloring of fur are definitely species-specific artifacts which is in strong contrast to the functional conservation of the *CFTR*-encoded anion channel.
Since the examination of chromosome 10 did not provide a possible explanation for a diverse manifestation of the CF gut-phenotype, and although I succeeded in enriching the desired genotype constellation on chromosome 10 and on chromosome 16 in almost 10 *CFTR*$^{-/-}$ piglets, but none of them showed an obvious improvement regarding the intestinal obstruction by meconium, the second postulated candidate region on chromosome 16 was not taken in further consideration.

Although the initial hypothesis of two independent loci on chromosomes 10 and 16 to protect CF piglets from MI has clearly been rejected by different methods, the assumption of a genetic background influencing the severity of the CF gut-phenotype appeared still convincing. Therefore, we conducted a second genome-wide survey (see also chapter IV.1.2.). For SNP-typing we employed the same genotyping array as used for the first analysis, namely the PorcineSNP60 v2 BeadChip (Illumina, San Diego, USA), but this time mapping was performed under more favorable conditions. Not only the amount of examined CF piglets showing the typical MI was extended to overall 198 animals, including 143 animals that have been investigated in the first GWAS and 55 additional piglets, but also 14 new heterozygous breeding animals have been incorporated into the pedigree. By integrating an extended population of control animals in the genotyping, the probability to figure out appropriate candidate regions along the porcine genome allowing for a proper distinction between the modified and the normal gut-phenotype in CF pigs, is increasing respectively. To analyze the obtained data, an alternative method based on a combined linkage disequilibrium and linkage analysis (cLDLA) has been applied corresponding to the method

proposed by MEUWISSEN et al. (2002). The cLDLA approach, based on reconstructed haplotypes, facilitate a more precise mapping and proved to be less sensitive to the absence of error-free marker maps and perfectly associated SNP than the SNP-GWAS approach (MEDUGORAC et al., 2017; MÜLLER et al., 2017). In view of promising results that have been realized in former studies, the alternative cLDLA method was considered as a useful complementary approach to the standard GWAS (ROTHAMMER et al., 2014; KUNZ et al., 2016). In this way, the analysis of our extended data set revealed two alternative candidate regions on chromosome 5 and on chromosome 13 potentially modifying the severity of the CF intestinal phenotype in pigs. A further examination of the two loci resulted in interesting features:

The first candidate region on chromosome 5 is packed by almost 12 genes. Because it is difficult to predict a causative variation among this high density of genes, the expression rate of every gene or genetic element in a broad spectrum of different organs as well as their described function according to the current literature has been checked in order to estimate a possible impact on modifying the CF gut-phenotype. In doing so, *ATP6V1E1*, located within the center of the candidate region, turned out to be a very promising one as its encoded protein is a component of the multi-unit vacuolar ATPase, a proton pump acting on the acidification of intracellular organelles and extracellular compartments (MCGUIRE et al., 2017). In view of an impaired regulation of the pH in the case of lacking *CFTR*, the involvement of *ATP6V1E1* in compensating this deficit, constitutes a logical approach. The consequences of lacking *CFTR* on lysosomal acidification are discussed contradictory (TEICHGRABER et al., 2008; HAGGIE & VERKMAN, 2009), however, there is no doubt about a co-localization of the vacuolar ATPase with CFTR on the apical side of respiratory epithelial cells (JAKAB et al., 2013; PLASSCHAERT et al., 2018). It is interesting to note that in human and other mammalian species, another anion channel, SLC25A18, is included in this region, but in sheep, cattle and pig it is lacking due to a large genomic deletion. Therefore, it has not been considered as a possible modifier of the intestinal phenotype in the CF pig model.

The second candidate region on chromosome 13 comprises only four genes and an implemented haplotype analysis restricted the region to a size of 180 kb. This segment resembles the upstream region of *TGFBR2*, including some of its well-characterized enhancer elements. While this region is apparently lost in pair-toed

species, it is partially highly conserved in the other investigated animals. *TGFB* is well known to modify pulmonary disease in CF (DRUMM et al., 2005; BREMER et al., 2008) and also its function as a promoter of growth in the intestinal epithelium is considered as secure (BARNARD et al., 1989). *TGFBR2* itself plays an important role in cell proliferation, including the continuous turnover of epithelial cells in the gut (FLENTJAR et al., 2007; ZHANG et al., 2016). A loss of function causes structural and functional damage of intestinal organoids (IHARA et al., 2018). Interestingly, a recent study of KLUGE et al. (2019) demonstrated a direct interaction between the *TGFB*-signaling axis and *ATP6V1E1* in regulating the extracellular bicarbonate concentration by epithelial cells. This finding supports the assumption of an independent or synergistic involvement of both proposed genes in controlling the extracellular pH and bicarbonate concentration of the intestine.

Taken together, an involvement of genetic variants of *ATP6V1E1* on chromosome 5 as well as *TGFBR2* on chromosome 13 in modifying the severity of the gut-phenotype in CF pigs deserves further attention. However, the new hypothesis has to be verified in future studies, whereby a more detailed characterization of the two submitted modifier genes is necessary. A first attempt would be the detailed sequencing of the candidate region, which has become a valuable approach due to the dramatically decreasing costs of whole-genome sequencing approaches. On the other hand, the limited availability of reference genomes as well requires the examination of numerous control animals, which makes this approach a demanding exploration. Second, the reproduction of suitable parental animals might produce new CF piglets with an improved phenotype and facilitates a more profound analysis of the genetic background. However, both strategies are time-consuming and therefore could not be conducted during my thesis. So far, there is good evidence for an influence of the genetic background on the gut-phenotype in our CF pig herd, but the exact molecular constellation still has to be identified. Pursuing the idea of a marker-assisted breeding will help to shape the genetic constellation of the breeding animals towards a regular production of CF piglets with an improved intestinal phenotype. Surviving the first critical days of life, will make the CF pig an ideal animal model for CF. It paves the way for a better long-term evaluation of the disease and allows for systematic preclinical testing of potential new forms of Cystic Fibrosis therapy.

As the new respiratory phenotype constitutes an interesting new modification of the CF pig model, it is crucial to analyze it in more detail. For a more precise description, it will be essential to increase the number of experimental animals. Since we did not obtain further animals with a similar modification of the respiratory CF phenotype after retiring the parental animals of the improved piglets from our breeding herd, new CF piglets must be generated in another way. One possible option is the re-cloning of one of the modified CF piglets via SCNT and ET. The production of airway-improved CF pigs by re-cloning is a fast and efficient method to generate a small number of animals with the desired genotype. However, it has to be considered that the re-cloned piglets might not exhibit the same level of improvement as the donor animals or even do not show any modification compared with normal CF piglets. In addition, this method is not suitable to produce a large number of viable animals due to a usually low cloning efficiency and a high rate of phenotypical abnormalities, so-called cloning artefacts, that might be explained with epigenetic reprogramming or genomic damage of the donor cells (CHO et al., 2007; HÖRMANSEDER et al., 2017). Alternatively, the parental animals of the airway-improved CF piglets themselves could be re-cloned and selectively mated at sexual maturity enabling a conventional breeding of a larger number of piglets. Nevertheless, this approach is very time-consuming and again, it is not certain if the resulting CF piglets will exhibit the desired phenotypical modification of the airways.

The new improved respiratory phenotype in the CF pig opens new prospects for the Cystic Fibrosis research and can thereby lead to a better understanding of pathophysiological mechanism of the disease.

VI. SUMMARY

Modifier genes of the intestinal and respiratory phenotype in Cystic Fibrosis pigs

Cystic Fibrosis (CF) is the most common lethal, autosomal recessive hereditary disease among Caucasians and affects more than 100,000 people worldwide. It is caused by mutations in the gene coding for the anion channel Cystic Fibrosis Transmembrane Conductance Regulator (CFTR), leading to a defective transepithelial electrolyte transport. While CF constitutes a multisystemic disease mainly affecting the airways, the gastrointestinal tract and the pancreas, the major cause for the decreased survival rate of CF patients is traced to pulmonary insufficiency. The overall knowledge about the disease increased tremendously, so that not only life expectancy of up to 40 years, but also the quality of patients' life has significantly been improved over the last decades.

From the CF animal models developed so far in six species, the porcine CF model proves to be the model showing the closest similarity to human CF disease. However, since a lethal neonatal meconium ileus (MI) occurs in 100 % of all CF piglets, the use of the pig as an animal model for CF is strongly limited. Nonetheless, a previous thesis done at the Chair for Molecular Animal Breeding and Biotechnology, describes the occurrence of three CF piglets that showed an improved intestinal phenotype as meconium has passed autonomously. An implemented genome-wide association study resulted in the hypothesis of two potential modifier loci on chromosome 10 (25.8–25.9 Mb) and on chromosome 16 (4.7–5.2 Mb) to rescue the severe gut-phenotype, whereby the three rectified piglets were homozygous for a specific haplotype at both loci.

As the aim of my thesis was to test this hypothesis, it was necessary to enrich the desired genetic constellation on both candidate regions in the CF breeding herd in order to increase the probability of generating CF piglets with the specific haplotypes. For this purpose, the CF breeding herd was screened for the proposed modifier loci by detecting informative markers. In addition, marker-specific PCRs have been established that discriminate the desired haplotype from any of the non-desired constellations. By selected mating, I succeeded in enriching the wanted

genotype in 10 CF piglets, but none of these animals showed the previously described improvement of the gut-phenotype. This finding was confirmed by a macroscopic and histological examination and correlated to the detailed SNP-based examination of the candidate region on chromosome 10 as the identified SNP patterns were not consistent with the marker-defined haplotypes. The initial hypothesis of a beneficial influence of the postulated regions on chromosomes 10 and 16 was therefore fully rejected. Instead, an alternative investigation of a more extended population of CF animals, based on a combined linkage disequilibrium and linkage analysis (cLDLA), revealed two new candidate regions on chromosome 5 and on chromosome 13 and suggested the potential involvement of genetic variants of *ATP6V1E1* (chromosome 5) and *TGFBR2* (chromosome 13).

Independently from the CF gut-phenotype, a variant respiratory phenotype was observed in some CF piglets during my thesis. These animals differed from normal CF piglets by showing a WT-like round trachea with greater diameter, while their genotype and a significant MI clearly indicated common signs of CF.

VII. ZUSAMMENFASSUNG

Modifier-Gene des intestinalen und respiratorischen Phänotyps in Schweinen mit Mukoviszidose

Die Mukoviszidose, auch zystische Fibrose (ZF) genannt, stellt die häufigste tödliche, autosomal rezessive Erbkrankheit unter Kaukasiern dar und betrifft weltweit mehr als 100.000 Menschen. Sie wird verursacht durch Mutationen im Gen, das für den Anionenkanal Cystic Fibrosis Transmembrane Conductance Regulator (CFTR) codiert, welche zu einem fehlerhaften transepithelialen Elektrolyttransport führen. Obwohl ZF eine multisystemische Erkrankung darstellt, welche hauptsächlich die Atemwege, den Verdauungstrakt sowie das Pankreas betrifft, ist die Hauptursache für die eingeschränkte Lebenserwartung der ZF-Patienten auf eine Lungeninsuffizienz zurückzuführen. Das allgemeine Wissen um die Krankheit hat sich enorm erweitert, sodass sich in den vergangenen Jahrzehnten nicht nur die Lebenserwartung der Patienten auf bis zu 40 Jahren erhöhte, sondern sich auch deren Lebensqualität signifikant verbesserte.
Von den bislang entwickelten sechs ZF-Tiermodellen, erweist sich das porcine Modell als dasjenige, welches die größte Ähnlichkeit mit der menschlichen ZF-Erkrankung aufweist. Dennoch ist der Nutzen des Schweins als Tiermodell für die Mukoviszidose stark begrenzt, da in 100 % aller ZF-Ferkel ein tödlicher neonataler Mekoniumileus (MI) auftritt. Nichtsdestotrotz beschreibt eine vorhergehende Doktorarbeit, erarbeitet am Lehrstuhl für Molekulare Tierzucht und Biotechnologie, das Vorkommen von drei ZF-Ferkeln, welche durch das selbstständige Absetzen von Mekonium einen verbesserten intestinalen Phänotyp aufzeigten. Eine durchgeführte genomweite Assoziationsstudie resultierte in der Hypothese zweier möglicher Modifier-Regionen auf Chromosom 10 (25,8-25,9 Mb) und auf Chromosom 16 (4,7-5,2 Mb), die vor einer schwerwiegenden Ausprägung des Darmphänotyps bewahren sollen, wobei die drei verbesserten Ferkel homozygot für einen bestimmten Haplotyp auf beiden Regionen waren. Da es das Ziel meiner Doktorarbeit war, diese Hypothese zu testen, war es notwendig, die gewünschte genetische Konstellation auf beiden Kandidatenregionen in der ZF-Zuchtherde anzureichern, um die

Wahrscheinlichkeit zu erhöhen, ZF-Ferkel mit den spezifischen Haplotypen zu produzieren. Aus diesem Grund wurde die ZF-Zuchtherde auf die vorgeschlagenen Modifier-Regionen überprüft, indem aussagekräftige Marker festgestellt wurden. Darüber hinaus wurden markerspezifische PCRs etabliert, welche den gewünschten Haplotyp von allen unerwünschten Konstellationen unterscheiden. Durch gezielte Verpaarung gelang es mir, den gesuchten Genotyp in 10 ZF-Ferkeln anzureichern, aber keines dieser Tiere zeigte die zuvor beschriebene Verbesserung des Darmphänotyps. Dieses Ergebnis wurde mit Hilfe makroskopischer und histologischer Untersuchung überprüft und korrelierte mit der ausführlichen, auf SNPs basierenden Untersuchung der Kandidatenregion auf Chromosom 10, da die Muster der identifizierten SNPs nicht mit den marker-definierten Haplotypen übereinstimmten. Die ursprüngliche Hypothese eines günstigen Einflusses der vorgeschlagenen Regionen auf den Chromosomen 10 und 16 wurde deshalb vollständig widerlegt. Stattdessen brachte die alternative Untersuchung eines erweiterten ZF-Tierbestandes, beruhend auf der cLDLA-Methode, zwei neue Kandidatenregionen auf Chromosom 5 und auf Chromosom 13 zum Vorschein und unterstellte eine mögliche Beteiligung genetischer Varianten von *ATP6V1E1* (Chromosom 5) und *TGFBR2* (Chromosom 13).

Unabhängig vom ZF-Darmphänotyp konnte während meiner Doktorarbeit in einigen ZF-Ferkeln ein abweichender respiratorischer Phänotyp festgestellt werden. Diese Tiere unterschieden sich von normalen ZF-Ferkeln, indem sie eine WT-ähnliche runde Trachea mit größerem Durchmesser aufwiesen, wohingegen ihr Genotyp sowie ein signifikanter MI eindeutig auf übliche Anzeichen von Mukoviszidose hinwiesen.

VIII. INDEX OF FIGURES

IX. INDEX OF TABLES

X. REFERENCES

Agrons GA, Corse WR, Markowitz RI, Suarez ES, Perry DR. Gastrointestinal manifestations of Cystic Fibrosis: radiologic-pathologic correlation. Radiographics 1996; 16: 871-93.

Ahmadi S, Xia S, Wu YS, Di Paola M, Kissoon R, Luk C, Lin F, Du K, Rommens J, Bear CE. SLC6A14, an amino acid transporter, modifies the primary CF defect in fluid secretion. Elife 2018; 7: e37963.

Aigner B, Renner S, Kessler B, Klymiuk N, Kurome M, Wunsch A, Wolf E. Transgenic pigs as models for translational biomedical research. J Mol Med 2010; 88: 653-64.

Akhurst RJ. TGF beta signaling in health and disease. Nat Genet 2004; 36: 790-92.

Aldersey JE, Sonstegard TS, Williams JL, Bottema CDK. Understanding the effects of the bovine polled variants. Anim Genet 2020; 51: 166-76.

Amodio J, Berdon W, Abramson S, Stolar C. Microcolon of prematurity: a form of functional obstruction. AJR 1986; 146: 239-44.

Andersen DH. Cystic Fibrosis of the pancreas and its relation to celiac disease: a clinical and pathologic study. JAMA Pediatrics 1938; 56: 344-99.

Arora K, Huang Y, Mun K, Yarlagadda S, Sundaram N, Kessler MM, Hannig G, Kurtz CB, Silos-Santiago I, Helmrath M, Palermo JJ, Clancy JP, Steinbrecher KA, Naren AP. Guanylate cyclase 2C agonism corrects CFTR mutants. JCI Insight 2017; 2: e93686.

Averill S, Lubner MG, Menias CO, Bhalla S, Mellnick VM, Kennedy TA,

Pickhardt PJ. Multisystem imaging findings of Cystic Fibrosis in adults: recognizing typical and atypical patterns of disease. AJR 2017; 209: 3-18.

Awasthi Mishra N, Drogemuller C, Jagannathan V, Keller I, Wuthrich D, Bruggmann R, Beck J, Schutz E, Brenig B, Demmel S, Moser S, Signer-Hasler H, Pienkowska-Schelling A, Schelling C, Sande M, Rongen R, Rieder S, Kelsh RN, Mercader N, Leeb T. A structural variant in the 5'-flanking region of the TWIST2 gene affects melanocyte development in belted cattle. PLoS One 2017; 12: e0180170.

Ballard ST, Evans JW, Drag HS, Schuler M. Pathophysiologic evaluation of the transgenic CFTR "gut-corrected" porcine model of Cystic Fibrosis. Am J Physiol Lung Cell Mol Physiol 2016; 311: L779-87.

Barnard JA, Beauchamp RD, Coffey RJ, Moses HL. Regulation of intestinal epithelial cell growth by transforming growth factor type beta. Proc Natl Acad Sci USA 1989; 86: 1578-82.

Bergstrom JH, Birchenough GM, Katona G, Schroeder BO, Schutte A, Ermund A, Johansson ME, Hansson GC. Gram-positive bacteria are held at a distance in the colon mucus by the lectin-like protein ZG16. Proc Natl Acad Sci USA 2016; 113: 13833-38.

Birket SE, Chu KK, Liu L, Houser GH, Diephuis BJ, Wilsterman EJ, Dierksen G, Mazur M, Shastry S, Li Y, Watson JD, Smith AT, Schuster BS, Hanes J, Grizzle WE, Sorscher EJ, Tearney GJ, Rowe SM. A functional anatomic defect of the Cystic Fibrosis airway. Am J Respir Crit Care Med 2014; 190: 421-32.

Blackman SM, Deering-Brose R, McWilliams R, Naughton K, Coleman B, Lai T, Algire M, Beck S, Hoover-Fong J, Hamosh A, Fallin MD, West K, Arking DE, Chakravarti A, Cutler DJ, Cutting GR. Relative contribution of genetic and nongenetic modifiers to intestinal obstruction in Cystic Fibrosis. Gastroenterology 2006; 131: 1030-39.

Blackman SM, Hsu S, Vanscoy LL, Collaco JM, Ritter SE, Naughton K, Cutting GR. Genetic modifiers play a substantial role in diabetes complicating Cystic Fibrosis. J Clin Endocrinol Metab 2009; 94: 1302-09.

Boucher RC. Evidence for airway surface dehydration as the initiating event in CF airway disease. J Intern Med 2007; 261: 5-16.

Bradley PA, Bourne FJ, Brown PJ. The respiratory tract immune system in the pig: I. Distribution of immunoglobulin-containing cells in the respiratory tract mucosa. Vet Pathol 1976; 13: 81-9.

Bremer LA, Blackman SM, Vanscoy LL, McDougal KE, Bowers A, Naughton KM, Cutler DJ, Cutting GR. Interaction between a novel TGFB1 haplotype and CFTR genotype is associated with improved lung function in Cystic Fibrosis. Hum Mol Genet 2008; 17: 2228-37.

Brodlie M, Haq IJ, Roberts K, Elborn JS. Targeted therapies to improve CFTR function in Cystic Fibrosis. Genome Med 2015; 7: 101.

Büscher R, Grasemann H. Disease modifying genes in Cystic Fibrosis: therapeutic option or one-way road? Naunyn-Schmiedeberg's Arch Pharmacol 2006; 374: 65-77.

Castellani C, Southern KW, Brownlee K, Dankert Roelse J, Duff A, Farrell M, Mehta A, Munck A, Pollitt R, Sermet-Gaudelus I, Wilcken B, Ballmann M, Corbetta C, de Monestrol I, Farrell P, Feilcke M, Ferec C, Gartner S, Gaskin K, Hammermann J, Kashirskaya N, Loeber G, Macek M, Jr., Mehta G, Reiman A, Rizzotti P, Sammon A, Sands D, Smyth A, Sommerburg O, Torresani T, Travert G, Vernooij A, Elborn S. European best practice guidelines for Cystic Fibrosis neonatal screening. J Cyst Fibros 2009; 8: 153-73.

Castellani C, Assael BM. Cystic Fibrosis: a clinical view. Cell Mol Life Sci 2017; 74: 129-40.

Castellani C, Duff AJA, Bell SC, Heijerman HGM, Munck A, Ratjen F, Sermet-Gaudelus I, Southern KW, Barben J, Flume PA, Hodková P, Kashirskaya N, Kirszenbaum MN, Madge S, Oxley H, Plant B, Schwarzenberg SJ, Smyth AR, Taccetti G, Wagner TOF, Wolfe SP, Drevinek P. ECFS best practice guidelines: the 2018 revision. J Cyst Fibros 2018a; 17: 153-78.

Castellani S, Di Gioia S, di Toma L, Conese M. Human cellular models for the investigation of lung inflammation and mucus production in Cystic Fibrosis. Anal Cell Pathol 2018b; 2018: 3839803; doi: 10.1155/2018/.

CFTR1. Cystic Fibrosis Mutation Database. 2015: http://www.genet.sickkids.on.ca/cftr/app. accessed Sept 15th, 2019.

Chen JH, Stoltz DA, Karp PH, Ernst SE, Pezzulo AA, Moninger TO, Rector MV, Reznikov LR, Launspach JL, Chaloner K, Zabner J, Welsh MJ. Loss of anion transport without increased sodium absorption characterizes newborn porcine Cystic Fibrosis airway epithelia. Cell 2010; 143: 911-23.

Cheng K, Ashby D, Smyth RL. Oral steroids for long-term use in Cystic Fibrosis. Cochrane Database Syst Rev 2013: CD000407; doi: 10.1002/14651858.CD000407.pub3.

Cho SK, Kim JH, Park JY, Choi YJ, Bang JI, Hwang KC, Cho EJ, Sohn SH, Uhm SJ, Koo DB, Lee KK, Kim T, Kim JH. Serial cloning of pigs by somatic cell nuclear transfer: restoration of phenotypic normality during serial cloning. Dev Dyn 2007; 236: 3369-82.

Collaco JM, Vanscoy L, Bremer L, McDougal K, Blackman SM, Bowers A, Naughton K, Jennings J, Ellen J, Cutting GR. Interactions between secondhand smoke and genes that affect Cystic Fibrosis lung disease. Jama 2008; 299: 417-24.

Course CW, Hanks R. Newborn screening for Cystic Fibrosis: Is there benefit for everyone? Paediatr Respir Rev 2019; 31: 3-5.

Cutting GR. Modifier genes in Mendelian disorders: the example of Cystic Fibrosis. Ann N Y Acad Sci 2010; 1214: 57-69.

Cutting GR. Cystic Fibrosis genetics: from molecular understanding to clinical application. Nat Rev Genet 2015; 16: 45-56.

Darrah R, McKone E, O'Connor C, Rodgers C, Genatossio A, McNamara S, Gibson R, Stuart Elborn J, Ennis M, Gallagher CG, Kalsheker N, Aitken M, Wiese D, Dunn J, Smith P, Pace R, Londono D, Goddard KA, Knowles MR, Drumm ML. EDNRA variants associate with smooth muscle mRNA levels, cell proliferation rates, and Cystic Fibrosis pulmonary disease severity. Physiol Genomics 2010; 41: 71-7.

Davies J, Alton E, Griesenbach U. Cystic Fibrosis modifier genes. J R Soc Med 2005; 98 (Suppl 45): 47-54.

Davis PB. Cystic Fibrosis since 1938. Am J Respir Crit Care Med 2006; 173: 475-82.

De Boeck K, Vermeulen F, Dupont L. The diagnosis of Cystic Fibrosis. Presse Med 2017; 46: e97-e108.

Di Sant'Agnese PA, Darling RC, Perera GA, Shea E. Abnormal electrolyte composition of sweat in Cystic Fibrosis of the pancreas: clinical significance and relationship to the disease. Pediatrics 1953; 12: 549-63.

Dmochewitz MD. The pig as an animal model for Cystic Fibrosis: approaches to overcome the lethal intestinal phenotype. LMU Munich 2016: Thesis.

Dorfman R, Sandford A, Taylor C, Huang B, Frangolias D, Wang Y, Sang R, Pereira L, Sun L, Berthiaume Y, Tsui L-C, Paré PD, Durie P, Corey M, Zielenski J. Complex two-gene modulation of lung disease severity in children with Cystic Fibrosis. J Clin Invest 2008; 118: 1040-49.

Dorfman R, Li W, Sun L, Lin F, Wang Y, Sandford A, Paré PD, McKay K, Kayserova H, Piskackova T, Macek M, Czerska K, Sands D, Tiddens H, Margarit S, Repetto G, Sontag MK, Accurso FJ, Blackman S, Cutting GR, Tsui L-C, Corey M, Durie P, Zielenski J, Strug LJJHG. Modifier gene study of meconium ileus in Cystic Fibrosis: statistical considerations and gene mapping results. 2009; 126: 763-78.

Dorfman R. Modifier gene studies to identify new therapeutic targets in Cystic Fibrosis. Curr Pharm Des 2012; 18: 674-82.

Drumm ML, Konstan MW, Schluchter MD, Handler A, Pace R, Zou F, Zariwala M, Fargo D, Xu A, Dunn JM, Darrah RJ, Dorfman R, Sandford AJ, Corey M, Zielenski J, Durie P, Goddard K, Yankaskas JR, Wright FA, Knowles MR. Genetic modifiers of lung disease in Cystic Fibrosis. N Engl J Med 2005; 353: 1443-53.

Dupuis A, Keenan K, Ooi CY, Dorfman R, Sontag MK, Naehrlich L, Castellani C, Strug LJ, Rommens JM, Gonska T. Prevalence of meconium ileus marks the severity of mutations of the Cystic Fibrosis Transmembrane Conductance Regulator (CFTR) gene. Genet Med 2016; 18: 333-40.

Durno C, Corey M, Zielenski J, Tullis E, Tsui LC, Durie P. Genotype and phenotype correlations in patients with Cystic Fibrosis and pancreatitis. Gastroenterology 2002; 123: 1857-64.

Edenborough FP. Women with Cystic Fibrosis and their potential for reproduction. Thorax 2001; 56: 649-55.

Fan Z, Perisse IV, Cotton CU, Regouski M, Meng Q, Domb C, Van Wettere AJ, Wang Z, Harris A, White KL, Polejaeva IA. A sheep model of Cystic Fibrosis generated by CRISPR/Cas9 disruption of the CFTR gene. JCI Insight 2018; 3: e123529.

Fanen P, Wohlhuter-Haddad A, Hinzpeter A. Genetics of Cystic Fibrosis: CFTR

mutation classifications toward genotype-based CF therapies. Int J Biochem Cell Biol 2014; 52: 94-102.

Fiorotto R, Amenduni M, Mariotti V, Cadamuro M, Fabris L, Spirli C, Strazzabosco M. Animal models for Cystic Fibrosis liver disease (CFLD). BBA - Mol Basis Dis 2019; 1865: 965-69.

Fisher JT, Zhang Y, Engelhardt JF. Comparative biology of Cystic Fibrosis animal models. Methods Mol Biol 2011; 742: 311-34.

Flentjar N, Chu PY, Ng AY, Johnstone CN, Heath JK, Ernst M, Hertzog PJ, Pritchard MA. TGF-betaRII rescues development of small intestinal epithelial cells in Elf3-deficient mice. Gastroenterology 2007; 132: 1410-19.

Gawenis LR, Bradford EM, Prasad V, Lorenz JN, Simpson JE, Clarke LL, Woo AL, Grisham C, Sanford LP, Doetschman T, Miller ML, Shull GE. Colonic anion secretory defects and metabolic acidosis in mice lacking the NBC1 Na+/HCO3- cotransporter. J Biol Chem 2007; 282: 9042-52.

Gentzsch M, Mall MA. Ion channel modulators in Cystic Fibrosis. Chest 2018; 154: 383-93.

Gibson LE, Cooke RE. A test for concentration of electrolytes in sweat in Cystic Fibrosis of the pancreas utilizing pilocarpine by iontophoresis. Pediatrics 1959; 23: 545-49.

Gill DR, Hyde SC. Delivery of genes into the CF airway. Thorax 2014; 69: 962-64.

Goldman MJ, Anderson GM, Stolzenberg ED, Kari UP, Zasloff M, Wilson JM. Human beta-defensin-1 is a salt-sensitive antibiotic in lung that is inactivated in Cystic Fibrosis. Cell 1997; 88: 553-60.

Gong J, Wang F, Xiao B, Panjwani N, Lin F, Keenan K, Avolio J, Esmaeili M, Zhang L, He G, Soave D, Mastromatteo S, Baskurt Z, Kim S, O'Neal WK, Polineni D, Blackman SM, Corvol H, Cutting GR, Drumm M, Knowles MR, Rommens JM, Sun L, Strug LJ. Genetic association and transcriptome integration identify contributing genes and tissues at Cystic Fibrosis modifier loci. PLoS Genet 2019; 15: e1008007.

Grainger DJ, Heathcote K, Chiano M, Snieder H, Kemp PR, Metcalfe JC, Carter ND, Spector TD. Genetic control of the circulating concentration of transforming growth factor type beta1. Hum Mol Genet 1999; 8: 93-7.

Grubb BR, Boucher RC. Pathophysiology of gene-targeted mouse models for Cystic Fibrosis. Physiol Rev 1999; 79: S193-214.

Guilbault C, Saeed Z, Downey GP, Radzioch D. Cystic Fibrosis mouse models. Am J Respir Cell Mol Biol 2007; 36: 1-7.

Guillon A, Chevaleyre C, Barc C, Berri M, Adriaensen H, Lecompte F, Villemagne T, Pezant J, Delaunay R, Moenne-Loccoz J, Berthon P, Bahr A, Wolf E, Klymiuk N, Attucci S, Ramphal R, Sarradin P, Buzoni-Gatel D, Si-Tahar M, Caballero I. Computed Tomography (CT) scanning facilitates early identification of neonatal Cystic Fibrosis piglets. PLoS One 2015; 10: e0143459.

Guo X, Pace RG, Stonebraker JR, O'Neal WK, Knowles MR. Meconium ileus in Cystic Fibrosis is not linked to central repetitive region length variation in MUC1, MUC2, and MUC5AC. J Cyst Fibros 2014; 13: 613-16.

Haggie PM, Verkman AS. Unimpaired lysosomal acidification in respiratory epithelial cells in Cystic Fibrosis. J Biol Chem 2009; 284: 7681-86.

Harutyunyan M, Huang Y, Mun KS, Yang F, Arora K, Naren AP. Personalized medicine in CF: from modulator development to therapy for Cystic Fibrosis patients with rare CFTR mutations. Am J Physiol Lung Cell Mol Physiol 2018; 314: L529-43.

Henderson LB, Doshi VK, Blackman SM, Naughton KM, Pace RG, Moskovitz J, Knowles MR, Durie PR, Drumm ML, Cutting GR. Variation in MSRA modifies risk of neonatal intestinal obstruction in Cystic Fibrosis. PLoS Genet 2012; 8: e1002580.

Hodson ME, Simmonds NJ, Warwick WJ, Tullis E, Castellani C, Assael B, Dodge JA, Corey M. An international/multicentre report on patients with Cystic Fibrosis (CF) over the age of 40 years. J Cyst Fibros 2008; 7: 537-42.

Hörmanseder E, Simeone A, Allen GE, Bradshaw CR, Figlmuller M, Gurdon J, Jullien J. H3K4 methylation-dependent memory of somatic cell identity inhibits reprogramming and development of nuclear transfer embryos. Cell Stem Cell 2017; 21: 135-43.

Hurley MN, McKeever TM, Prayle AP, Fogarty AW, Smyth AR. Rate of improvement of CF life expectancy exceeds that of general population - observational death registration study. J Cyst Fibros 2014; 13: 410-15.

Ihara S, Hirata Y, Hikiba Y, Yamashita A, Tsuboi M, Hata M, Konishi M, Suzuki N, Sakitani K, Kinoshita H, Hayakawa Y, Nakagawa H, Ijichi H, Tateishi K, Koike K. Adhesive interactions between mononuclear phagocytes and intestinal epithelium perturb normal epithelial differentiation and serve as a therapeutic target in Inflammatory Bowel Disease. J Crohns Colitis 2018; 12: 1219-31.

Illumina. PorcineSNP60 v2 Genotyping BeadChip. 2020: https://www.illumina.com/products/by-type/microarray-kits/porcine-snp60.html. accessed Jan 22th, 2020.

Ivanov M, Matsvay A, Glazova O, Krasovskiy S, Usacheva M, Amelina E, Chernyak A, Ivanov M, Musienko S, Prodanov T, Kovalenko S, Baranova A, Khafizov K. Targeted sequencing reveals complex, phenotype-correlated genotypes in Cystic Fibrosis. BMC Med Genomics 2018; 11 (Suppl 1): 13.

Jakab RL, Collaco AM, Ameen NA. Characterization of CFTR high expresser

cells in the intestine. Am J Physiol Gastrointest Liver Physiol 2013; 305: G453-65.

Kelly T, Buxbaum J. Gastrointestinal manifestations of Cystic Fibrosis. Dig Dis Sci 2015; 60: 1903-13.

Kerem E, Corey M, Kerem BS, Rommens J, Markiewicz D, Levison H, Tsui LC, Durie P. The relation between genotype and phenotype in Cystic Fibrosis - analysis of the most common mutation (delta F508). N Engl J Med 1990; 323: 1517-22.

Kerem E, Konstan MW, De Boeck K, Accurso FJ, Sermet-Gaudelus I, Wilschanski M, Elborn JS, Melotti P, Bronsveld I, Fajac I, Malfroot A, Rosenbluth DB, Walker PA, McColley SA, Knoop C, Quattrucci S, Rietschel E, Zeitlin PL, Barth J, Elfring GL, Welch EM, Branstrom A, Spiegel RJ, Peltz SW, Ajayi T, Rowe SM. Ataluren for the treatment of nonsense-mutation Cystic Fibrosis: a randomised, double-blind, placebo-controlled phase 3 trial. Lancet Respir Med 2014; 2: 539-47.

Klimova B, Kuca K, Novotny M, Maresova P. Cystic Fibrosis revisited - a review study. Med Chem 2017; 13: 102-09.

Kluge M, Namkoong E, Khakipoor S, Park K, Roussa E. Differential regulation of vacuolar H(+) -ATPase subunits by transforming growth factor-beta1 in salivary ducts. J Cell Physiol 2019; 234: 15061-79.

Klymiuk N, Mundhenk L, Kraehe K, Wuensch A, Plog S, Emrich D, Langenmayer MC, Stehr M, Holzinger A, Kroner C, Richter A, Kessler B, Kurome M, Eddicks M, Nagashima H, Heinritzi K, Gruber AD, Wolf E. Sequential targeting of CFTR by BAC vectors generates a novel pig model of Cystic Fibrosis. J Mol Med 2012; 90: 597-608.

Knowles MR, Drumm M. The influence of genetics on Cystic Fibrosis phenotypes. Cold Spring Harb Perspect Med 2012; 2: a009548.

Kunz E, Rothammer S, Pausch H, Schwarzenbacher H, Seefried FR, Matiasek K, Seichter D, Russ I, Fries R, Medugorac I. Confirmation of a non-synonymous SNP in PNPLA8 as a candidate causal mutation for Weaver syndrome in Brown Swiss cattle. Genet Sel Evol 2016; 48: 21.

Lands LC, Milner R, Cantin AM, Manson D, Corey M. High-dose ibuprofen in Cystic Fibrosis: Canadian safety and effectiveness trial. J Pediatr 2007; 151: 249-54.

Lavelle GM, White MM, Browne N, McElvaney NG, Reeves EP. Animal models of Cystic Fibrosis pathology: phenotypic parallels and divergences. Biomed Res Int 2016; 2016: 5258727; doi: 10.1155/2016/.

Leung AY, Wong PY, Yankaskas JR, Boucher RC. cAMP- but not Ca(2+)-regulated Cl- conductance is lacking in Cystic Fibrosis mice epididymides and seminal vesicles. Am J Physiol 1996; 271: C188-93.

Li W, Soave D, Miller MR, Keenan K, Lin F, Gong J, Chiang T, Stephenson AL, Durie P, Rommens J, Sun L, Strug LJ. Unraveling the complex genetic model for Cystic Fibrosis: pleiotropic effects of modifier genes on early Cystic Fibrosis-related morbidities. Hum Genet 2014; 133: 151-61.

Liu X, Li T, Riederer B, Lenzen H, Ludolph L, Yeruva S, Tuo B, Soleimani M, Seidler U. Loss of Slc26a9 anion transporter alters intestinal electrolyte and HCO3(-) transport and reduces survival in CFTR-deficient mice. Pflugers Arch 2015; 467: 1261-75.

Marino CR, Matovcik LM, Gorelick FS, Cohn JA. Localization of the Cystic Fibrosis transmembrane conductance regulator in pancreas. J Clin Invest 1991; 88: 712-16.

McCarron A, Donnelley M, Parsons D. Airway disease phenotypes in animal models of Cystic Fibrosis. Respir Res 2018; 19: 54.

McGuire C, Stransky L, Cotter K, Forgac M. Regulation of V-ATPase activity. Front Biosci (Landmark Ed) 2017; 22: 609-22.

Medugorac I, Seichter D, Graf A, Russ I, Blum H, Gopel KH, Rothammer S, Forster M, Krebs S. Bovine polledness - an autosomal dominant trait with allelic heterogeneity. PLoS One 2012; 7: e39477.

Medugorac I, Graf A, Grohs C, Rothammer S, Zagdsuren Y, Gladyr E, Zinovieva N, Barbieri J, Seichter D, Russ I, Eggen A, Hellenthal G, Brem G, Blum H, Krebs S, Capitan A. Whole-genome analysis of introgressive hybridization and characterization of the bovine legacy of Mongolian yaks. Nat Genet 2017; 49: 470-75.

Mekus F, Ballmann M, Bronsveld I, Bijman J, Veeze H, Tummler B. Categories of deltaF508 homozygous Cystic Fibrosis twin and sibling pairs with distinct phenotypic characteristics. Twin Res 2000; 3: 277-93.

Meng X, Clews J, Kargas V, Wang X, Ford RC. The Cystic Fibrosis Transmembrane Conductance Regulator (CFTR) and its stability. Cell Mol Life Sci 2017; 74: 23-38.

Meuwissen TH, Karlsen A, Lien S, Olsaker I, Goddard ME. Fine mapping of a quantitative trait locus for twinning rate using combined linkage and linkage disequilibrium mapping. Genetics 2002; 161: 373-79.

Meyerholz DK, Stoltz DA, Namati E, Ramachandran S, Pezzulo AA, Smith AR, Rector MV, Suter MJ, Kao S, McLennan G, Tearney GJ, Zabner J, McCray PB, Jr., Welsh MJ. Loss of Cystic Fibrosis Transmembrane Conductance Regulator function produces abnormalities in tracheal development in neonatal pigs and young children. Am J Respir Crit Care Med 2010a; 182: 1251-61.

Meyerholz DK, Stoltz DA, Pezzulo AA, Welsh MJ. Pathology of gastrointestinal organs in a porcine model of Cystic Fibrosis. Am J Pathol 2010b; 176: 1377-89.

Müller MP, Rothammer S, Seichter D, Russ I, Hinrichs D, Tetens J, Thaller G, Medugorac I. Genome-wide mapping of 10 calving and fertility traits in Holstein dairy cattle with special regard to chromosome 18. J Dairy Sci 2017; 100: 1987-2006.

Navis A, Bagnat M. Loss of CFTR function leads to pancreatic destruction in larval zebrafish. Dev Biol 2015; 399: 237-48.

NCBI. NCBI databases. https://www.ncbi.nlm.nih.gov/. accessed Jan 29th, 2020.

O'Neal WK, Knowles MR. Cystic Fibrosis disease modifiers: complex genetics defines the phenotypic diversity in a monogenic disease. Annu Rev Genomics Hum Genet 2018; 19: 201-22.

O'Sullivan BP, Freedman SD. Cystic fibrosis. Lancet 2009; 373: 1891-904.

Olivier AK, Yi Y, Sun X, Sui H, Liang B, Hu S, Xie W, Fisher JT, Keiser NW, Lei D, Zhou W, Yan Z, Li G, Evans TI, Meyerholz DK, Wang K, Stewart ZA, Norris AW, Engelhardt JF. Abnormal endocrine pancreas function at birth in Cystic Fibrosis ferrets. J Clin Invest 2012; 122: 3755-68.

Olivier AK, Gibson-Corley KN, Meyerholz DK. Animal models of gastrointestinal and liver diseases. Animal models of Cystic Fibrosis: gastrointestinal, pancreatic, and hepatobiliary disease and pathophysiology. Am J Physiol Gastrointest Liver Physiol 2015; 308: G459-71.

Pabst R, Binns RM. The immune system of the respiratory tract in pigs. Vet Immunol Immunopathol 1994; 43: 151-56.

Paranjape SM, Mogayzel PJ, Jr. Cystic Fibrosis in the era of precision medicine. Paediatr Respir Rev 2018; 25: 64-72.

Parkins MD, Somayaji R, Waters VJ. Epidemiology, biology, and impact of

clonal Pseudomonas aeruginosa infections in Cystic Fibrosis. Clin Microbiol Rev 2018; 31: e00019-18.

Pierucci-Alves F, Akoyev V, Stewart JC, 3rd, Wang LH, Janardhan KS, Schultz BD. Swine models of Cystic Fibrosis reveal male reproductive tract phenotype at birth. Biol Reprod 2011; 85: 442-51.

Plasschaert LW, Zilionis R, Choo-Wing R, Savova V, Knehr J, Roma G, Klein AM, Jaffe AB. A single-cell atlas of the airway epithelium reveals the CFTR-rich pulmonary ionocyte. Nature 2018; 560: 377-81.

Pratap U, Quinn S, Blizzard LB, Reid DW. Population-based study of Cystic Fibrosis disease severity and haemochromatosis gene mutations. Respirology 2010; 15: 141-49.

Proesmans M, Vermeulen F, De Boeck K. What's new in Cystic Fibrosis? From treating symptoms to correction of the basic defect. Eur J Pediatr 2008; 167: 839-49.

Pulleyn LJ, Newton R, Adcock IM, Barnes PJ. TGFbeta1 allele association with asthma severity. Hum Genet 2001; 109: 623-27.

Quinton PM. Chloride impermeability in Cystic Fibrosis. Nature 1983; 301: 421-22.

Rafeeq MM, Murad HAS. Cystic fibrosis: current therapeutic targets and future approaches. J Transl Med 2017; 15: 84.

Ramos AM, Crooijmans RP, Affara NA, Amaral AJ, Archibald AL, Beever JE, Bendixen C, Churcher C, Clark R, Dehais P, Hansen MS, Hedegaard J, Hu ZL, Kerstens HH, Law AS, Megens HJ, Milan D, Nonneman DJ, Rohrer GA, Rothschild MF, Smith TP, Schnabel RD, Van Tassell CP, Taylor JF, Wiedmann RT, Schook LB, Groenen MA. Design of a high density SNP genotyping assay in

the pig using SNPs identified and characterized by next generation sequencing technology. PLoS One 2009; 4: e6524.

Ratjen FA. Cystic fibrosis: pathogenesis and future treatment strategies. Respir Care 2009; 54: 595-605.

Reid DW, Lam QT, Schneider H, Walters EH. Airway iron and iron-regulatory cytokines in Cystic Fibrosis. Eur Respir J 2004; 24: 286-91.

Riordan JR, Rommens JM, Kerem B, Alon N, Rozmahel R, Grzelczak Z, Zielenski J, Lok S, Plavsic N, Chou JL, et al. Identification of the Cystic Fibrosis gene: cloning and characterization of complementary DNA. Science 1989; 245: 1066-73.

Rogers CS, Hao Y, Rokhlina T, Samuel M, Stoltz DA, Li Y, Petroff E, Vermeer DW, Kabel AC, Yan Z, Spate L, Wax D, Murphy CN, Rieke A, Whitworth K, Linville ML, Korte SW, Engelhardt JF, Welsh MJ, Prather RS. Production of CFTR-null and CFTR-DeltaF508 heterozygous pigs by adeno-associated virus-mediated gene targeting and somatic cell nuclear transfer. J Clin Invest 2008a; 118: 1571-77.

Rogers CS, Stoltz DA, Meyerholz DK, Ostedgaard LS, Rokhlina T, Taft PJ, Rogan MP, Pezzulo AA, Karp PH, Itani OA, Kabel AC, Wohlford-Lenane CL, Davis GJ, Hanfland RA, Smith TL, Samuel M, Wax D, Murphy CN, Rieke A, Whitworth K, Uc A, Starner TD, Brogden KA, Shilyansky J, McCray PB, Jr., Zabner J, Prather RS, Welsh MJ. Disruption of the CFTR gene produces a model of Cystic Fibrosis in newborn pigs. Science 2008b; 321: 1837-41.

Rogers GB, Taylor SL, Hoffman LR, Burr LD. The impact of CFTR modulator therapies on CF airway microbiology. J Cyst Fibros 2019; doi: 10.1016/j.jcf.2019.07.008. [Epub ahead of print]

Rosen BH, Chanson M, Gawenis LR, Liu J, Sofoluwe A, Zoso A, Engelhardt JF. Animal and model systems for studying Cystic Fibrosis. J Cyst Fibros 2018; 17:

S28-34.

Rothammer S, Kremer PV, Bernau M, Fernandez-Figares I, Pfister-Schar J, Medugorac I, Scholz AM. Genome-wide QTL mapping of nine body composition and bone mineral density traits in pigs. Genet Sel Evol 2014; 46: 68.

Rothammer S, Kunz E, Krebs S, Bitzer F, Hauser A, Zinovieva N, Klymiuk N, Medugorac I. Remapping of the belted phenotype in cattle on BTA3 identifies a multiplication event as the candidate causal mutation. Genet Sel Evol 2018; 50: 36.

Rowe SM, Heltshe SL, Gonska T, Donaldson SH, Borowitz D, Gelfond D, Sagel SD, Khan U, Mayer-Hamblett N, Van Dalfsen JM, Joseloff E, Ramsey BW. Clinical mechanism of the Cystic Fibrosis Transmembrane Conductance Regulator potentiator ivacaftor in G551D-mediated Cystic Fibrosis. Am J Respir Crit Care Med 2014; 190: 175-84.

Rowe SM, Daines C, Ringshausen FC, Kerem E, Wilson J, Tullis E, Nair N, Simard C, Han L, Ingenito EP, McKee C, Lekstrom-Himes J, Davies JC. Tezacaftor-Ivacaftor in residual-function heterozygotes with Cystic Fibrosis. N Engl J Med 2017; 377: 2024-35.

Rozmahel R, Wilschanski M, Matin A, Plyte S, Oliver M, Auerbach W, Moore A, Forstner J, Durie P, Nadeau J, Bear C, Tsui LC. Modulation of disease severity in Cystic Fibrosis Transmembrane Conductance Regulator deficient mice by a secondary genetic factor. Nat Genet 1996; 12: 280-87.

Santis G, Osborne L, Knight RA, Hodson ME. Independent genetic determinants of pancreatic and pulmonary status in Cystic Fibrosis. Lancet 1990; 336: 1081-84.

Semaniakou A, Croll RP, Chappe V. Animal models in the pathophysiology of Cystic Fibrosis. Front Pharmacol 2018; 9: 1475; doi: 10.3389/fphar.2018.01475.

Shanthikumar S, Neeland MN, Saffery R, Ranganathan S. Gene modifiers of Cystic Fibrosis lung disease: a systematic review. Pediatr Pulmonol 2019; 54: 1356-66.

Skov M, Hansen CR, Pressler T. Cystic fibrosis - an example of personalized and precision medicine. Apmis 2019; 127: 352-60.

Smith DJ, Klein K, Hartel G, Wainwright CE, Bell SC, Anderson GJ, Reid DW. Mutations in the HFE gene can be associated with increased lung disease severity in Cystic Fibrosis. Gene 2019; 683: 12-7.

Snouwaert JN, Brigman KK, Latour AM, Malouf NN, Boucher RC, Smithies O, Koller BH. An animal model for Cystic Fibrosis made by gene targeting. Science 1992; 257: 1083-88.

Sontag MK, Corey M, Hokanson JE, Marshall JA, Sommer SS, Zerbe GO, Accurso FJ. Genetic and physiologic correlates of longitudinal immunoreactive trypsinogen decline in infants with Cystic Fibrosis identified through newborn screening. J Pediatr 2006; 149: 650-57.

Stanke F, Becker T, Hedtfeld S, Tamm S, Wienker TF, Tummler B. Hierarchical fine mapping of the Cystic Fibrosis modifier locus on 19q13 identifies an association with two elements near the genes CEACAM3 and CEACAM6. Hum Genet 2010; 127: 383-94.

Stoltz DA, Meyerholz DK, Pezzulo AA, Ramachandran S, Rogan MP, Davis GJ, Hanfland RA, Wohlford-Lenane C, Dohrn CL, Bartlett JA, Nelson GAt, Chang EH, Taft PJ, Ludwig PS, Estin M, Hornick EE, Launspach JL, Samuel M, Rokhlina T, Karp PH, Ostedgaard LS, Uc A, Starner TD, Horswill AR, Brogden KA, Prather RS, Richter SS, Shilyansky J, McCray PB, Jr., Zabner J, Welsh MJ. Cystic Fibrosis pigs develop lung disease and exhibit defective bacterial eradication at birth. Sci Transl Med 2010; 2: 29ra31; doi: 10.1126/scitranslmed.3000928.

Stoltz DA, Rokhlina T, Ernst SE, Pezzulo AA, Ostedgaard LS, Karp PH, Samuel MS, Reznikov LR, Rector MV, Gansemer ND, Bouzek DC, Abou Alaiwa MH, Hoegger MJ, Ludwig PS, Taft PJ, Wallen TJ, Wohlford-Lenane C, McMenimen JD, Chen JH, Bogan KL, Adam RJ, Hornick EE, Nelson GAt, Hoffman EA, Chang EH, Zabner J, McCray PB, Jr., Prather RS, Meyerholz DK, Welsh MJ. Intestinal CFTR expression alleviates meconium ileus in Cystic Fibrosis pigs. J Clin Invest 2013; 123: 2685-93.

Stoltz DA, Meyerholz DK, Welsh MJ. Origins of Cystic Fibrosis lung disease. N Engl J Med 2015; 372: 351-62.

Sun L, Rommens JM, Corvol H, Li W, Li X, Chiang TA, Lin F, Dorfman R, Busson PF, Parekh RV, Zelenika D, Blackman SM, Corey M, Doshi VK, Henderson L, Naughton KM, O'Neal WK, Pace RG, Stonebraker JR, Wood SD, Wright FA, Zielenski J, Clement A, Drumm ML, Boelle PY, Cutting GR, Knowles MR, Durie PR, Strug LJ. Multiple apical plasma membrane constituents are associated with susceptibility to meconium ileus in individuals with Cystic Fibrosis. Nat Genet 2012; 44: 562-69.

Sun X, Sui H, Fisher JT, Yan Z, Liu X, Cho HJ, Joo NS, Zhang Y, Zhou W, Yi Y, Kinyon JM, Lei-Butters DC, Griffin MA, Naumann P, Luo M, Ascher J, Wang K, Frana T, Wine JJ, Meyerholz DK, Engelhardt JF. Disease phenotype of a ferret CFTR-knockout model of Cystic Fibrosis. J Clin Invest 2010; 120: 3149-60.

Sun X, Olivier AK, Yi Y, Pope CE, Hayden HS, Liang B, Sui H, Zhou W, Hager KR, Zhang Y, Liu X, Yan Z, Fisher JT, Keiser NW, Song Y, Tyler SR, Goeken JA, Kinyon JM, Radey MC, Fligg D, Wang X, Xie W, Lynch TJ, Kaminsky PM, Brittnacher MJ, Miller SI, Parekh K, Meyerholz DK, Hoffman LR, Frana T, Stewart ZA, Engelhardt JF. Gastrointestinal pathology in juvenile and adult CFTR-knockout ferrets. Am J Pathol 2014; 184: 1309-22.

Tan W, Carlson DF, Lancto CA, Garbe JR, Webster DA, Hackett PB, Fahrenkrug SC. Efficient nonmeiotic allele introgression in livestock using custom endonucleases. Proc Natl Acad Sci USA 2013; 110: 16526-31.

Taylor-Cousar JL, Munck A, McKone EF, van der Ent CK, Moeller A, Simard C, Wang LT, Ingenito EP, McKee C, Lu Y, Lekstrom-Himes J, Elborn JS. Tezacaftor-Ivacaftor in patients with Cystic Fibrosis homozygous for Phe508del. N Engl J Med 2017; 377: 2013-23.

Teichgraber V, Ulrich M, Endlich N, Riethmuller J, Wilker B, De Oliveira-Munding CC, van Heeckeren AM, Barr ML, von Kurthy G, Schmid KW, Weller M, Tummler B, Lang F, Grassme H, Doring G, Gulbins E. Ceramide accumulation mediates inflammation, cell death and infection susceptibility in Cystic Fibrosis. Nat Med 2008; 14: 382-91.

Thermofisher. Axiom™ Porcine Genotyping Array. https://www.thermofisher.com/order/catalog/product/550588#/550588. accessed Jan 22th, 2020.

Tuggle KL, Birket SE, Cui X, Hong J, Warren J, Reid L, Chambers A, Ji D, Gamber K, Chu KK, Tearney G, Tang LP, Fortenberry JA, Du M, Cadillac JM, Bedwell DM, Rowe SM, Sorscher EJ, Fanucchi MV. Characterization of defects in ion transport and tissue development in Cystic Fibrosis transmembrane conductance regulator (CFTR)-knockout rats. PLoS One 2014; 9: e91253.

Turner MW. The role of mannose-binding lectin in health and disease. Mol Immunol 2003; 40: 423-29.

Uc A, Olivier A, A Griffin M, Meyerholz D, Yao J, Abu-El-Haija M, Buchanan K, G. Vanegas Calderon O, Abu-El-Haija M, Pezzulo A, Reznikov L, J Hoegger M, Rector M, S Ostedgaard L, Taft P, Gansemer N, S Ludwig P, Hornick E, A Stoltz D, Norris A. Glycemic regulation and insulin secretion are abnormal in Cystic Fibrosis pigs despite sparing of islet cell mass. Clinical Science 2014; 128: 131-42.

van der Doef HP, Slieker MG, Staab D, Alizadeh BZ, Seia M, Colombo C, van der Ent CK, Nickel R, Witt H, Houwen RH. Association of the CLCA1 p.S357N variant with meconium ileus in European patients with Cystic Fibrosis. J Pediatr

Gastroenterol Nutr 2010; 50: 347-49.

Vanscoy LL, Blackman SM, Collaco JM, Bowers A, Lai T, Naughton K, Algire M, McWilliams R, Beck S, Hoover-Fong J, Hamosh A, Cutler D, Cutting GR. Heritability of lung disease severity in Cystic Fibrosis. Am J Respir Crit Care Med 2007; 175: 1036-43.

Wainwright CE, Elborn JS, Ramsey BW, Marigowda G, Huang X, Cipolli M, Colombo C, Davies JC, De Boeck K, Flume PA, Konstan MW, McColley SA, McCoy K, McKone EF, Munck A, Ratjen F, Rowe SM, Waltz D, Boyle MP. Lumacaftor-Ivacaftor in patients with Cystic Fibrosis homozygous for Phe508del CFTR. N Engl J Med 2015; 373: 220-31.

Weiler CA, Drumm ML. Genetic influences on Cystic Fibrosis lung disease severity. Front Pharmacol 2013; 4: 40.

Welsh MJ, Smith AE. Molecular mechanisms of CFTR chloride channel dysfunction in Cystic Fibrosis. Cell 1993; 73: 1251-54.

Welsh MJ, Rogers CS, Stoltz DA, Meyerholz DK, Prather RS. Development of a porcine model of Cystic Fibrosis. Trans Am Clin Climatol Assoc 2009; 120: 149-62.

Whiting P, Al M, Burgers L, Westwood M, Ryder S, Hoogendoorn M, Armstrong N, Allen A, Severens H, Kleijnen J. Ivacaftor for the treatment of patients with Cystic Fibrosis and the G551D mutation: a systematic review and cost-effectiveness analysis. Health Technol Assess 2014; 18: 1-106.

Wu L, Chau J, Young RP, Pokorny V, Mills GD, Hopkins R, McLean L, Black PN. Transforming growth factor-beta1 genotype and susceptibility to chronic obstructive pulmonary disease. Thorax 2004; 59: 126-29.

Zhang M, Liao Y, Lonnerdal B. EGR-1 is an active transcription factor in TGF-

beta2-mediated small intestinal cell differentiation. J Nutr Biochem 2016; 37: 101-08.

Zhou L, Dey CR, Wert SE, DuVall MD, Frizzell RA, Whitsett JA. Correction of lethal intestinal defect in a mouse model of Cystic Fibrosis by human CFTR. Science 1994; 266: 1705-08.

Zielenski J, Corey M, Rozmahel R, Markiewicz D, Aznarez I, Casals T, Larriba S, Mercier B, Cutting GR, Krebsova A, Macek M, Jr., Langfelder-Schwind E, Marshall BC, DeCelie-Germana J, Claustres M, Palacio A, Bal J, Nowakowska A, Ferec C, Estivill X, Durie P, Tsui LC. Detection of a Cystic Fibrosis modifier locus for meconium ileus on human chromosome 19q13. Nat Genet 1999; 22: 128-29.

XI. ACKNOWLEDGMENTS

First of all, I would like to thank Prof. Dr. Eckhard Wolf for providing me the opportunity to perform my doctoral thesis at the Chair for Molecular Animal Breeding and Biotechnology and for reviewing this manuscript.

I would like to sincerely thank my mentors Prof. Dr. Nikolai Klymiuk and Dr. Andrea Bähr for their patient support and constant guidance.

I am thankful to my fellow graduate students Steffi, Florian, Petra, Lina, Sophia, Claudia and Hannah for all their help and eternal moral support! Special thanks also go to the animal caretaker Harald Paul.

Finally, I would like to express my deepest gratitude to my family and friends and particularly to Marcus. Thank you for your love, your understanding and your inestimable and never-ending support during the last years. Thanks for always believing in me! Without you, this work would not have been possible.